EFFECT OF IRRADIATION OF ULTRAVIOLET ON THE QUANTITATION METHOD OF ENHANCED GREEN FLUORESCENT PROTEIN

HOR CHEE HENG
(KE11029)

BACHELOR OF CHEMICAL ENGINEERING (BIOTECHNOLOGY)
UNIVERSITI MALAYSIA PAHANG

Thesis Access Form

No_____Location_____

Author : ……

Title : ……

Status of access OPEN / RESTRICTED / CONFIDENTIAL

Moratorium period:_____ years, ending_____/_____200____

Conditions of access proved by (CAPITALS): **DR CHEW FEW NE**

Supervisor (Signature)……

Faculty: ……

Author's Declaration: *I agree the following conditions:*

OPEN access work shall be made available in the Universiti Malaysia Pahang only and not allowed to reproduce for any purposes.

*The statement itself shall apply to **ALL** copies:*

This copy has been supplied on the understanding that it is copyright material and that no quotation from the thesis may be published without proper acknowledgement.

Restricted/confidential work: All access and any photocopying shall be strictly subject to written permission from the University Head of Department and any external sponsor, if any.

Author's signature…….Date: ……

users declaration: for signature during any Moratorium period (Not Open work):
I undertake to uphold the above conditions:

Date	Name (CAPITALS)	Signature	Address

EFFECT OF IRRADIATION OF ULTRAVIOLET ON THE QUANTITATION METHOD OF ENHANCED GREEN FLUORESCENT PROTEIN

HOR CHEE HENG
(KE11029)

Thesis submitted in partial fulfilment of the requirements
for the award of the degree of
Bachelor of Chemical Engineering (Biotechnology)

Faculty of Chemical & Natural Resources Engineering
UNIVERSITI MALAYSIA PAHANG

JANUARY 2015

SUPERVISOR'S DECLARATION

We hereby declare that we have checked this thesis and in our opinion, this thesis is adequate in terms of scope and quality for the award of the degree of Bachelor of Chemical Engineering (Biotechnology).

Signature :
Name of main supervisor : DR. CHEW FEW NE
Position : SENIOR LECTURER
Date :

STUDENT'S DECLARATION

I hereby declare that the work in this thesis is my own except for quotations and summaries which have been duly acknowledged. The thesis has not been accepted for any degree and is not concurrently submitted for award of other degree.

Signature :
Name : HOR CHEE HENG
ID Number : KE11029
Date :

Dedication

Highest gratitude to
my supervisor, my family members and my friends
for all your care, support and trust on me.
Special dedication to
Faculty of Chemical Engineering and Natural Resources of
University Malaysia Pahang
on providing all the related environment
and appropriate equipment
on finishing my research.

ACKNOWLEDGEMENT

I would like to thanks the following people and organisations;

- My supervisors Dr. Chew Few Ne for her guidance through an effective well-arranged weekly meeting.
- My PSM co-student, Ooi Chee Beng for his knowledge and excellent lab skill during performing PSM.

ABSTRACT

In last 30 years, green fluorescent protein (GFP) has changed from an unknown protein to a commonly used protein in bioscience application due to its visible fluorescence. As the usage of GFP increases, fluorescent detection and measurement devices are becoming more important. To detect and measure the GFP, a gel-based imaging system using a native polyacrylamide gel was developed. The ultimate aim of this study is to investigate the effect of ultraviolet (UV) light on the GFP quantitation method. In the research, enhanced GFP (EGFP) was expressed in *Escherichia coli* strain BL21(DE3) and purified using immobilized metal ions affinity chromatography. Different dilution of EGFP was prepared and their concentrations were determined by Lowry's method using bovine serum albumin as the standard. The EGFP dilution samples were then loaded into a native polyacrylamide gel. After electrophoresis, fluorescent image of EGFP on the gel was captured using gel imaging system under different UV irradiation exposure period. The UV irradiation has a marked influence on the EGFP fluorescence intensity. The fluorescence intensity was increased as the UV exposure period increased from 5-35 s. However, the fluorescence intensity decreased when the exposure period was increased further. Highest fluorescence intensity happened at around 35 s of UV exposure. By using different concentration of purified EGFP, the photobleaching process followed a first order reaction with rates between 3712-8213 int/s. The linearity showed insignificant change and lied within 0.922-0.946. It became more reliable when the UV exposure time increases. However, UV exposure time affected the fluorescence intensity, it is better to choose around 35s as UV exposure time due to highest fluorescence intensity when using gel-based imaging method as quantitation method.

Key words: GFP, EGFP, UV, gel-based imaging method, quantitation

ABSTRAK

Dalam 30 tahun yang lalu, protein perndarfluor hijau (GFP) telah berubah daripada protein yang tidak diketahui kepada protein yang biasa digunakan dalam kegunaan biosainas kerana sifatnya yang boleh bercahaya hijau dan dapat dilihat. Oleh sebab kenaikan penggunaan GFP, alat pengesanan dan pengukuran telah menjadi semakin penting. Untuk mengesan dan mengukur GFP, system pengimejan yang berasaskan gel dengan menggunakan gel polyacrylamide asli telah dibangunkan. Matlamat utama kajian ini adalah untuk mengkaji kesan cahaya ultraugu (UV) pada kaedah kuantiti GFP. Dalam kajian ini, enhanced GFP (EGFP) telah ditunjukkan dalam Escherichia coli strain BL 21 (DE 3) dan disucikan dengan mengunakan ion logam bergerak pertalian kromatografi. Pencairan EGFP yang berbeza telah disesdiakan dan kepekatan mereka telah ditentukan dengan oleh kaedah Lowry dengan menggunakan albumin serum lembu sebagai standard. Sample pencairan EGFP kemudian diisikan ke dalam gel polyacrylamide asli. Selepas elektroforeis, imej pendarflour EGFP yang berada dalam gel ditangkap gambar di bawah sinaran UV dalam tempoh pendedahan yang berbeza. Sinaran UV telah menpengaruhi intensiti pendarfluor EGFP. Intensiti pendarfluor EGFP telah ditingkatkan apabila tempoh pendedahan UV telah dinaikan dari 5 hingga 35 s. Walaubagaimanapun, intensiti perdarflour menurun apabila tempoh pendedahan itu telah meningkat. Intensiti pendarfluor yang paling tinggi ialah 35 saat apabila didedahkan oleh sinarran UV. Dengan menggunakan pelbagai kepekatan EGFP yang telah disucikan, proses ‘photobleaching’ diikuti tindak balas tertib pertama dengan kadar antara 3712 – 8213 int/s. Kelinearan menunjukkan perubahan yang tidak ketara dan berada dalam 0.922-0.946. Kelinearan itu menjadi lebih linear apabila masa pendedahan UV meningkat. Walaubagaiamanapun, masa pendedahan UV menjejaskan intensity pendarfluor. Oleh itu, masa 35s adalah lebih baik dipilihkan sebagai masa

pendedahan UV kerana intensity pendarfluor adalah paling tinggi apabila menggunakan kaedah berasaskan gel sebagai kaedah quantitation.

Kata kunci: GFP, EGFP, UV, kaedah pengimejan berasaskan gel, kuantiti

TABLE OF CONTENTS

LIST OF FIGURES

LIST OF TABLES

LIST OF ABBREVIATIONS

APS	-	*Ammonium persulfate*
A.victoria	-	*AequoreaVictoria*
BSA	-	*Bovine serum albumin*
C.elegans	-	*Caenorhabditiselegans*
DNA	-	*Dioxyribonucleic acid*
E.coli	-	*Escherichia coli*
EGFP	-	*Enhanced green fluorescent protein*
GFP	-	*Green fluorescent protein*
IPTG	-	*Isopropyl- β-D-thiogalactoside*
LB	-	*Luria bertani*
NA	-	*Nucleic acid*
n-PAGE	-	*Native-polyacrylamide gel electrophoresis*
OD	-	*Optical density*
PAGE	-	*Polyacrylamide gel electrophoresis*
RNA	-	*Ribonucleic acid*
R.reniformis	-	*Renillareniformis*
Temed	-	*Tetramethylethylenediamine*
UV	-	*Ultraviolet*
wtGFP	-	*Wild type green fluorescent protein*
D-D	-	*Dye to dye*
D-O	-	*Dye to oxygen*
QD	-	*Quantum Dots*

1 INTRODUCTION

1.1 Background of green fluorescent protein

Fluorescent proteins can be found from the mostly marine creatures. Green fluorescent protein (GFP) is originated from the bioluminescent jellyfish which also known as *Aequorea victoria (A. victoria)* in the sea of north pacific (Zimmer, 2002; Chalfie *et al.*, 1994). GFP is a 27 kDa protein which is made of 238 amino acids polypeptide and composed of 11- strand β sheet with a central coaxial α helix in a novel 3-D configuration (Yang *et al.*, 1996; Ormo *et al.*, 1996). GFP chromophore is lied within the β sheet. This chromophore is formed when tri-peptide,-(Ser_{56}-Tyr_{66}-Gly_{67})-,of GFP is going through cyclisation, oxidation and dehydration reactions (Yang *et al.*, 1996; Ormo *et al.*, 1996). The chromophore is the source of green light where it absorbs light energy from the ultraviolet (UV) and emits a low energy green light. This phenomenon happens when the Ca^{2+} ions react with Aequorin. Nowadays, there are many types of GFP derivatives and the basic form of the GFP is the wild type GFP (wtGFP). The wtGFP with 238 polypeptides is stable and proteolysis-resistant. It has the excitation peak at 395 nm and a minor peak at 475 nm (Ward *et al.*,1980). GFP has been modified into different type of GFP derivatives like enhanced GFP (EGFP) and S65T by modifying certain location of amino acid. Random mutagenesis affects the proteins spectral characteristic, hence these mutant GFPs has a more powerful green fluorescence intensity when are excited at specific absorbance (Philip, 1997). In this study, EGFP will be used as the model protein due to its better fluorescence properties compared to GFP.

1.2 Motivation and problem statement

Around 30 years ago, the GFP was discovered by Osamu Shimomura and this discovery was further developed into many applications which are important and useful in the science life today. These applications including protein markers, tag for protein localization, and protein-protein interactions. In 2008, the Royal Swedish Academy of Sciences had awarded the Nobel Prize to Osamu Shimomura, Martin Chalfie and Roger Yonchien Tsien for the discovery and development of the GFP (Tongea and Meechb, 2009; Nienhaus, 2008). Given its large number of applications, the reliable quantitation methods such as spectrofluorometer, flow cytometry, fluorescent microscopy and gel-based imaging system are designed to analyze the GFP samples. In this research, gel-based imaging system is used for GFP quantitation. This analytical method only required microgram amount and small volume of samples for the analysis. Furthermore, gel-based imaging system is able to quantify the denatured GFP from its native form (Chew *et al.*, 2011). Gel-based imaging system uses UV lamps as the illumination source for green fluorescent detection. The UV radiation may affect the reproducibility and accuracy during the quantitation. Prolonged irradiation of UV on GFP may induce photoconversion in the chromophore (Patterson *et al.*, 1997). It causes initial increase in the fluorescence and photobleaching effects on different type of mutant GFPs. Patterson (2007) has reported that the EGFP photobleaching rate was increased rapidly when it was exposed under the high power of UV light for a long period. Thus, the exposure time effect of the UV irradiation on GFP fluorescence is crucial for reliable and accurate GFP quantitation using the gel-based imaging method.

1.3 Objectives

This research study was to investigate the effect of UV irradiation period on different concentration of purified EGFP quantitation using gel-based imaging method.

1.4 Scope of this research

The following are the scopes of this research:

(i) Expression of EGFP in *E.coli* strain BL21 (DE3)

(ii) Purification using affinity chromotagraphy.

(iii) Determination of the amount of EGFP by using Lowry's method.

(iv) Investigation of the effect of UV irradiation period and EGFP concentration on the quantitation method.

2 LITERATURE REVIEW

2.1 Properties of green fluorescent protein

GFP is from marine creatures: a jellyfish, *Aequorea victoria*, from North-west pacific and a sea pansy, *Renilla reniformis*, from Georgia coastline (Ward *et al.*, 1980). Although both *Aequorea* GFP and *Renilla* GFP share the identical chromophore, *Aequorea* GFP has two absorbance peaks at 395 and 475 nm while *Renilla* GFP has only a single absorbance peak at 198 nm (Deluca and Mcelroy, 1981). Besides, *Renilla* GFP has 5.5-folds greater monomer extinction coefficient than the *Aequorea* GFP which has a 395 nm peak absorbance (Deluca and Mcelroy, 1981). Hence, only *Aequorea* GFP genes are cloned for various application (Tsien, 1998). GFP is an acidic, compact, globular protein with 27 kDa molecular weights (Chalfie and Kain, 2005). Table 2-1 and Table 2-2 show the comparisons of the physical properties and the amino acid compositions of the *Aequorea* GFP and *Renilla* GFP.

Table 2-1**:** Comparisons of the physical properties of the Aequorea GFP and Renilla GFP [Adapted from Chalfie and Kain (2005)]

	Aequorea	*Renilla*
Monomer molecular weight[a]	27 kDa 26.9 kDa[c]	27 kDa[b]
Isoelectric point(s) (pI)	4.6–5.1[d]	5.34 ± 0.07[b]
Fluorescence emission maximum	508[e]–509 nm	509 nm[b]
Fluorescence quantum yield	0.72–0.78[e] 0.80	0.80[b]
Molar extinction coefficient (monomer) $\varepsilon\lambda^{1M}$ (liter mol^{-1} cm^{-1})		
λ = 498 nm	3,000	133,000[b]
λ = 475 nm	14,000	53,000[b]
λ = 397 nm	27,600	<1,000[b]
λ = 280 nm	22,000	22,000[b]
Absorption ratio (highest purity achieved) 498 nm/280 nm		5.6[b]–6.0
397 nm/380 nm	1.25	

[a] At moderate protein concentration of *Aequorea* GFP (<0.5 mg mL^{-1}) the monomeric form predominates. At higher protein concentrations of *Aequorea* GFP (>2.0 mg mL^{-1}) the dimeric form predominates. Renilla GFP is dimeric (2 × 27 kDa) at all concentrations unless denatured. [b] From Ward and Cormier (1979). [c] From Prasher et al. (1992). Based upon sequence of cDNA. [d] From Cutler (1995). Nine isoforms have been characterized. [e] From Morise et al. (1974).

Table 2-2: The amino acid compositions of Renillas GFP and Aequorea GFP [Adapted from Chalfie and Kain (2005)]

Amino Acids	*Renilla* GFP Nearest Integer per 27,000 Da[a]	*Aequorea* GFP from cDNA Sequence gfp 10[b]
Lysine	19	20
Histidine	8	10
Arginine	7	6
Half-cystine	2[c]	2
Methionine	9	6
Aspartic acid	20	18
Asparagine		13
Glutamic acid	27	16
Glutamine		8
Threonine	17	15
Serine	15	10
Proline	11	10
Glycine	22	22
Alanine	14	8
Valine	18	17
Isoleucine	14	12
Tyrosine	11	11
Phenylalanine	13	13
Tryptophan	0[d]	1
Amino sugars	0[e]	0

[a] From Ward and Cormier (1979). Each value represents the average from hydrolyses of 24, 48, and 72 h unless otherwise indicated.
[b] From Prasher et al. (1992).
[c] Determined as cysteic acid following performic acid oxidation.
[d] Determined by hydrolysis in the presence of thioglycolate.
[e] Determined by hydrolysis with *p*-toluenesulfonic acid.

2.2 The formation and mechanism of GFP chromophore

GFP is made of 238-amino acid polypeptides which consists of β barrel with 11 strands GFP that surrounding α helix in a cylindrical structure (Yang *et al.*, 1996; Ormo *et al.*, 1996;McRae *et al.*, 2005). This cylindrical structure is named as 'β-can' which has the function to protect the chromophore that position in the middle of the α helix (Phillips, 1997). Water molecules can form 'stripes' around the cylinder surface and give resistance and stability for chromophore from being unfold caused by denaturants and heat (Phillips, 1997). The α helix contains p-hydroxybenzylideneimadazolinone chromophore which undergoes cyclization of tripeptide (Ser65, Tyr66 and Gly67) and 1,2-dehydrogentaion of the tryrosine (Cody *et al.*, 1993). Based on Figure 2-1, when the translated apoprotein evades

precipitation into inclusion bodies, cyclization of amino group, Gly-67 to the carbonyl group, Ser-65 is occurred to form an imidazolidin-5-one, where the absence of O_2 would stop the process. Then, the new N=C double bond would further to cause dehydrogenation to form a conjugated chromophore (imidazolidin-5-ones). The conjugated chromophore will change to the chromophore completely by undergoing autoxidative formation of double bonds at 4-position. This process needs around one step with a time constant of 4 h (Kidwai and Devasia, 1962).Chromophore is the source of emitting the low energy green light after absorbing the UV light. This phenomenon happens when the Ca^{2+} ions react with Aequorin. The Aequorin which emits the blue light will become an intermediate molecule that further produce a reaction product named blue fluorescent protein (BFP). The excited BFP will further transfer energy to GFP and causes it moves into excited state and emits the green light.

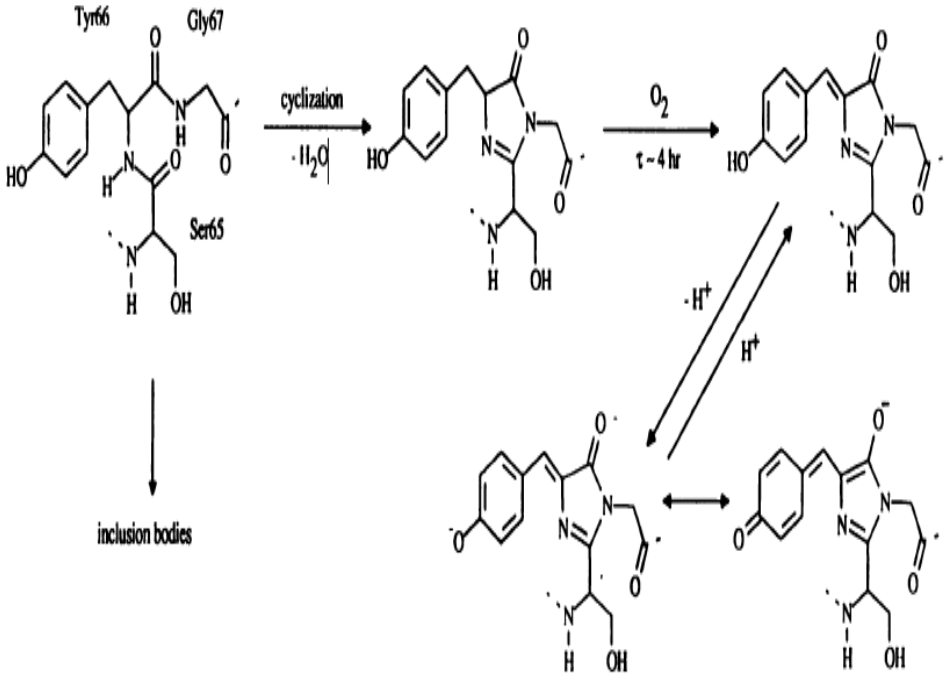

Figure 2-1: The chromophore formation process [Adapted from Heim *et al.* (1994)]

2.3 The derivatives of GFP

GFP is engineering mutated in order to improve its properties. Random mutation is carried out by substituting the certain location of amino acid with other amino acids in the chromophore structure. However, most of the mutations in GFP encountered failures, for example loss of fluorescence without obvious change at certain absorption or emission peaks. The failures are due to the failure formation of chromophore, quenching of the fluorescence and misfolding of the protein (Cubitt *et al.,* 1995). Some successful examples of mutated GFP are S65T and EGFP. For S65T, since the Ser65 is substituted with Thr, it has higher fluorescence intensity, less photobleaching rate, extinction coefficient as well as quantum efficiency compared to wtGFP (Cubitt *et al.,* 1995). For the EGFP, it is a mutant where its fluorescence intensity is increased by 35-fold compared to wtGFP (Cormack *et al.,* 1996). Its enhanced fluorescence intensity causes EGFP becomes so popular in the aspect of the protein marker and reporter (Zhao *et al.*, 1998).

2.4 Applications of green fluorescent protein

2.4.1 GFP as a marker of gene expression and cell lineage

GFP can be used as the gene expression marker in vivo without the needs of the cofactors (Chalfie *et al.,* 1994). This application works when the DNA of GFP is expressed in prokaryotic [*Escherichia coli* (*E.coli*)] or eukaryotic [*Caenorhabditiselegans* (*C.elegans*)] cells (Chalfie *et al.,* 1994). GFP was expressed in the *E.coli* after the induction using Isopropyl- β-D-thiogalactoside (IPTG). Green fluorescence was observed in control bacteria under the illumination UV light. After GFP purification, *the recombinant GFP* exhibits same fluorescence excitation and emission spectra as the purified native protein (Chalfie *et al.,* 1994). This shows that the chromphore of GFP can be formed in the *E.coli* in the absence of other

A.victoria products. As for the *C.elegans,* fluorescent of GFP was produced during the transformation process (Brenner, 1974). Hence, alike with native protein, GFP performs well in term of expression in those cells when illuminated under 450 nm to 490 nm of light.

2.4.2 GFP as a protein tag

GFP can be used as a fluorescent tag for the N- (amino) or C- (carboxyl) termini of proteins (Wang and Hazelrigg, 1994). The ideal fusion of GFP with a host protein preserves both the fluorescence of GFP and all the targeting and physiological function of the host protein. Fusion process happens when both the N- and C-termini are fused with the cytosolic and membrane-bound proteins. The process is functioned successfully without flexible linkers when the amino terminus of GFP is fused at the carboxyl terminus of the host protein. This successful fusion might be enhanced by linker sequences (Cubitt *et al.,* 1995). Application of GFP using as a protein tag is becoming popular. It can be applied in many fields especially in medicine like using GFP to tag lactic acid bacterium strains for live vaccine vectors (Geoffroy *et al.,* 2000).

2.4.3 Monitoring protein-protein interactions

GFP is widely applied in protein-protein interaction application due to its small monomeric reporter molecule that might avoid the obstacles to development of an ideal system to study protein-protein interactions for various applications. (Paulmurugan and Gambhir, 2003).Protein-protein interaction happens when a donor chromophore is fused with an acceptor chromophore such as expressing fusions of two different-colored GFP mutants (Cubitt *et al.,* 1995). For example, blue mutation Y66H acts as the donor, which has maximum excitation of 382 nm and maximum emission of 448 nm while S65T acts as the acceptor which has which

has maximum excitation of 489 nm and maximum emission of 511 nm (Cubitt *et al.,* 1995). This application requires the overlapping between the emission spectrum of the donor and the absorption spectrum of the acceptor (Cubitt *et al.,* 1995). wtGFP is not advisable to be used in this protein-protein interaction because it has the 395nm excitation peak which is almost the same as Y66H which has the 382 nm absorption peak. This will directly excite wtGFP without any energy transfer (Cubitt *et al.,* 1995). Fluorescence resonance energy transfer (FRET) can be used to detect this interaction.

2.5 Quantitation methodss of GFP

There are many analysis methods to detect and measure GFP which including flow cytometry, fluorescent microscopy, spectrofluorometer and gel-based imaging system.

2.5.1 Flow cytometry

Flow cytometry is a technology which is contributive to clinical medicine and cell biology in a very significant manner. Flow cytometry consists of fluidic system, laser, optic system and electronics. Hydrodynamic focusing is applied in flow cytometry (Robinson, 2004). The fluid system transports the samples to the interrogating point that is focused by the laser beam and this produces many optical signals. Flurophores are attached on the cells or particles will emit light when its expose to laser beam at 488nm. Forward scatter (FSC), side scatter (SSC) and fluorescent signals will be collected. FSC is a signal that is used to detect physical size of the particles like cell diameter. SSC is used to detect internal composition, for example red blood cell and white blood cell. Fluorescent signals will follow the same direction as the SSC and pass through a series of short-pass, long-pass and band-pass filters to allow certain wavelength to reach the suitable detectors. Based

on the certain wavelength of the light magnitude, electrical signals are generated and then further analyzed by the computer system. GFP labelled bacteria can be quantified by using flow cytometry. It can quantify fluorescence intensity of various groups of GFP-labelled microorganisms. By using flow cytometry, the quantitation of GFP within a population is allowed because this device is able to analyze the optical properties of hundreds of single cells per second passing through focused laser beam (Errampalli *et al.*, 1999). Flow cytometry is able to identify fluorophores with emission spectra relatively close to each other. Besides, multi-parameter measurements can be obtained concurrently. Additionally, it is able to analyze a huge number of particles in a very short time, however, the generated data will be difficult to be analyzed. Examples of the applications of flow cytometry are transgenic product (GFP), cell viability, cell pigments, DNA and RNA content, chromosome analysis (Castano and Comas, 2012).

2.5.2 Fluorescence microscopy

Fluorescent microscopy is widely applied in the biological sciences due to its magnificent specificity to visualize certain bio-molecule and its ability to study the three-dimensional interior of cells and organisms through fluorescent labeling (Li *et al.*, 2009). The fluorescent microscopy is consists of excitation light source, objective lens,detector, dichroic mirror, emission filter and excitation filter. The fluorescence microscope starts with illuminating the light to let the chromophore absorb the light and cause them to emit low energy light. Then, the microscope has a filter which allows the certain wavelength radiation pass through that matches the fluorescing sample. The radiation will react with the atoms of the specimen and excited the electrons to a higher energy level. They will emit energy when they are in lower level power. The fluorescence that laminated from the sample is separated

from the much brighter excitation light in a second filter, so that it is visible to the human eye. In terms of detecting GFP, the fluorescent microscopic examination is characterized by higher sensitivity. Besides, the spectrofluorometric analysis of cellular lysates reduce screening time to optimize the complementation assay based on reassembly of GFP in order to maximize the percentage of cells showing GFP fragment reassembly (Torrado *et al.*, 2008). The advantage of using fluorescence microscope is that it is able to observe the specific cellular components via molecule-specific labeling and also structures inside a live sample in real time. However, the wavelength of light had limited fundamentally its moderate spatial resolution (Gustafsson *et al.*, 2008). This fluorescence microscope are normally used for the imaging the structural components of organisms like cells, genetic material like DNA and RNA as well as study on the cell populations (Bradbury and Evennett, 1996).

2.5.3 Spectrofluorometer

Spectrofluorometer is used for analysis of fluorescence spectra of liquids, surfaces and glasses (Lakowicz, 2006). The spectrofluorometer consists of a light source (xenon lamp), a sample holder, an excitation monochromator, an emission monochromator and a photo detector (PMT, CCD detector and photodiode) (Lakowicz, 2006).Based on Figure 2-2, a reference sample such as rhodamine is set and it is used to correct for lamp output in order to verify the excitation wavelength as well as correct for difference in detector sensitivity. A high intensity light sources from xenon lamp is then used to cause the maximum molecules inside the sample to become excited state at any one point in time. The light is either passed through an excitation filter or monochromator that enables to select a wavelength of interest to use as the exciting light. The exciting light will pass through the samples and is

collected at **90** ° to the exciting light. The emission is finally passed through an emission monochromator to the detector. The signal which can be analog or digital is detected by the computer system (Lakowicz, 2006). The advantage of using spectroflurometer is verification of the wavelength selection is allowed; a sample of different range of wavelength can be scanned (Lakowicz, 2006). As for the disadvantages, they are expensive and can only give specificity and sensitivity in comparison (Lakowicz, 2006). Besides that, this device needs huge amount of samples to be detected and it is hard to distinguish denatured proteins from its native form (Chew *et al.*,2011; Lakowicz, 1999) .

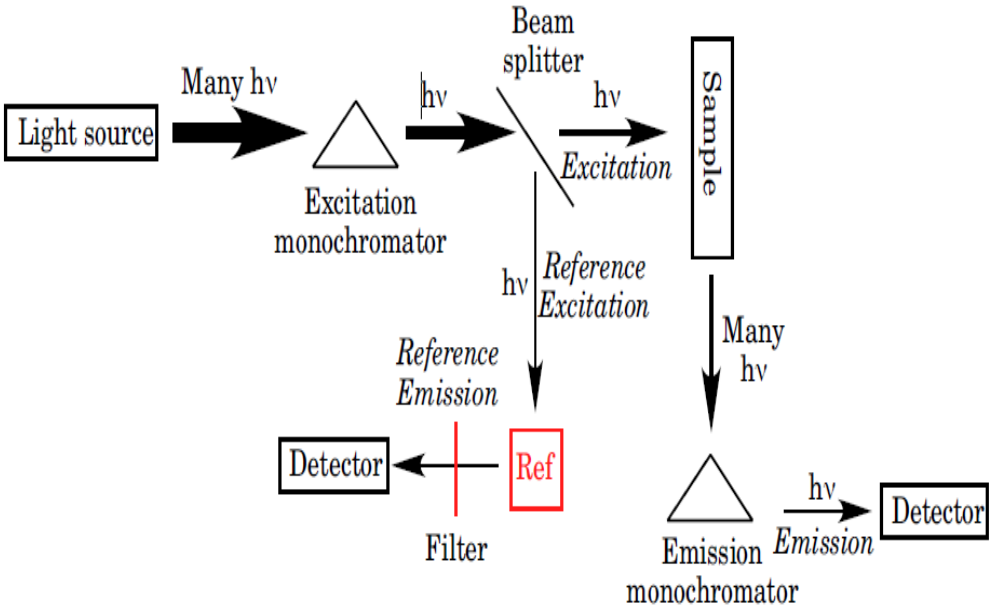

Figure 2-2: The components of spectrofluorometer [Adapted from Lakowicz (2006)]

2.5.4 Gel-based imaging system

The gel-based imaging system is widely used in the molecular biology, medicine and cell biology. The gel-based imaging system consists of a gel electrophoresis system and a gel documentation imaging system. But technically, the components that are required to carry out this method are an electrophoresis system, a

polyacrylamide gel, and a gel documentation imaging system. During the electrophoresis process, the polyacrylamide gel acts as a molecular sieve and is used to separate the molecules in the mixture for GFP quantitation (Chew *et al.,* 2009a). The gel documentation imaging system is used to measure the intensity of GFP fluorescent band on the gel. The principle of gel-based imaging system is basically using electrophoresis in which the charged molecule will move in an electric field towards opposite sign electrode (Descalzo *et al.,* 2012). The charged molecules in this research are the GFP with isoelectric point lower than the buffer pH and thus it is able to migrate through the polyacrylamide gel when subjected to an electric field. The polyacrylamide gel is consisted of two gels which are stacking gel and resolving gel. The stacking gel has lower acrylamide percentage (larger pore) and has a lower pH compared with the resolving gel. When the gel is connected to a constant electric current, the charged protein molecules will be squeezed down toward the anode. At the same time, the glycine from electrophoresis buffer will enter the stacking gel. The glycine will become a zwitterion and moves slowly. The protein encounter resolving gel, due to the smaller pore size of resolving gel, this cause the protein slow down and allow the following protein to stack. For glycine that reaches the resolving gel will become anionic and moves faster than protein due to higher charge to mass ratio. The proteins now becomes the sole carrier of current and are separated based on their molecular mass. The advantage of using this gel-based imaging system is that it is able to identify the denatured protein sample from its native form and it only require microgram samples to be detected (Chew *et al.,* 2009a). As for disadvantage, the prolonged ultraviolet irradiation may affect the accuracy and reproducibility of this method and it is hard to automate the gel-based technique (Tonge *et al.,* 2001; Lilley *et al.,* 2002).

2.6 Summary of the quantitation methods

Quantitation Method	Type	Principle	Limitation	Reference
Flow cytometry	Solution	suspended within a stream of liquid are interrogated in a very short time when they go through a light source focused at small region.	may create great amounts of data and this will cause the analyses complicated.	(Jahan-Tigh *et al.*, 2012; Robinson, 2004)
Spectroflurometer	Solution	generates the wavelength of light required to excite the analyte of interest; it selectively transmits the wavelength of light emitted, then it measures the intensity of the emitted light.	Need huge amount of samples to be detected. Hard to distinguish denatured proteins from its native form. can only give specificity and sensitivity in comparison	(Li *et al*., 2009; Gustafsson *et al.*, 2008)
Fluorecent microscopy	Imaging	used in molecular cell due to its high specific image and magnificent ability to study the three-dimensional interior of cells .	wavelength of light had limited fundamentally its moderate spatial resolution.	(Chew *et al.*, 2011a; Lakowicz, 2011)

Gel-based imaging system	Imaging	Using native polyacrylamide gel which contains the GFP protein for the quantitation and is detected by using bio-imaging system.	Difficulties in automation of the gel-based technique. Poor reproducibility due to the effect of UV irradiation.	(Chew *et al.,* 2011a; Tonge *et al.,* 2001; Lilley *et al.,* 2002)

2.7 Parameters influencing the fluorescent intensity

2.7.1 Effect of the irradiation period of ultraviolet

The UV irradiation shows its effect when it exposes on the GFP. Based on research by Patterson (2007), the fluorescence level decreased rapidly when EGFP is prolonged irradiated under the higher power of UV light. Figure 2-3 indicates that the fluorescence intensity decreased when a longer irradiation time was applied. Restricting the UV exposure period on chromophore may reduce the photobleaching effect. Photobleaching is basically caused by the irreversible damage of chromophore because of the prolonged exposure of UV light or high-intensity excitation light (Diaspro *et al.,* 2006).Based on research done by Patterson et al. (1997), the EGFP, wtGFP two-photon excitation (TPE), EBFP,TPE and fluorescein at 488 nm irradiation showed typical multiexponential photobleaching decay while the wtGFP at 488 nm showed an initial increase in fluorescence followed by a rapid decrease when those GFP variants were exposed continuously to UV irradiation. The initial increase in fluorescence seen in wtGFP is due to the photoconversion or photoisomerisation (Figure 2-4). Figure 2-5 shows the photoconversion of the wtGFP between the 475 nm and 397 nm absorption peaks by 488 nm irradiation

(Patterson *et al.,* 1997). Prolonged UV exposure period on the different type fluorescein protein may have different effect on the fluorescence intensity such as photoconversion and photobleaching. This shows obviously the intensity of the fluorescence image is affected by the intensity of excitation light. In other words, the photobleaching and photoconversion (fluorescence intensity) is directly caused by the irradiation of the UV light (excitation light). Hence, the effect of the irradiation period of UV on the GFP fluorescent intensity is investigated in order to improve the reliability of gel-based imaging system for GFP quantitation.

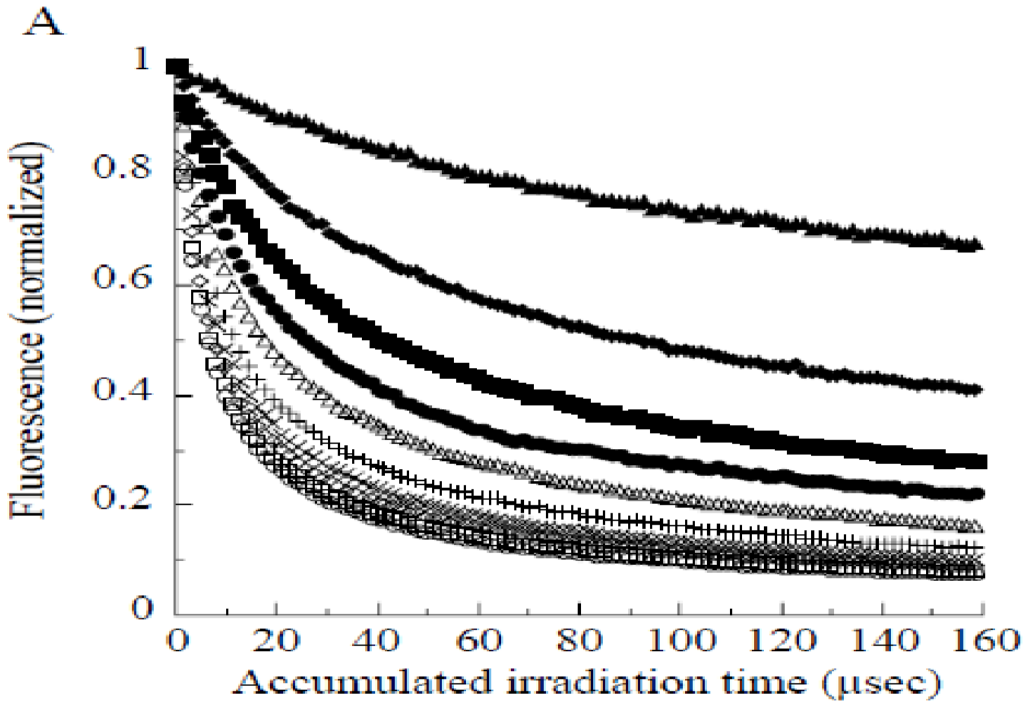

Figure 2-3: Effect of irradiation period on the fluorescence intensity [Adapted from Patterson (2007)]

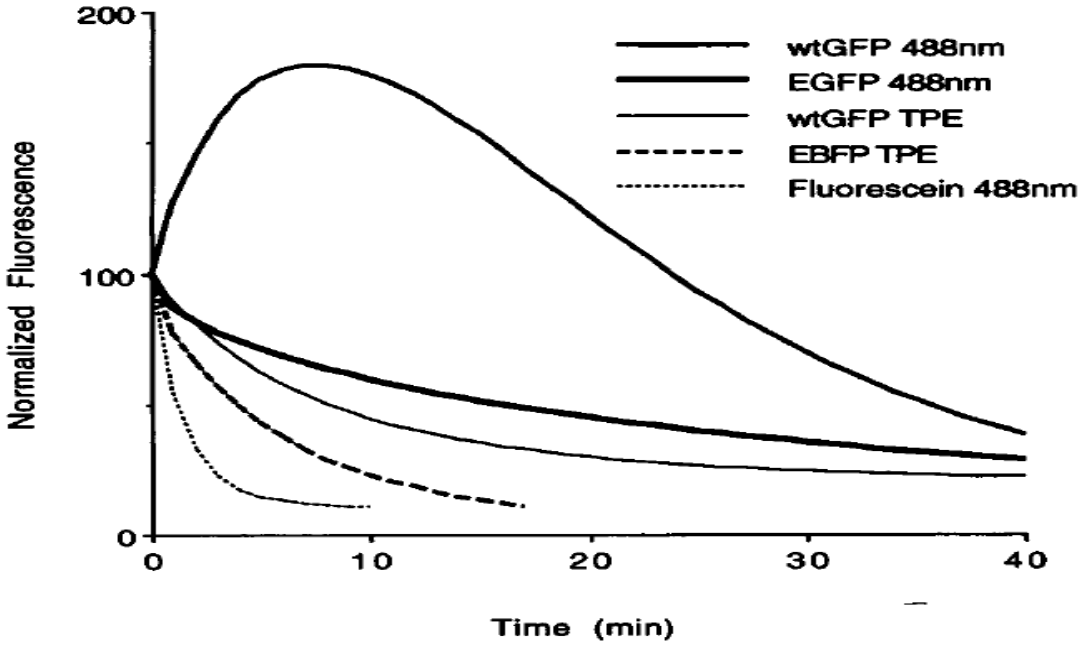

Figure 2-4: Time-resolved fluorescence changes during irradiation [Adapted from Patterson *et al*. (1997)]

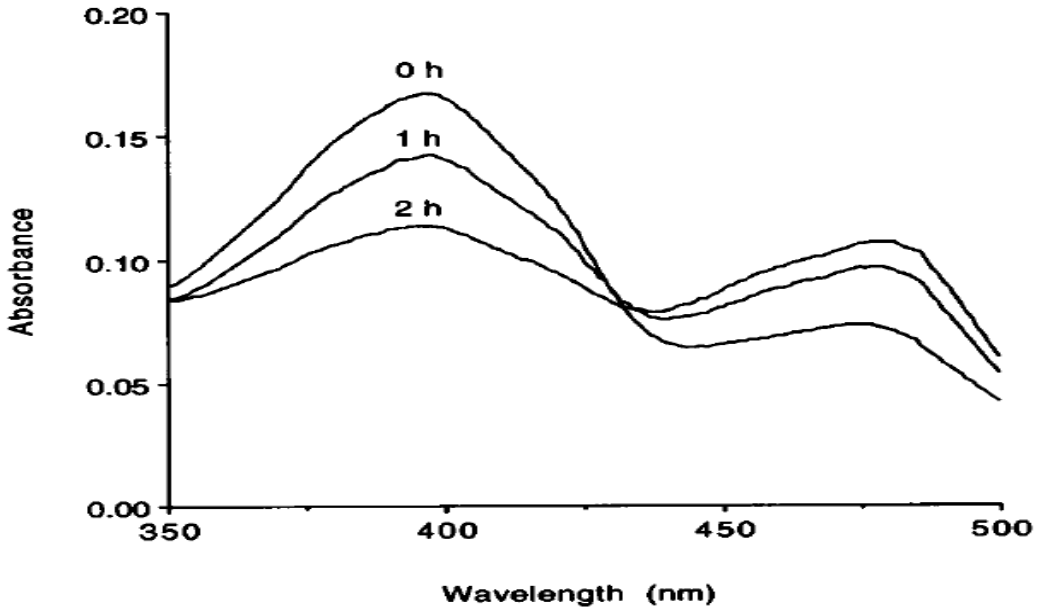

Figure 2-5: Photoconversion between the 475 nm and 397 nm absorption peaks by 488 nm irradiation [Adapted from Patterson *et al*. (1997)]

2.7.2 Effect of the fluorescent protein concentration

Indeed, the fluorescence intensity increases when the concentration of the fluorophore increases. However, Hamann *et al.* (2002) reported that high concentration of the flurophores causes particular fluorophores undergo self-quenching and finally reduced the fluorescence intensity. Fluorescence intensity of a sample is reduced during the quenching process (Lakowicz, 2006). This phenomenon can be caused by a variety of molecular interactions which includes molecular rearrangements, energy transfer, excited-state reactions, ground-state complex formation, and collision quenching. When the fluorophore is collisional encountered with the quencher, collision quenching is occurred in which the excited fluorophore experiences non-radiative transitions to the ground state (Lakowicz, 2006) (Figure 2-6). The common example of those quenchers includes O_2, I-, Cs^+ and acrylamide. Hamann *et al.* (2002) have reported that the fluorescent intensity was increased as the concentration of calcein (a type of chromophore) increased from 0 to 4 mM (Figure 2-7). However, the fluorescent intensity decreased when the concentration of calcein was increased further. Acrylamide is one of the listed quencher, and this might resulted in collision quenching when the chromophore in GFP is in contact with acrylamide. Hence, under the different UV exposure period, the effect of EGFP concentration on the fluorescent intensity was investigated for better GFP quantitation performance.

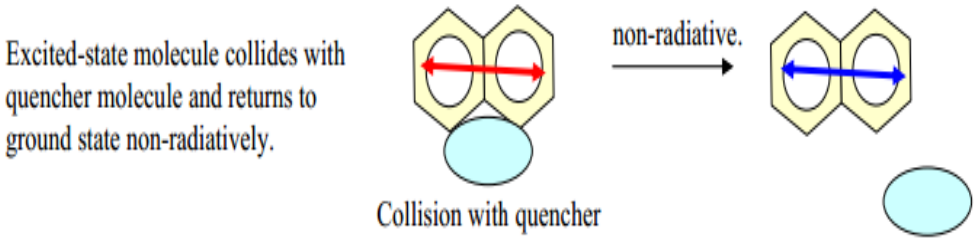

Figure 2-6: The process of collision quenching [Adapted from Lakowicz (2006)]

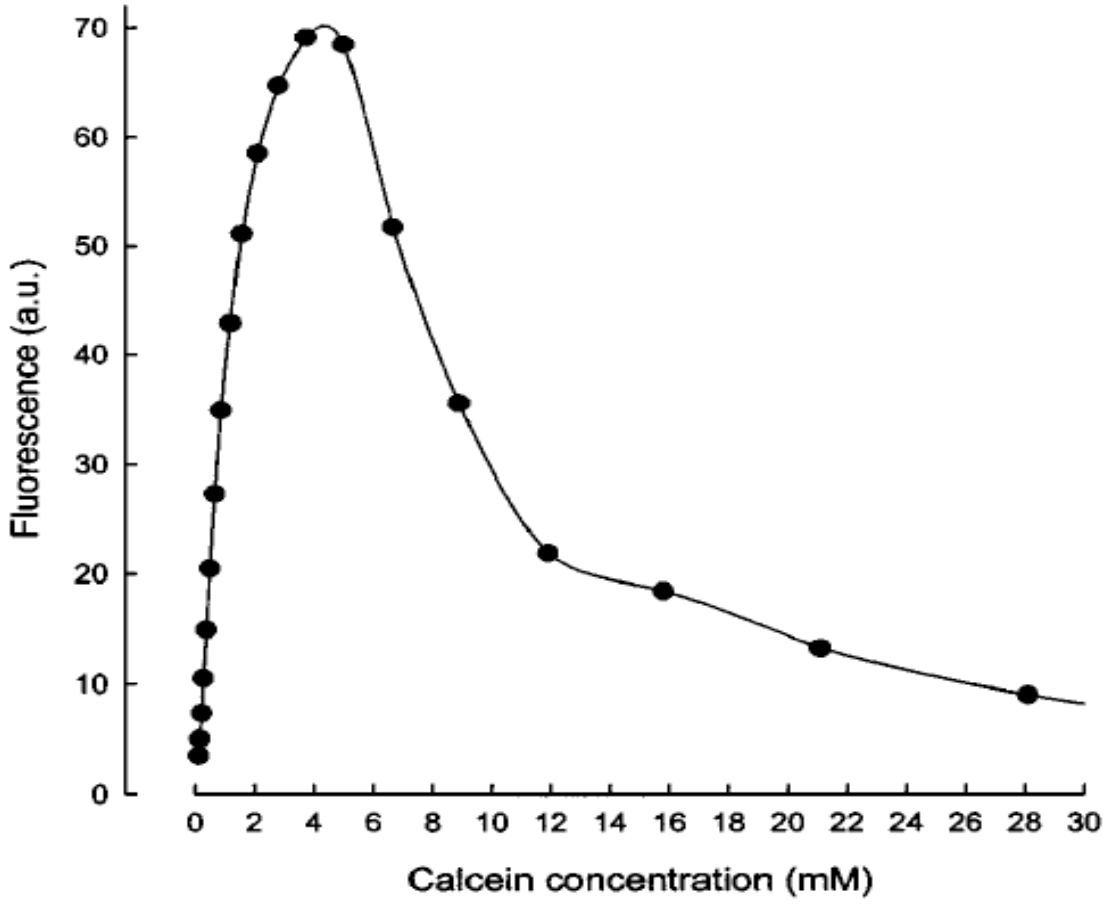

Figure 2-7: The effect of the concentration on the fluorescence [Adapted from Hamann *et al.* (2002)]

3 MATERIALS AND METHODS

3.1 Chemicals

Chemicals	*Company*	*Process*
LB broth	Lennox	Fermentation
LB agar	Lennox	
Ampicilin	Cole-Parmer	
Isopropyl B-D-Thiogalactopyranoside(IPTG)	Thermo-Scientific	
Disodium phosphate	Biobasic Canda INC	Purification
Monosodium phosphate	Biobasic Canda INC	
Sodium Chloride	Merck	
Imidazole	Merck	
Sodium carbonate	Fisher Scientific	Quantition(Lowry's method)
Sodium hydroxide	Fisher Scientific	
Sodium citrate	Sigma-Aldrich	
Copper (II)sulphate	Fisher Scientific	
Folin&Ciocalteu's phenol reagent	Sigma-Aldrich	
Bovine serum albumin (BSA)	Fisher Scientific	
Potassium sodium tatratetetrahydrate	Sigma-Aldrich	
Tris base	Cole-Parmer	Quantitation (Gel-imaging method)
Hydrochloric acid	OXONE	
Acrylamide	Merck	
Glycine	Biobasic Canda INC	
2-methyl-q-propanol(isobutanol)	Fisher Scientific	
Ammonium persulfate	Biobasic Canda INC	
Tetramethylethylenediamine(Temed)	Biobasic Canda INC	

3.2 Summary of methodology

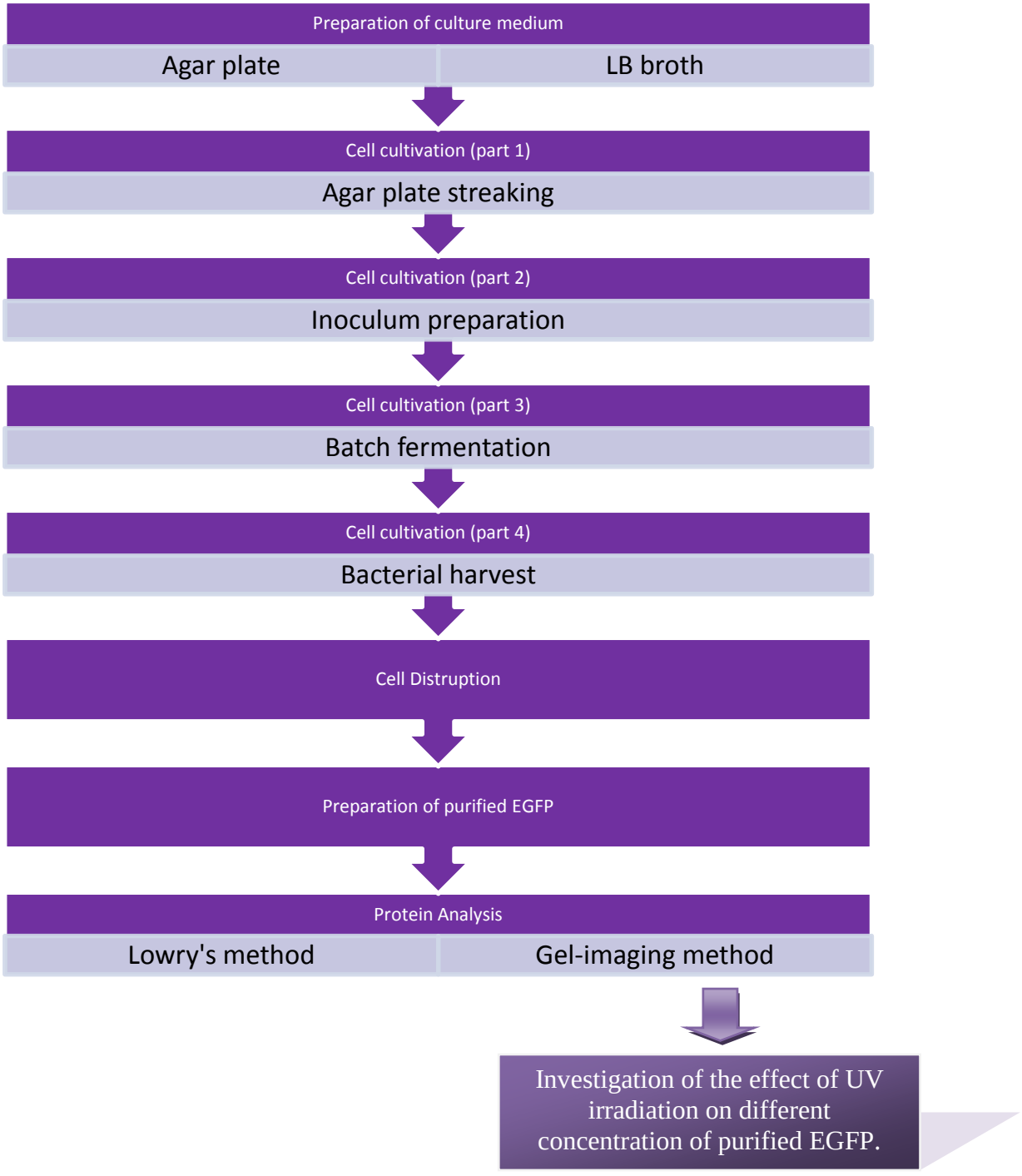

3.3 Methodology

3.3.1 Preparation of culture medium

3.3.1.1 Agar plate

3.5 g of Luria Bertani (LB) agar broth powder was weighed and poured inside the beaker. The powder was dissolved and top up to 100 mL with distilled water. The LB agar broth was poured into a bottle and autoclaved. 15-20 mL of sterilized nutrient agar per petri plate was poured inside the laminar flow hood near the flame and let it cool until warm to obtain nutrient agar plate. 0.10 mL of ampicilin (final concentration at 100 µg/mL) was added before pouring into the plate. The cover was closed and sealed it with parafilm after solidify and the agar plate was kept in 4℃ chiller until use.

3.3.1.2 Luria Bertani broth

1g of nutrient broth powder was weighed and added into the beaker. The powder was dissolved and then top up the mixture to final volume of 50 mL with distilled water. The broth powder was dissolved by stirring using a hot plate stirrer. For the cultivation, ratio of LB broth to the flask volume was remained at 0.2. The pH of the nutrient broth was adjusted to pH 7.0 by using 0.1 mol of hydrochloric acid or sodium hydroxide. The mouth of flask with cotton wool was covered in a cotton dressing and aluminum foil. The broth was sterilized at 121 ℃ for 20 min.

3.3.2 Preparation of culture medium

3.3.2.1 Agar plate streaking

Inoculation loop was flamed to redness to be sterilized and let it cool. A single loop of one broth culture was obtained aseptically from a glycerol stock containing the *Escherichia coli (E. coli)* strain BL21 (DE3) carrying the pRSETEGFP plasmid encoding the EGFP. Four sections of streaks were aseptically done onto the surface of agar inside a laminar hood. The petri dish was sealed with a parafilm and

incubated inside an incubator (Memmert, Loading Modell 100-800) at 37 ℃ for 18 h.

3.3.2.2 Innoculum preparation

After 18 h cultivation, single *E. coli* colony was obtained aseptically from the petri dish by using an inoculation needle into a sterilized 250 mL Erlenmeyer flask containing 50 mL autoclaved LB broth and 0.05 mL of ampicilin (final concentration at 100 μg/mL) . The Erlenmeyer flask was incubated for 18 h at 30 ℃ and 200 rpm in an incubator shaker (Stuart, S1500).

3.3.2.3 Batch fermentation

Batch fermentation method was extracted from Chew *et al.* (2009b).1000 mL Erlenmeyer flasks containing 200 mL of autoclaved LB broth and 100 μg/mL of ampicillin were prepared. 5% v/v of inoculum was aseptically transferred into the Erlenmeyer flask. The culture was grown to an optical density (OD_{600}) of 0.8-1.0 by shaking at 30 ℃ and 200 rpm (Stuart, S1500). IPTG at final concentration of 0.5 mM was added to induce the expression of the recombinant EGFP for another 16 h.

3.3.2.4 Bacteria harvest

After 16h, *E coli* cell which containing EGFP was harvested by centrifugation (5000 xg, 30 min and 4 ℃) (Eppendorf, centrifuge 5810R). Sample buffer (20 mM sodium phosphate, 0.5 M sodium chloride, pH 7.4) was then added to wash the cell pellet followed by centrifugation at the same conditions. Cell pellet was re-suspended in sample buffer and 15 % (v/v) biomass suspension was prepared. The process followed by keeping the biomass suspension in a freezer (-80 ℃) for bacterial lysis process.

3.3.2.5 Cell disruption

The biomass suspension was removed from the freezer (15 min) and thaw by hand warmth (10 min). Thaw lysis was carried out for 3 cycles. Cell debris was removed by centrifugation (5000 x g, 10 min, 4℃) and the supernatant was filtered through 0.45µm filter prior to purification process.

3.3.3 Preparation of purified EGFP

3.3.3.1 Purification of EGFP

The clarified lysate was purified using HisTrap™ Fast Flow 1 mL column (GE Healthcare, Sweden) pre-packed with pre-charged Nickel Sepharose™ 6 Fast Flow. The syringe was filled with distilled water. The stopper was removed and the column was connected to the syringe 'drop to drop' to avoid introducing air bubbles into the system. The snap-off end was removed at the column outlet. The column was washed with 5 mL of distilled water. The column was equilibrated with at least 5 mL of binding buffer (20 mM sodium phosphate, 0.5 M sodium chloride and 20 mM imidazole, pH 7.4). 1 mL/min was applied for the 1 mL columns. The clarified lysate was loaded using a syringe. The protein sample was washed with 20 mL binding buffer to remove unwanted proteins. After the washing step, the purified EGFP was eluted from the column using 5 mL elution buffer (20 mM sodium phosphate, 0.5 m sodium chloride and 500 mM imidazole, pH 7.4)

3.3.3.2 Histrap desalting

The desalting column was equilibrated with 25 mL sample buffer at 5ml/min to remove ethanol storage. Then, 1.5 mL of purified EGFP was loaded with 10 mL sample buffer. Purified EGFP sample was collected when it was eluted from the column.

3.3.4 Analytical Procedure

3.3.4.1 Lowry's method

Purified EGFP eluted from HisTrap desalting column was diluted to several dilutions using sample buffer. The concentration of each diluted protein was determined using Lowry's method. A series of concentration BSA stock solution (200, 500, 1000, 1500, and 2000 μg/mL) were prepared. 1mL of Lowry reagent (Table 3-1) was added into 0.2 mL of each BSA concentration and mixed well and leaved it in dark place. After 10 min, 0.1 mL of 1.0 N Folin & Ciocalteu reagent was added, mixed well and leaved at room temperature. After 30 min, the optical density (OD) of the mixture was measured at 750 nm against blank (replace the 0.2 mL of BSA with 0.2 mL distilled water) by using spectrophotometer (Hitachi, U-1800). The standard calibration curve was plotted (OD versus concentration) for each BSA concentration. The concentration of EGFP dilution samples were determined by replacing the 0.2 mL BSA sample with 0.2 mL of protein sample and the procedure was repeated as mentioned. Duplicate independent experiments with duplicate measurements were implemented.

Table 3-1: Reagents for Lowry's method

Reagent	Preparation procedure	Notes
A	Dissolve 5g of sodium carbonate and 1 g of sodium, hydroxide in 250 mL distilled water.	Keep refrigerated (4 ℃)
B	Dissolve 1.25g of copper sulphate ($CuSO_4.5H_2O$) and 2.5 g of sodium citrate in 500 mL distilled water.	Wrap the bottle with aluminium foil to avoid discolorization and keep refrigerated (4 ℃).

Lowry solution	Mix reagent A and B in a 50:1 ratio.	Freshly prepared and keep refrigerated (4 ℃).
Folin-Ciocalteu reagent (stock 2.0 N)	Dilute the stock with distilled water in 1:1 ratio.	Freshly prepared.

3.3.4.2 Gel-based imaging method

The intensities of EGFP dilution samples were quantified using gel imaging method (Chew *et al.,* 2009a). Polyacrylamide gel using 15 and 4% (w/v) acrylamide as resolving and stacking gels respectively were prepared. The gel formulation was depicted in Table 3-2. For the preparation of resolving gel, 4x native lower buffer, distilled water, acrylamide mix, APS and TEMED were added accordingly inside a beaker and mixed it fast. The solution was loaded into the gap of the gel plate. 400 mL of isobutanol was layered above the gel solution to make the gel form a uniform flat surface and wait for 40 min for polymerization. After polymerization, the resolving gel overlay was washed with distilled water to remove the isobutanol. Stacking gel solution was mixed and loaded on top of the resolving gel. A comb was placed in the stacking gel mixture and wait for 30 min at room temperature. After the stacking gel had polymerized, the comb was taken out .The wells were cleaned with electrode buffer (0.025 M Tris and 0.192 M glycine) and the cathode and anode reservoirs were filled with the electrode buffer. A series of EGFP dilution samples mixed with equal volume of 2x native sample buffer [125 mM Tris hydrochloride (pH 6.8), 20% (w/v) glycerol and 0.01% (w/v) bromophenol blue] were loaded into the well. The electrophoresis apparatus was connected to the power supply at a constant current of 15 mA. The gel was electrophoresis for 2 hours.

After electrophoresis, the gel was carefully taken out from gel plates and viewed and captured under different UV exposure time (5, 35, 95, 185, 305, 455, 635, 845, 1085 and 1355 sec) using a gel documentation system (Alpha Ease@ FluroChem). Before viewing, the position of the gel was placed in the same position by using a standard. The EGFP fluorescent intensity on the gel was analysed using AlphaEaseFC software. The imaging system was set by following the conditions such as aparture: 8.00; zoom: 70.00; focus: 1.90 ; UV lamp wavelength:302 nm ; exposure time: 2 sec ; translumination: UV ; filter type : Fluorescein.

Table 3-2: Composition of resolving gel and stacking gel

Chemicals	Resolving gel (15%) composition (µL)	stacking gel (4%) composition(µL)
4x native lower buffer (4 ℃) [(1.5M Tris hydrochloride(pH 8.8)]	2350	-
4x native upper buffer (4 ℃) [(0.5M Tris hydrochloride(pH 6.8)]	-	937.50
Distilled water	3517.50	2437.50
Acrylamide mix [40% (w/v) acrylamide and 0.8% (w/v) bisacrylamide]	3520.50	375.0
10%(w/v) ammonium persulfate (APS)	58.75	25.05
tetramethylethylenediamine (TEMED)	9.50	5.25

4 RESULTS AND DISCUSSION

4.1 Effect of exposure time of UV light on the different concentration of EGFP fluorescence

The 1x dilution of concentration was determined by Lowry's method and divided by 200 µ/L and the rest concentration was mixed by calculation (Figure 4-1). The signal to noise (SNR) based on the fluorescence over background was calculated from 4 experimental results (Table 4-1).

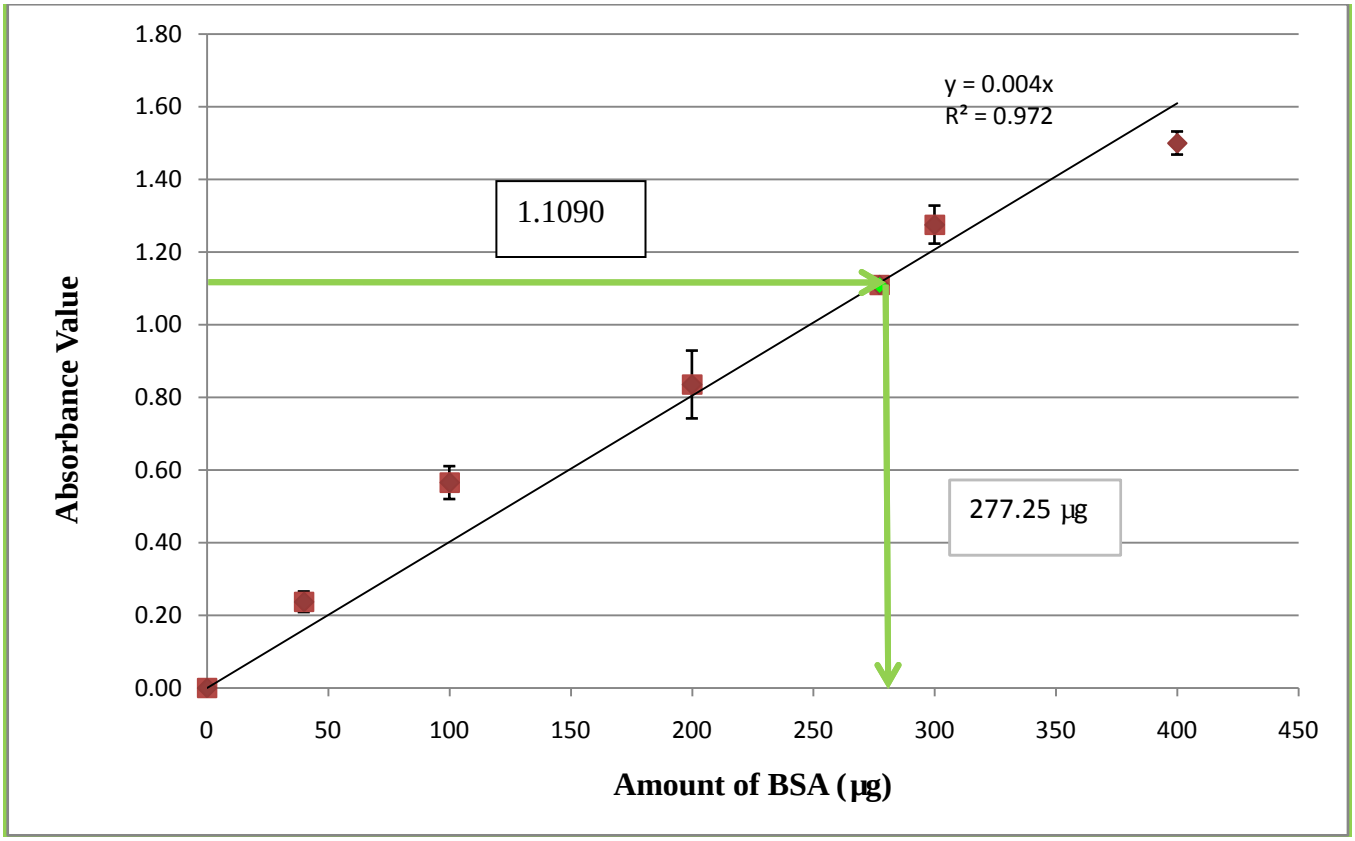

Figure 4-1: The amount of EGFP is calculated based on Lowry's method

For the UV exposure time ranging from 0-35 s, the fluorescence of different concentration of EGFP (from 0.87 µg/µL to 1.386 µg/µL) was increased (see Figure 4-2), A further increase in the UV exposure time resulted in a decrease of EGFP

fluorescence. However, EGFP concentration with 8x dilution rate just showed a decreasing trend for exposure time of 0-1355 s. The deviation of trend might be due to the low values of signal to noise ratios (SNR). For an object that can be detected as an image, the contrast of the object (signal) must be higher than its surrounding image noise (Smith, 1999). According to ICH Harmonised Tripartite Guidline (1994), the acceptable value for the detection limit based on SNR is at least 2:1. The exact value for minimum detectable SNR depends on the size of the object; the larger the object, the easier to be detected (Smith, 1999). Hence, results for EGFP concentration with 1x - 6x dilution rate are more reliable if compared with the 8x dilution rate of EGFP concentration (Table 4-1).

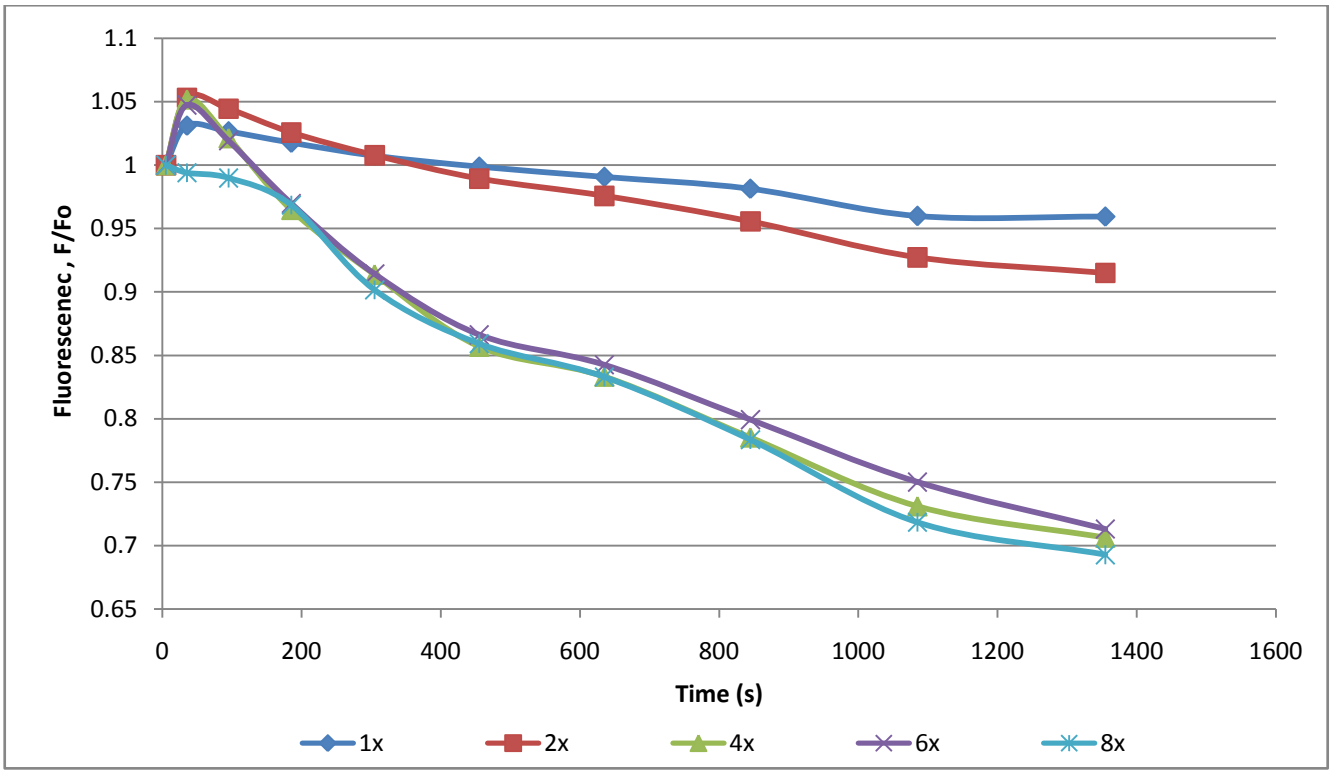

Figure 4-2: The EGFP relative fluorescence as function of time for different EGFP concentration

Table 4-1: The dilution rate of EGFP and signal to noise ratio (SNR) for different concentration of EGFP and amount of EGFP.

Amount of EGFP (μg)	**Concentration of EGFP (μg/μL) (5 μL)**	**Dilution rate**	**SNR (Range)**
6.93	1.386	1x	3.6-4.8
3.47	0.694	2x	3.1-3.7
1.73	0.346	4x	2.2-2.4
1.16	0.232	6x	1.8-1.9 (<2.0)
0.87	0.174	8x	1.5-1.6 (<2.0)

EGFP fluorescence increased at the beginning of UV irradiation (0-35s), this might be due to photoisomerisation of the EGFP. Photo-isomerisation is a process in which structural change between isomers caused by photoexcitation. Figure 4.3 shows the mechanism for the GFP photoisomerisation in which involve of proton transfer processes. The three-proton relay involves green chromophore, Ser205, Glu222 and water W22 in which residues are connected with arrow symbols (Figure 4-3) (Zhang *et al.*, 2010). There is no proton transfer on the excited state at 475 nm, and the emission of 503 nm is from the B* to B state of GFP. The I state is electronically similar to B state (anionic state chromophore), but environmentally very similar to A state. Normally, the proton transfer finally reverses back to the ground state during the light absorption (395 nm or 490 nm) or emission (580 nm) cycles. However, instead of reversing back to the gound state, the neutral chromophore is photo-isomerized to the anionic form and this involves a slower structural relaxation like the rotation of the

Thr203 side chain and the stabilization of the phenolate oxyanions. Irradiation of 395-nm or 490-nm light can induce the photoisomerisation of the wild type GFP (wtGFP) (Sullivan and Kay, 1999). Since the overall structure of wtGFP is extremely close to EGFP, it is logical that EGFP will also undergo photoisomerisation but at different wavelength. The UV wavelength used in this experiment is 302 nm and this may cause photoisomerisation of EGFP when it was irradiated by 302 nm UV light although the EGFP excitation wavelength is at 488 nm. During the photoisomerisation, the fluorescence intensity will be increased as shown exactly in the Figure 4-2 (Sullivan and Kay, 1999).

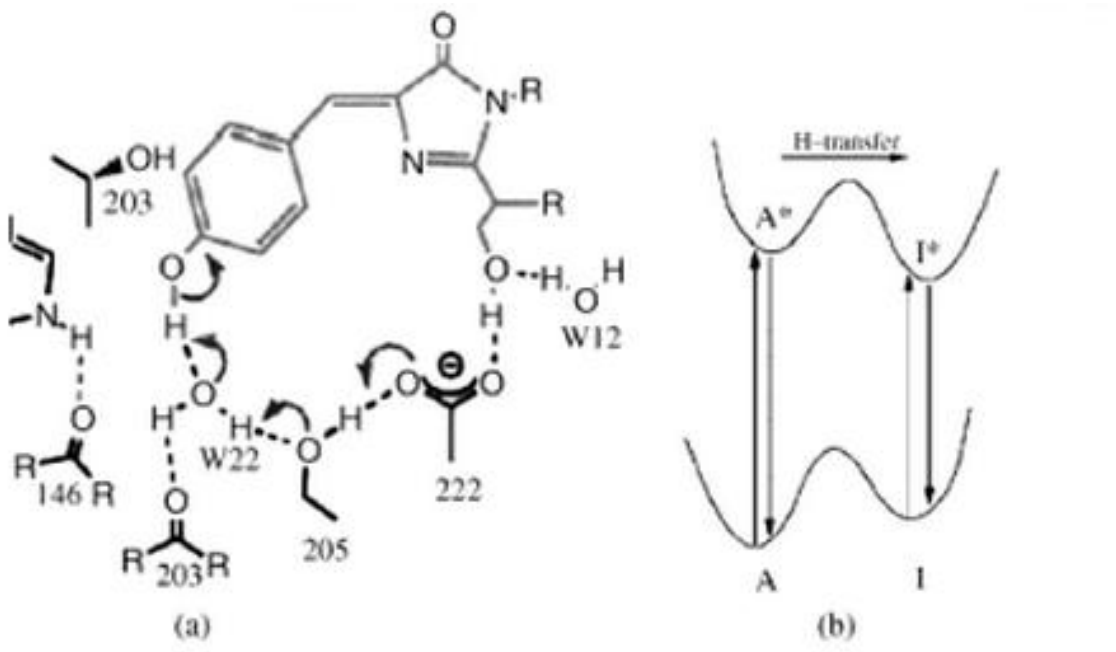

Figure 4-3: The photo-isomerisation mechanism [Adapted from Zhang *et al.* (2010)]

The data in Figure 4-2 indicate the highest EGFP fluorescence intensity is around 35 s of UV radiation time. Beyond this time, the fluorescence of EGFP decreased dramatically. GFP gene from bioluminescent jellyfish causes protein to fluoresce under radiation of UV light. However, proteins and genes are sensitive to the UV light (Neves-Petersen *et al.*, 2012). Long UV irradiation period can cause photodamage in GFP which resulted photobleaching (Sullivan and Kay, 1999). UV can be classified into

3 catagories, which are UVA (315-400 nm), UVB (280-315 nm), and UVC (200-280 nm) (Masumaa *et al.*, 2013). Protein and DNA absorb UV at maximal wavelength of 280 nm and 260 nm respectively (Masumaa *et al.*, 2013). The tyrosine (Tyr) which is in the chromophore of GFP is one of the amino acid residues that its side chains absorb UV light in the UV range (UVB, 280-315 nm) (Neves-Petersen *et al.*, 2012). UVA is absorbed by chromophore for the formation of reactive oxygen species like singlet and triplet reaction which will further damage the DNA in the chromophore (IARC, 2005). Besides that, UVB is also absorbed by the chromophore for the formation of the singlet oxygen species (IARC, 2005). UVB is the most energetic UV type (Masumaa *et al.*, 2013). The singlet oxygen species is an oxidative compound which is highly reactive and it can induce DNA damage indirectly. In this research, the UV wavelength used is 302 nm which is under category of UVB and this shows its destructive effect on the fluorescence intensity of EGFP.

The light-emitting ability of the fluorophore will be lost over few times of absorption and emission circles. Figure 4-4 shows that long period of UV irradiation will cause the fluorophore undergo many absorption and emission circles and resulted in loses of the EGFP fluorescent intensity. When the fluorophore molecule absorbed photon energy, there are few number of routes so that it can return to the ground state. The fluorophore molecule is exposed to UV light (a type of photon radiation), it will absorb the photon energy so that becoming excited and jump from electronic ground state (S_0) to higher energy state (S_2). The later internal conversion system will cause the energy inside the molecule to pass down to lower energy level (S_1) and emit light to fluorescence and this process is called as singlet state. There is a reaction that is linked between singlet state and triplet state which is intersystem crossing. During the intersystem crossing, the higher energy level of triplet state (T_2) and undergo internal conversion to T_1 and further

releases phosphorescence. During this whole process which includes adsorption and emission will keep repeating when the UV exposure period increases and this will lead to photobleaching. During photobleaching, modification of fluorophore may be happened due to chemical reaction with oxygen. Fluorphore may return to the ground state as a new molecule that no longer absorbs light at the excitation wavelength (Xiao, 2009).

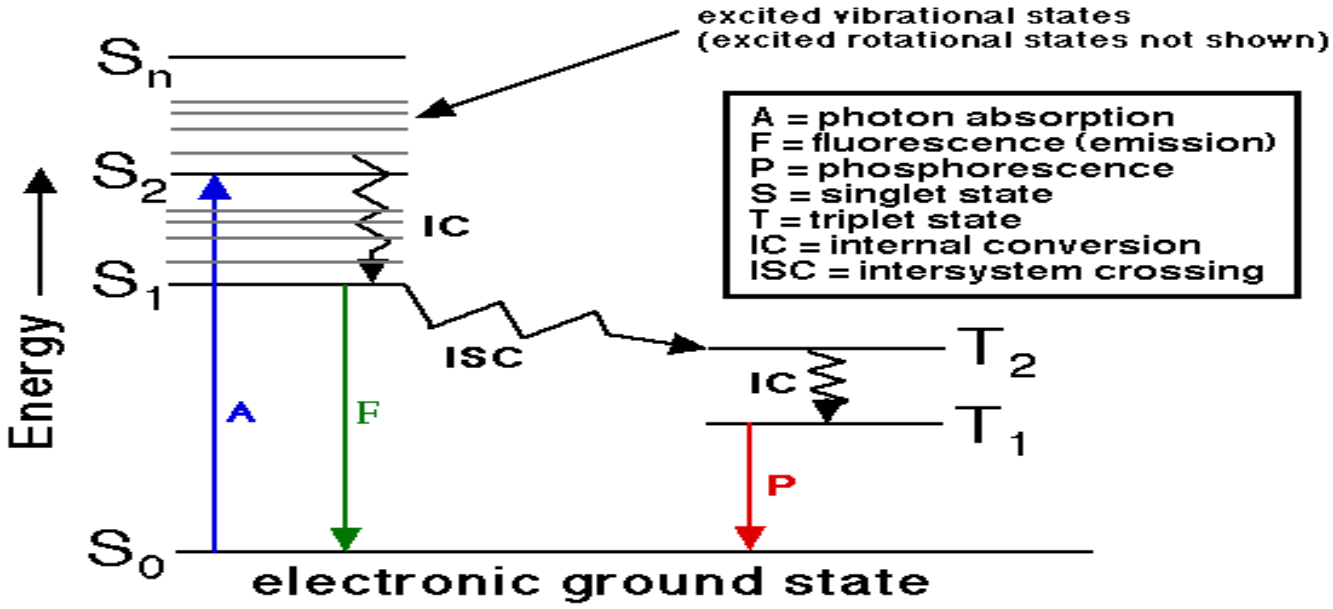

Figure 4-4: Jablonski diagram [Adapted from www.chemicool.com]

The formation of oxygen is occurred during the UV irradiation on EGFP (Jiménez-Banzo *et al.*, 2008). Hence, it can be assumed that the longer UV irradiation period, the more oxygen is produced. Oxygen is required for the oxidation process of fluorophore molecule formation. However, oxygen is one of the fluorescence quenching elements. Besides, histidine tagged with the EGFP could highly react with oxygen and hence reduced the fluorescence of EGFP (Ma *et al.*, 2006). Based on Kasche and Lindqvist (1963), the reaction of the triplet state of fluorescein and oxygen is related to photobleaching. In principle, photobleaching occurs when oxygen is reacted with singlet excited state or triplet state dye molecule (such as fluorescein) (Song *et*

al.,1995). Lindqvist (1960) demonstrated that the triplet excited state fluorescein molecules became depopulated via two major pathways: dye to dye (D-D) and dye to oxygen (D-O) mechanisms. D-D mechanism is the reaction between a triplet and another triplet or a ground state dye molecule while D-O mechanism is the reaction between a triplet dye molecule and an oxygen molecule (Song *et al.*,1995). The reaction between a dye molecule (eg: fluorecein) and an oxygen molecule can lead to irreversible photobleaching (Song *et al.*,1995). Hence, D-O mechanism is not only main cause of the photobleaching and it is also involved D-D mechanism (Song *et al.*,1995). Besides, in the absence of all D-D reactions, the D-O mechanism bleached the dye molecule due to the concentration of fluorescein is lower than oxygen (Song *et al.*,1995). The mechanism of the photobleaching described above can be used to apply on EGFP because both EGFP and fluorescein undergo same mechanism of photobleaching (Day and Davidson, 2014 ; kalies *et al.*, 2011).

The effect of EGFP concentration on the photobleaching rate is presented in Figure 4-5. Photobleaching rate was increased as the concentration of EGFP increased from 0.174 μg/μL and 1.386 μg/μL. However the photobleachng rate decreased when the EGFP concentration was increased further. The photobleaching rate is within the range of 3712 int/s and 8213 int/s. Ma *et al.* (2006) have reported that a lower Quantum Dots (QD) concentration increases photobleaching rate. QD is a nanocrystal made of semiconductior material that able to emit light as EGFP. It was reported that QD experienced photobleaching due to photooxidation of cellular QDs (Ma *et al.*, 2006). Hence, it is logical to relate QD's photobleaching rate with GFP. In our research, the reason that it does not continue show the increasing trend in photobleaching rate in 6x and 8x dilution EGFP concentration is because of both of the SNR is low. Hence, it will

cause some inaccurate data under observation using bio-imaging system. For higher dilution EGFP concentration (1.386 g/L, 0.694 g/L and 0.346 g/L), their result is more reliable and accurate due to their SNR is high. Hence, it is correct to refer the photobleaching rate trend at 1.386 g/L (1x), 0.694 g/L (2x) and 0.346g/L (4x). To be more convincing, the GFP was also compared with the QD concentration and indicated that QD has higher photostability than GFP (Ma *et al.*, 2006). According to Ma *et al.* (2006), it shows that the experiment by testing QD concentration does have influence on the QD photostability, however, there is not enough details can explain the relevant parameters which can have effect on the photostability (Ma *et al.*, 2006; Eggeling *et al.*, 1999). Due to its photostability of the GFP, it is advantageous to use higher concentration of GFP, so that the photobleaching rate can be reduced.

The photobleaching rate is mainly caused by the photo-oxidation. The two necessary elements for photo-oxidation are light and oxygen. The photo-oxidation mechanism is shown in **Error! Reference source not found.** The free-radical R generated in the initiation reaction (1) reacts with oxygen to form the free-radical ROO- as shown in reaction (2). This propagation process is followed by (3) to produce hydroperoxide (ROOH) and a further free-radical R-. Branching process (4) can form two new polymer free-radical RO- and OH- without consuming each other. The termination of the photo-oxidation mechanism can be happened by recombination of free radicals in (5), (6) and (7). Reaction (5) involves the formation of stable intermediate products (R-R) like ketones and alchohols while reaction (6) and (7) will form the carbonyl groups (ROOR). In our case, chromophore in GFP is the carbonyl groups which will absorb the UV radiation (Schulz, 2009). When the chromophore absorbs the UV radiation, it will also absorb the photon energy that may break the chemical bonds inside the

chromophore. This may lead to the changing inside chromophore structure that cause it loses the fluorescence intensity. Hence, the increasing the light irradiation period and the existence of oxygen in the system will accelerate the bleaching of GFP. The reason of higher concentration of GFP has lower photobleaching rate is mainly because it may take longer time for oxygen to react with all chromophores molecule for photooxidation. Thus, the ratio of GFP to oxygen must be high, so it will result in a slower photobleaching rate. To avoid quick photobleaching, increasing GFP concentration is required for those subcellular organelles with high oxygen density. The fluorescence intensity reached the saturation point around 1085s. This is due to the photobleaching process had destroyed some chromophores inside EGFP (kalies *et al.*, 2011).

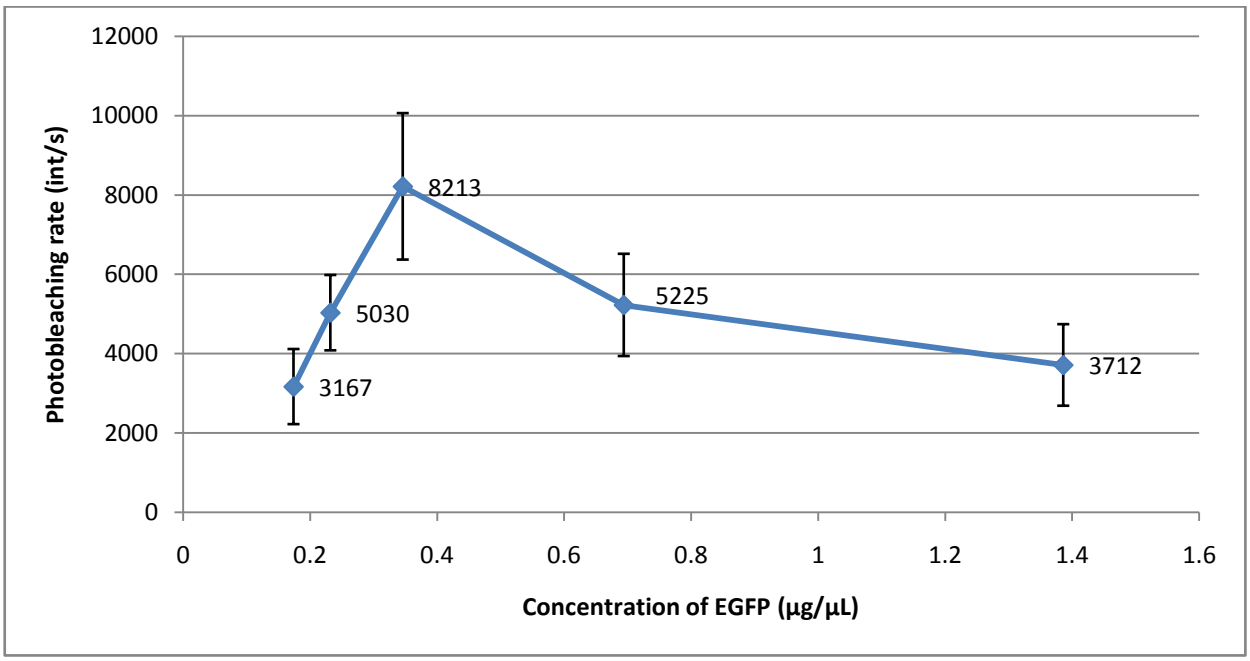

Figure 4-5: The effect of the concentration of EGFP (µg/(µL) on the photobleaching rate (int/s)

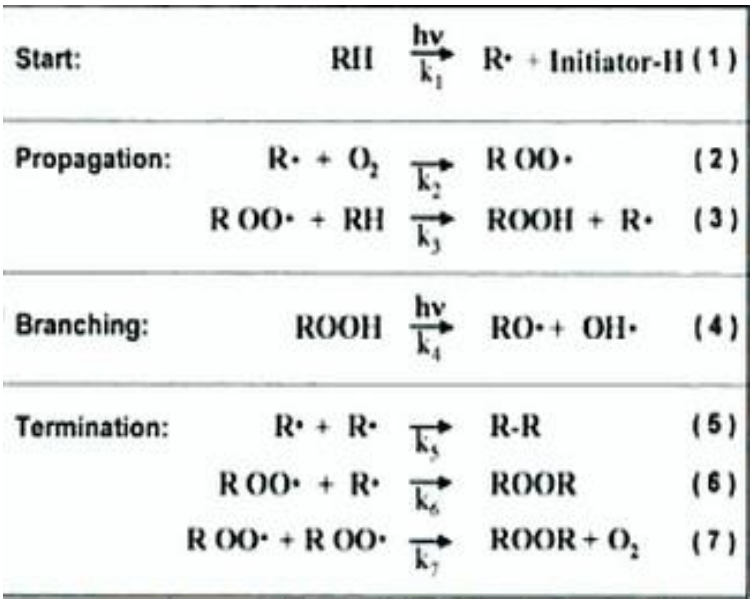

Figure 4-6: The photo-oxidation mechanism [Adapted from Schulz (2009)]

The UV irradiation period and purified EGFP concentration have a marked influence on the quantitation data using gel-based imaging method. Under different UV exposure time, the linearity of standard curve (R^2) was between 0.922 and 0.946 (Figure 4-7). Higher R^2 value was obtained for higher UV exposure time, and this resulted more reliable standard curve for EGFP quantitation. However, higher UV exposure time will leads to high photobleaching, Hence, it is suggested to develop the standard curve at exposure time of 35 s because of the highest value of EGFP intensity.

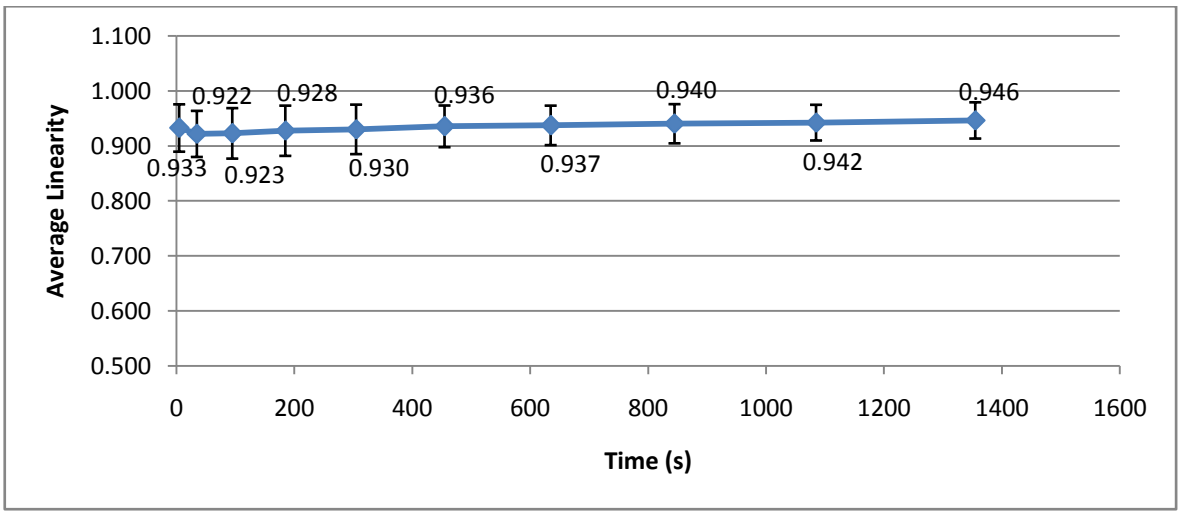

Figure 4-7: The effect of UV exposure time on the linearity of EGFP quantitation method.

5 CONCLUSION

5.1 Conclusion

The fluorescent intensity of EGFP was dependent on the concentration of the EGFP and UV irradiation period. Higher concentration of the EGFP and shorter period of UV irradiation will result in lower photobleaching rate. The main reason for photobleaching rate is due to photo-oxidation. The linearity of different UV exposure time is between 0.922 and 0.946 in which the difference is insignificant. However, in term of UV irradiation period and EGFP concentration, they will affect greatly on the fluorescence intensity. The best period of UV is around 35s because fluorescence intensity is the highest. To increase the reliability of the bio-imaging system, the concentration of EGFP should reach a certain level and the over-irradiation must be avoided.

5.2 Recommendation

It is advisable to increase the EGFP concentration during the purification step in order to solve the SNR limitation.

5.3 Future work

This experiment can be conducted with other type of fluorescent protein and fluorescein because the effect of the UV irradiation period and concentration may not only have effect on GFP, but also on other fluorescent protein and fluorescein. This will be also an improvement for the reliability of the imaging method like gel-based imaging system and spectrofluorometer.

REFRENCES

1. Bradbury, S., and Evennett, P. (1996). *Fluorescence microscopy*. United Kingdom: Ltd.: Oxford.
2. Brenner, S. (1974). The genetics of Caenorhabditis elegans. *Genetics Volume 77* , 71-94.
3. Castano, E.,and Comas, J. (2012). *Flow cytometry in the analysis of cellular populations.* Barcelona: Handbook of instrumental techniques for materials, chemical and biosciences research, Centres Cient fics i Tecnol ògics.
4. Chalfie, M., and Kain, S. R. (2005). *Methods of Biochemical Analysis, Green Fluorescent Protein.* John Wiley & Sons, Inc.: USA.
5. Chalfie, M., Tu, Y., Euskirchen, G., Ward, W. W., and Prasher, D. C. (1994). Green fluorescent protein as a marker for gene-expression. *Science Volume 263* , 802-805.
6. Chew, F. N. (2011). Fluorescent quantitation method for differentiating the nativity of green. *Journal of Bioscience and Bioengineering Volume 111* , 246–248.
7. Chew, F. N., Tan, W. S., and Tey, B. T. (2009b). Single-step purificaiton of the recombinant green fluorescent protein from intact Escherichia coli cells using preparative PAGE. *Electrophoresis Volume 30* , 3017-3023.
8. Chew, F. N., Tan, W. S.,Ling, T. C.,Tan C. S. and Tey, B. T. (2009a). Quantitation of green fluorescent protein using gel-based imaging method. *Analytical Biochemistry Volume 384* , 353–355.
9. Cody, C. W., Prasher, D. C., Westler, W. M., Prendergast, F. G., and Ward, W. W. (1993). Chemical structure of the hexapeptide chromophore of the Aequorea green-fluorescent protein. *Biochemistry Volume 32* , 1212-1218.
10. Cormack, B. P., Valdivia, R. H. and Falkow, S. (1996). FACS-optimized mutants of the green fluorescent protein (GFP). *Gene 173* , 33-38.
11. Cubitt, A. B., Heim, R., Adams, S. R., Boyd, A. E., Gross, L. A., and Tsien, R. Y. (1995). Understanding, improving and using green fluorescent proteins. *Trends in Biochemical Science Volume 20* , 448-455.
12. Day, R. N., and Davidson, M. W. (2014). *The Fluorescent Protein Revolution.* United State: CRC Press.
13. DeLuca, M. A., and McElroy, W. D. (1981). bioluminescene and Chemiluminescence. *Academic New York* , 235-242.
14. Descalzo, L. G., L ópez, E. G., Alcazar, A., Baquero, F., and Cid, C. (2012). Gel Electrophoresis of Proteins. In S. Magdeldin, *Gel Electrophoresis - Principles and Basics* (pp. 57-68). Croatia: InTech.
15. Diaspro, A., Chirico, G., Usai, C., Ramoino, P., and Dobrucki, J. (2006). Photobleaching In Handbook of biological confocal microscopy. *Handbook of biological Confocal Microscopy* , 690-702.
16. Eggeling, C., Widengren, J., Rigler, R., and Seidel, C. A. M. (1999). Photostability of Fluorescent Dyes for Single-Molecule Spectroscopy: Mechanisms and Experimental Methods for Estimating Photobleaching in Aqueous Solution. In W. S. Rettig, *Applied Fluorescence in Chemistry, Biology and Medicine* (pp. 193-240). Berlin : Springer.
17. Errampalli, D., Leung, K., Cassidy, M. B., Kostrzynska, M., Blears, M., Lee, H., and Trevors, J. T. (1999). Applications of the green fluorescent protein as a molecular marker in environmental microorganisms. *Journal of Microbiological Methods Volume 35* , 187-199.

18. Geoffroy, M. C., Guyard, C., Quatannens, B., Pavan, S., Lange, M., and Mercenier, A. (2000). Use of Green Fluorescent Protein To Tag Lactic Acid Bacterium Strains under Development as Live Vaccine Vectors. *Applied and environmental microbiology Volume 66* , 383-391.
19. Gustafsson, M. G. L., Shao, L., Carlton, P. M., Wang, C. J. R., and olubovskaya, I. N. (2008). Three-Dimensional Resolution Doubling in Wide-Field Fluorescence Microscopy by Structured Illumination. *Biophysical Journal Volume 94* , 4957–4970.
20. Hamann, S., Kiilgaard, J. F., Litman, T., Alvarez-Leefmans F. J., Winther, B. R., and Zeuthen, T. (2002). Measurement of Cell Volume Changes by Fluorescence Self-Quenching. *Journal of Fluorescence, Volume 12* , 139-145.
21. Heim, R., Prasher, D. C., and Tsien, R. Y. (1994). Wavelength mutations and posttranslational autoxidation of green fluorescent protein. *Proceedings of the National Academy of Sciences Volume 91* , 12051-12054.
22. IARC. (2005). *Exposure to artificial UV radiation and skin cancer.* Lylon, France: World Health Organization .
23. ICH Harmonised Tripartite Guideline. (1994). *Validation of Analytical Procedures: Text and Methodology.* European Union, Japan and USA: International Conference on Harmonisation of Technical Requirements for Registration of Pharmaceuticals for Human Use.
24. Jahan-Tigh, R. R., Ryan, C., Obermoser, G., and Schwarzenberger, K. (2012). Flow Cytometry. *Journal of Investigative Dermatology Volume 132* , 1-5.
25. Jiménez-Banzo, A., Nonell, S., Hofkens, J., and Flors, C. (2008). Singlet oxygen photosensitization by EGFP and its chromphore HBDI. *Biophysical Journal Volume 94* , 168-172.
26. kalies, S., Kuetemeyer, K., and Heisterkamp, A. (2011). Mechanisms of high-order photobleaching and its relationship to intracellular ablation. *Biomed Opt Express Volume 4* , 805-816.
27. Kasche, V., and Lindqvist, L. (1964). Reaction between the triplet state of fluorescein and oxygen. *Journal Chemical Physics, Volume 4* , 817-823.
28. Kidwai, A. R., and Devasia, G. M. (1962). new method for the synthesis of amino acids. Synthesis of amino acids and their derivatives through 2,4-disubstituted-2-imidazolin-5-ones. *The Journal of Organic Chemistry Volume 27* , 4527-2531.
29. Lakowicz, J. R. (1999). *Instrumentation for fluorescence spectroscopy. In Princples of fluorescence spectroscopy.* US: Springer.
30. Lakowicz, J. R. (2006). *Principles of fluorescence.* Baltimore, USA: Springer.
31. Li, Q. F., Wu, S. S. H., and Chou, K. C. (2009). Subdiffraction-Limit Two-Photon Fluorescence Microscopy for GFP-Tagged Cell Imaging. *Biophysical Journal Volume 97* , 3224–3228.
32. Lilley, K. S., Razzaq, A., and Dupree, P. (2002). Two-dimensional gel electrophoresis: recent advances in sample preparation, detection and quantitation. *Current Opinion in Chemical Biology, volume 6* , 46-50.
33. Lindqvist, L. (1960). A flash photocolysis study of fluorescein. *Arkivfor Kemi. Vol 16* , 79-138.
34. Ma, J., Chen, J. Y., Guo, J., Wang, C. C.,Tang, W. L., and Wang, P. N. (2006). Photostability of Thiol-Capped CDTE Quantum Dots In Living Cells: the effect of photo-oxidation. *Nanotechnology Volume 17* , 2083-2089.

35. Masumaa, R.,Kashimaa, S., Kurasaki, M.,and Okuno, T. . (2013). Effects of UV wavelength on cell damages caused by UV irradiation in PC12 cells. *Journal of Photochemistry and Photobiology B: Biology Volume 125* , 202-208.
36. McRae, S. R., Brown, C. L., and Bushell, G. R. (2005). Rapid purification of EGFP, EYFP, and ECFP with high yield and purity. *Protein Expression and Purification Volume 41* , 121-127.
37. Neves-Petersen, M. T., Gajula, G. P., and Petersen, S. B. (2012). UV Light Effects on Proteins: From Photochemistry to Nanomedicine. *Molecular Photochemistry—Various Aspects* , 125-158.
38. Nienhaus, G. U. (2008). The green fluorescent protein: a key tool to study chemical. *Angewandte Chemie-International Edition, Volume 47* , 8992–8994.
39. Ormo, M., Cubitt, A.B., Kalio, K., Gross,L.A., Tsien, R.Y., and Remington,S.J. (1996). Crystal structure of the Aequorea victoria green fluorescent protein. *Science Volume 273* , 1392–1395.
40. Patterson, G. . (2007). Photobleaching and Photoactivation of Fluorescent Proteins for Studies in Cell Biology. *Microscopy and Microanalysis Volume 13* , 294-295.
41. Patterson, G. H., Knobel, S. M., Sharif, W. D., Kain, S. R., and Piston, D. W. (1997). Use of the Green Fluorescent Protein and Its Mutants in Quantitative. *Biophysical Journal Volume 73* , 2782-2790.
42. Pattison, D. I., and Davies, M. J. (2006). Actions of ultraviolet light on cellular structures. *Cancer: Cell Structures, Carcinogens and Genomic Instability* , 131-157.
43. Paulmurugan, R., and Gambhir, S. S. (2003). Monitoring Protein-Protein Interactions Using Split Synthetic Renilla Luciferase Protein-Fragment-Assisted Complementation. *Analytical Chemistry Volume 75* , 1584-1589.
44. Phillips Jr, G. N. (1997). Structure and dynamics of green fluorescent protein. *Current Opinion in Structural Biology Volume 7* , 821–827.
45. Robinson, J. P. (2004). Flow Cytometry. *Encyclopedia of Biomaterials and Biomedical Engineering* , 602-612.
46. Schulz, U. (2009). *Accelerated Testing: Nature and Artificial Weathering in the Coatings Industry.* Vincentz Network GmbH & Co KG.
47. Smith, S. W. (1999). *The Scientist and Engineer's Guide to Digital Signal Processing 2nd edition.* San Diego, California: California Technical Publishing.
48. Song, L., Hennink E. J., Young, T., and Tanke, H.J. (1995). Photobleaching Kinetics of Fluorescein in Quantitative Fluorescence Microscopy. *Biophysical Journal Volume 68* , 2588-2600.
49. Sullivan, K. F., and Kay, S. A. (1999). *Green Fluorescent Proteins.* San Diego, California: Academic Press.
50. Tonge, R. P., Shaw, J., and Middleton, B. (2001). Validation and development of fluorescence two-dimensional differential gel electrophoresis proteomics technology. *Proteomics volume 1* , 377-396.
51. Tongea, P. J., and Meechb, S. R. (2009). Excited state dynamics in the green fluorescent protein. *Journal of Photochemistry and Photobiology A: Chemistry, Volume 205* , 1-11.
52. Torrado, M., Iglesias, R., and Mikhailov, A. T. (2008). Detection of protein interactions based on GFP fragment complementation by fluorescence microscopy and spectrofluorometry. *BioTechnique Volume 44* , 70-74.
53. Tsien, R. Y. (1998). The green fluorescent protein. *Annual Reviews of Biochemistry Volume 67* , 509-544.

54. Wang, S., and Hazelrigg, T. (1994). Implications for bed mRNA localisation from spatial distribution of exu protein in Drosophila oogenesis. *Nature Volume 369* , 400-403.
55. Ward, W. W., Cody, C. W., Hart, R. C., and Cormier, M. J. (1980). Spectrophotometric identity of the energy transfer chromophores in Renilla and Aequorea green-fluorescent proteins. *Photochemistry and Photobiology Volume 31* , 611–615.
56. Xiao, J. (2009). Single-molecule imaging in live cells. In P. a. Hinterdorfer, *In Handbook of Single-Molecule Biophysics* (pp. 43-93). Unites State: Springer.
57. Yang, F., Moss, L. G., and Phillips Jr, G. N. (1996). The molecular structure of green fluorescent protein. *Nature Biotechnology Volume 14* , 1246–1251.
58. Zhang, H., Sun, Q., Wang, S. F., Olsen, Seth., and Smith S.C. (2010). Theoritical studies of green and red fluorescent proteins. In K. L. Han, *Hydrogen bonding and transfer in the excited state Volume 1 and 2* (pp. 815-837). Brisbane, Austria: John Wiley & Sons.
59. Zhao, X., Jiang, X., Huang, C., Kain, S. R., and Li, X. (1998). Generation of a destabilized form of enhanced green fluorescent protein. *Journal of Biological Chemistry Volume 273* , 34970-34975.
60. Zimmer, M. (2002). Green Fluorescent Protein (GFP): Applications, Structure, and Related Photophysical Behavior. *Chemistry Review Volume 102* , 759-782.

APPENDIX A: Raw data of Lowry's assay

Table A-1: Standard curve of Lowry's assay using BSA as standard protein

Concentration (ug/mL)	Ug	1st run	2nd run	Average	STD
0	0	0	0	0	0
200	40	0.2170	0.2570	0.2370	0.028284
500	100	0.5330	0.5970	0.5650	0.045255
1000	200	0.7690	0.9010	0.8350	0.093338
1500	300	1.2380	1.3120	1.2750	0.007071
2000	400	1.4770	1.5220	1.4995	0.052326
GFP		1.1040	1.1140	1.1090	0.03182

- **The amount of EGFP = 1.1090/0.004=277.27 µg in 200 µL**

Table A-2: The amount and concentration of EGFP for each dilution

Dilution rate	Amount of EGFP (µg)	Concentration of EGFP (µg/ µL)
1x	6.93	1.386
2x	3.47	0.694
4x	1.73	0.346
6x	1.16	0.232
8x	0.87	0.174

For 1x:

- **The amount of EGFP in 200 µL is 277.27 µg**
- **The amount of EGFP in 5 µL is 6.93 µg**
- **Concentration of EGFP is 6.93 µg/5 µL=1.386 µg/ µL**

For 2x:

- **The amount of EGFP in 5 µL is 6.93 µg/2 = 3.47 µg**
- **Concentration of EGFP is 3.47 µg/5 µL= 0.694 µg/ µL**

For 4x:

- **The amount of EGFP in 5 µL is 6.93 µg/4 = 1.73 µg**
- **Concentration of EGFP is 3.47 µg/5 µL= 0.346 µg/ µL**

For 6x:

- **The amount of EGFP in 5 µL is 6.93 µg/6 = 1.16 µg**
- **Concentration of EGFP is 3.47 µg/5 µL= 0.232 µg/ µL**

For 8x:

- **The amount of EGFP in 5 µL is 6.93 µg/8 = 0.87 µg**
- **Concentration of EGFP is 3.47 µg/5 µL= 0.174 µg/ µL**

APPENDIX B: Raw data of gel-based imaging assay

Table B-1: 1st run raw data

- **Intensity= IDV Sample – IDV background**
- **Signal to noise ratio (SNR)= IDV(Sample) / IDV (background)**

	5 sec				35 sec			
Concentration	IDV (sample)	IDV (background)	SNR	Intensity	IDV (sample)	IDV (background)	SNR	Intensity
1x	68803294	16060757	4.3	52742537	70903841	16533975	4.3	54369866
2x	60735436	16452615	3.7	44282821	63197524	16942887	3.7	46254637
4x	41238749	15223934	2.7	26014815	43980538	15848107	2.8	28132431
6x	35925475	15770423	2.3	20155052	38415062	16433778	2.3	21981284
8x	27620436	15250857	1.8	12369579	29383373	15920542	1.8	13462831

	95 sec				185 sec			
Concentration	IDV (sample)	IDV (background)	SNR	Intensity	IDV (sample)	IDV (background)	SNR	Intensity
1x	70506981	15798951	4.5	54708030	69373877	15180825	4.6	54193052
2x	63049399	16317940	3.9	46731459	61627334	15566659	4.0	46060675
4x	43609175	15212895	2.9	28396280	42370473	14468584	2.9	27901889
6x	37862077	15871818	2.4	21990259	36445829	15106072	2.4	21339757
8x	28830554	15485532	1.9	13345022	28216536	14848937	1.9	13367599

	305 sec				455 sec			
Concentration	IDV (sample)	IDV (background)	SNR	Intensity	IDV (sample)	IDV (background)	SNR	Intensity
1x	68893328	14813796	4.7	54079532	66381609	13473243	4.9	52908366
2x	60759780	14923392	4.1	45836388	57504111	13641870	4.2	43862241
4x	41453964	13984822	3.0	27469142	37829046	12834949	2.9	24994097
6x	35453493	14525408	2.4	20928085	32463863	13342405	2.4	19121458
8x	27422586	14187070	1.9	13235516	24900119	12859352	1.9	12040767

	635 sec				845 sec			
Concentration	IDV (sample)	IDV (background)	SNR	Intensity	IDV (sample)	IDV (background)	SNR	Intensity
1x	66053219	13105034	5.0	52948185	64574863	12587418	5.1	51987445
2x	57091740	13381673	4.3	43710067	55349654	12768281	4.3	42581373
4x	37265682	12608179	3.0	24657503	35208623	12066378	2.9	23142245
6x	31968464	13121231	2.4	18847233	30309299	11960876	2.5	18348423
8x	24464779	12364332	2.0	12100447	23254876	11940884	1.9	11313992

	1085 sec				1355 sec			
Concentration	**IDV (sample)**	**IDV (background)**	**SNR**	**Intensity**	**IDV (sample)**	**IDV (background)**	**SNR**	**Intensity**
1x	63313436	11920505	5.3	51392931	64711155	12159794	5.3	52551361
2x	53693764	12055762	4.5	41638002	54575764	12255578	4.5	42320186
4x	33410579	11540545	2.9	21870034	34063240	11763623	2.9	22299617
6x	28923291	11326979	2.6	17596312	28736397	11179569	2.6	17556828
8x	22051384	11228326	2.0	10823058	21967940	11112608	2.0	10855332

Table B-2: 2nd run raw data

	5 sec				35 sec			
Concentration	IDV (sample)	IDV (background)	SNR	Intensity	IDV (sample)	IDV (background)	SNR	Intensity
1x	91186727	29966852	3.0	61219875	90604142	27902206	3.2	62701936
2x	64202404	21655368	3.0	42547036	74510370	28460106	2.6	46050264
4x	43030340	19799437	2.2	23230903	50299022	26297893	1.9	24001129
6x	37740789	20635668	1.8	17105121	44895633	27749668	1.6	17145965
8x	35754138	22417502	1.6	13336636	43964056	32379024	1.4	11585032

	95 sec				185sec			
Concentration	IDV (sample)	IDV (background)	SNR	Intensity	IDV (sample)	IDV (background)	SNR	Intensity
1x	84100196	22691592	3.7	61408604	83709109	21307941	3.9	62401168
2x	67894317	23031898	2.9	44862419	66105091	21455405	3.1	44649686
4x	43309499	21161837	2.0	22147662	40564303	20093713	2.0	20470590
6x	39417605	23448906	1.7	15968699	37215982	22052473	1.7	15163509
8x	37415208	25825564	1.4	11589644	36172798	24388306	1.5	11784492

	305 sec				455 sec			
Concentration	IDV (sample)	IDV (background)	SNR	Intensity	IDV (sample)	IDV (background)	SNR	Intensity
1x	80722694	19666831	4.1	61055863	85342790	23402465	3.6	61940325
2x	63099575	19734508	3.2	43365067	67332197	23135388	2.9	44196809
4x	37299471	18705212	2.0	18594259	40454699	22357366	1.8	18097333
6x	35660060	21959594	1.6	13700466	36582906	23107178	1.6	13475728
8x	32938450	22964379	1.4	9974071	37156867	27243294	1.4	9913573

	635 sec				845 sec			
Concentration	IDV (sample)	IDV (background)	SNR	Intensity	IDV (sample)	IDV (background)	SNR	Intensity
1x	80472733	19802377	4.1	60670356	81492593	21311622	3.8	60180971
2x	62482652	19418139	3.2	43064513	63083390	20841064	3.0	42242326
4x	35735796	18926124	1.9	16809672	36162399	20353853	1.8	15808546
6x	32000129	19377089	1.7	12623040	32473404	20825992	1.6	11647412
8x	31916095	23023999	1.4	8892096	32878506	24265140	1.4	8613366

	1085 sec				1355 sec			
Concentration	IDV (sample)	IDV (background)	SNR	Intensity	IDV (sample)	IDV (background)	SNR	Intensity
1x	77350250	19172449	4.0	58177801	79106994	20682875	3.8	58424119
2x	59481555	18945728	3.1	40535827	60422625	20394814	3.0	40027811
4x	32273427	18232105	1.8	14041322	33144167	19662370	1.7	13481797
6x	28611873	18019552	1.6	10592321	29365594	19584575	1.5	9781019
8x	28850901	21597022	1.3	7253879	29821121	23036802	1.3	6784319

Table B-3: 3rd run raw data

	5 sec				35 sec			
Concentration	IDV (sample)	IDV (background)	SNR	Intensity	IDV (sample)	IDV (background)	SNR	Intensity
1x	78729876	18588779	4.2	60141097	82317411	19640066	4.2	62677345
2x	61237673	18583227	3.3	42654446	64255823	19459194	3.3	44796629
4x	44495411	18142042	2.5	26353369	46938398	19031446	2.5	27906952
6x	34249741	18530627	1.8	15719114	36256914	19343255	1.9	16913659
8x	30702945	21675273	1.4	9027672	32493910	22886870	1.4	9607040

	95 sec				185sec			
Concentration	IDV (sample)	IDV (background)	SNR	Intensity	IDV (sample)	IDV (background)	SNR	Intensity
1x	81186417	18902409	4.3	62284008	79337592	18480737	4.3	60856855
2x	63608853	18845326	3.4	44763527	61793382	17990804	3.4	43802578
4x	46241069	18348137	2.5	27892932	44044544	17230999	2.6	26813545
6x	35639826	18644664	1.9	16995162	33626817	17506246	1.9	16120571
8x	31916526	21963796	1.5	9952730	29926171	20457189	1.5	9468982

	305 sec				455 sec			
Concentration	IDV (sample)	IDV (background)	SNR	Intensity	IDV (sample)	IDV (background)	SNR	Intensity
1x	77980422	17192850	4.5	60787572	75305221	16183870	4.7	59121351
2x	60410171	16957037	3.6	43453134	57415982	15748401	3.6	41667581
4x	42058542	16417564	2.6	25640978	38837663	15108039	2.6	23729624
6x	32033673	16577987	1.9	15455686	29723414	15449924	1.9	14273490
8x	28234161	19251893	1.5	8982268	25971393	17646266	1.5	8325127

	635 sec				845 sec			
Concentration	IDV (sample)	IDV (background)	SNR	Intensity	IDV (sample)	IDV (background)	SNR	Intensity
1x	75889773	16468991	4.6	59420782	74855609	15807475	4.7	59048134
2x	57967297	16337454	3.5	41629843	56853918	15592186	3.6	41261732
4x	39394295	15251344	2.6	24142951	37737092	14780844	2.6	22956248
6x	30202222	15547421	1.9	14654801	28936912	15037302	1.9	13899610
8x	26495117	17771434	1.5	8723683	25175260	17052124	1.5	8123136

	1085 sec				1355 sec			
Concentration	IDV (sample)	IDV (background)	SNR	Intensity	IDV (sample)	IDV (background)	SNR	Intensity
1x	72794683	15473127	4.7	57321556	71456319	14861380	4.8	56594939
2x	54887386	15053131	3.6	39834255	53444818	14518140	3.7	38926678
4x	35812475	14159509	2.5	21652966	34037605	13827069	2.5	20210536
6x	27410358	14401184	1.9	13009174	26120341	14024470	1.9	12095871
8x	23596703	16002825	1.5	7593878	22535176	15427665	1.5	7107511

Table B-4: 4th run raw data

	5 sec				35 sec			
Concentration	IDV (sample)	IDV (background)	SNR	Intensity	IDV (sample)	IDV (background)	SNR	Intensity
1x	95151547	28285025	3.4	66866522	93847496	25120405	3.7	68727091
2x	72648336	27602350	2.6	45045986	70991090	24292652	2.9	46698438
4x	51713590	26390708	2.0	25322882	49056299	22934993	2.1	26121306
6x	39116296	26004197	1.5	13112099	36358189	23173799	1.6	13184390
8x	38425070	27034979	1.4	11390091	35326484	24129236	1.5	11197248

	95 sec				185sec			
Concentration	IDV (sample)	IDV (background)	SNR	Intensity	IDV (sample)	IDV (background)	SNR	Intensity
1x	90897970	21942670	4.1	68955300	88001391	20232874	4.3	67768517
2x	67454631	21504465	3.1	45950166	64328284	19822757	3.2	44505527
4x	44795591	20156891	2.2	24638700	41221594	19043456	2.2	22178138
6x	32731681	20317037	1.6	12414644	29969143	18500254	1.6	11468889
8x	32001886	21232627	1.5	10769259	29365459	19313902	1.5	10051557

	305 sec				455 sec			
Concentration	IDV (sample)	IDV (background)	SNR	Intensity	IDV (sample)	IDV (background)	SNR	Intensity
1x	85447706	18597483	4.6	66850223	83377712	16648985	5.0	66728727
2x	61448349	18215115	3.4	43233234	59242892	16295260	3.6	42947632
4x	37885993	17380684	2.2	20505309	35292681	15633156	2.3	19659525
6x	27349181	17001733	1.6	10347448	26092082	15710540	1.7	10381542
8x	26869705	17469817	1.5	9399888	25851927	16497366	1.6	9354561

	635 sec				845 sec			
Concentration	IDV (sample)	IDV (background)	SNR	Intensity	IDV (sample)	IDV (background)	SNR	Intensity
1x	81510321	15823827	5.2	65686494	80532709	15265905	5.3	65266804
2x	57467261	15569736	3.7	41897525	55822776	15096595	3.7	40726181
4x	33348229	14854450	2.2	18493779	31611506	14260635	2.2	17350871
6x	24442788	14878371	1.6	9564417	23076678	14139618	1.6	8937060
8x	24342501	15638925	1.6	8703576	22991717	14897014	1.5	8094703

	1085 sec				1355 sec			
Concentration	IDV (sample)	IDV (background)	SNR	Intensity	IDV (sample)	IDV (background)	SNR	Intensity
1x	79069448	14655116	5.4	64414332	78279452	14651493	5.3	63627959
2x	54199140	14366060	3.8	39833080	52267221	13821405	3.8	38445816
4x	29895706	13669147	2.2	16226559	28424863	13132862	2.2	15292001
6x	22008934	13627981	1.6	8380953	20718386	13011331	1.6	7707055
8x	21911271	14445427	1.5	7465844	21013801	13802867	1.5	7210934

Table B-5: The average raw data of 4 data

Time (s)	AVERAGE Intensity								
	1x	STD	COV	2x	STD	COV	4x	STD	COV
5	60242508	5804959	9.64	43632572	1232299	2.82	25230492	1400346	5.55
35	62119060	5898234	9.50	45949992	815124	1.77	26540454.5	1917078	7.22
95	61838986	5827399	9.42	45576893	938863	2.06	25768893.5	2932880	11.38
185	61304898	5590446	9.12	44754617	946084	2.11	24341040.5	3580105	14.71
305	60693298	5221429	8.60	43971956	1246235	2.83	23052422	4186129	18.16
455	60174692	5772979	9.59	43168566	1131406	2.62	21620144.75	3270458	15.13
635	59681454	5242242	8.78	42575487	979846	2.30	21025976.25	3962018	18.84
845	59120839	5470751	9.25	41702903	858546	2.06	19814477.5	3788650	19.12
1085	57826655	5328187	9.21	40460291	852061	2.11	18447720.25	3930044	21.30
1355	57799595	4595469	7.95	39930123	1725496	4.32	17820987.75	4122799	23.13

Time (s)	AVERAGE Intensity					
	6x	STD	COV	8x	STD	COV
5	16522847	2933209	17.75	11530995	1848427	16.03
35	17306324.5	3606729	20.84	11463037.75	1584238	13.82
95	16842191	3953571	23.47	11414163.75	1450367	12.71
185	16023181.5	4072513	25.42	11168157.5	1765541	15.81
305	15107921.25	4421096	29.26	10397935.75	1934919	18.61
455	14313054.5	3618481	25.28	9908507	1566366	15.81
635	13922372.75	3893188	27.96	9604950.5	1665810	17.34
845	13208126.25	3982404	30.15	9036299.25	1537013	17.01
1085	12394690	3949392	31.86	8284164.75	1698393	20.50
1355	11785193.25	4244848	36.02	7989524	1919160	24.02

Table B-6: The raw data of intensity of each UV exposure period for each concentration

	Intensity				
Concentration (µg/ µL) Time (s)	1.386	0.694	0.346	0.232	0.174
5	60242508	43632572	25230492	16522847	11530995
35	62119060	45949992	26540455	17306325	11463038
95	61838986	45576893	25768894	16842191	11414164
185	61304898	44754617	24341041	16023182	11168158
305	60693298	43971956	23052422	15107921	10397936
455	60174692	43168566	21620145	14313055	9908507
635	59681454	42575487	21025976	13922373	9604951
845	59120839	41702903	19814478	13208126	9036299
1085	57826655	40460291	18447720	12394690	8284165
1355	57799595	39930123	17820988	11785193	7989524

- **Fo = Intensity at 5 seconds**
- **F= Intensity at different time**

Table B-7: The raw data of relative intensity of each UV exposure period for each concentration

	Relative Intensity (F/Fo)				
Concentration (µg/ µL) Time (s)	1.386	0.694	0.346	0.232	0.174
5	1	1	1	1	1
35	1.031	1.053	1.052	1.047	0.994
95	1.027	1.045	1.021	1.019	0.990
185	1.018	1.026	0.965	0.970	0.969
305	1.007	1.008	0.914	0.914	0.902
455	0.999	0.989	0.857	0.866	0.859
635	0.991	0.976	0.833	0.843	0.833
845	0.981	0.956	0.785	0.799	0.784
1085	0.960	0.927	0.731	0.750	0.718
1355	0.959	0.915	0.706	0.713	0.693

Table B-8: The 1st raw data for photobleaching rate

Concentration (µg/ µL) / Time (s)	Intensity				
	1.386	0.694	0.346	0.232	0.174
35	54369866	46254637	28132431	21981284	13462831
95	54708030	46731459	28396280	21990259	13345022
185	54193052	46060675	27901889	21339757	13367599
305	54079532	45836388	27469142	20928085	13235516
455	52908366	43862241	24994097	19121458	12040767
635	52948185	43710067	24657503	18847233	12100447
845	51987445	42581373	23142245	18348423	11313992

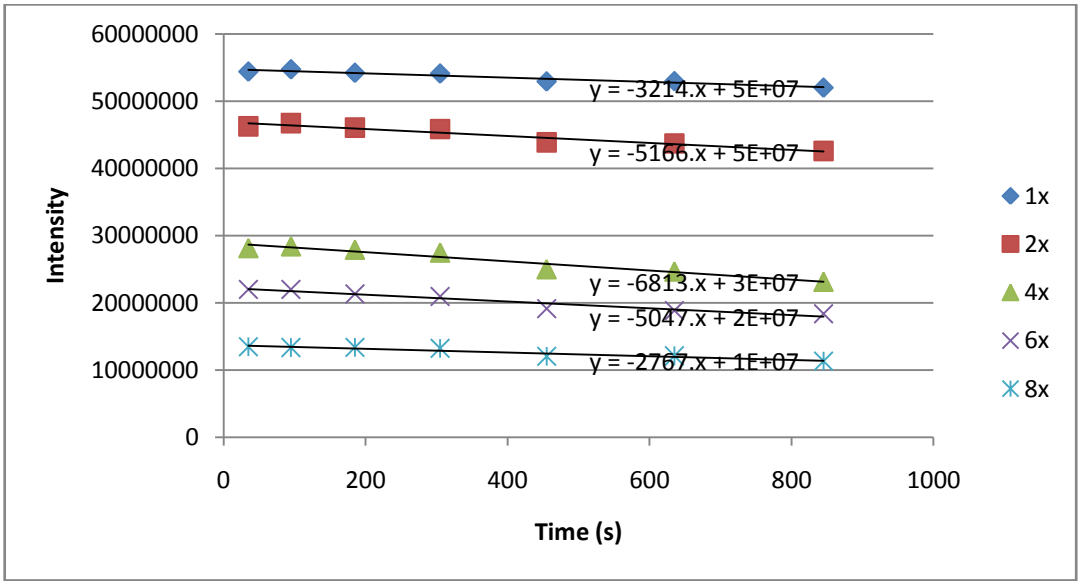

Figure B-1: The effect of UV exposure time on the fuorescence intensity with different photobleaching rate (int/s) for each EGFP concentration (1st raw data)

Table B-9: The 2nd raw data for photobleaching rate

Time (s) \ Concentration (µg/ µL)	Intensity				
	1.386	0.694	0.346	0.232	0.174
35	62701936	46050264	24001129	17145965	11585032
95	61408604	44862419	22147662	15968699	11589644
185	62401168	44649686	20470590	15163509	11784492
305	61055863	43365067	18594259	13700466	9974071
455	61940325	44196809	18097333	13475728	9913573
635	60670356	43064513	16809672	12623040	8892096
845	60180971	42242326	15808546	11647412	8613366

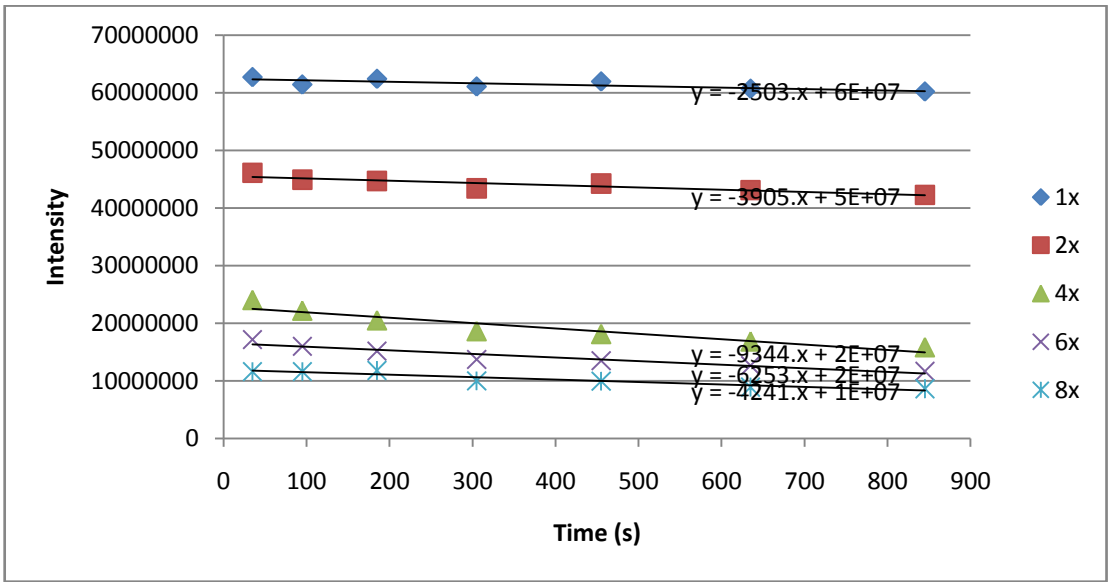

Figure B-2: The effect of UV exposure time on the fuorescence intensity with different photobleaching rate (int/s) for each EGFP concentration (2nd raw data)

Table B-10: The 3rd raw data for photobleaching rate

Concentration (µg/ µL) / Time (s)	Intensity				
	1.386	0.694	0.346	0.232	0.174
35	62677345	44796629	27906952	16913659	9607040
95	62284008	44763527	27892932	16995162	9952730
185	60856855	43802578	26813545	16120571	9468982
305	60787572	43453134	25640978	15455686	8982268
455	59121351	41667581	23729624	14273490	8325127
635	59420782	41629843	24142951	14654801	8723683
845	59048134	41261732	22956248	13899610	8123136

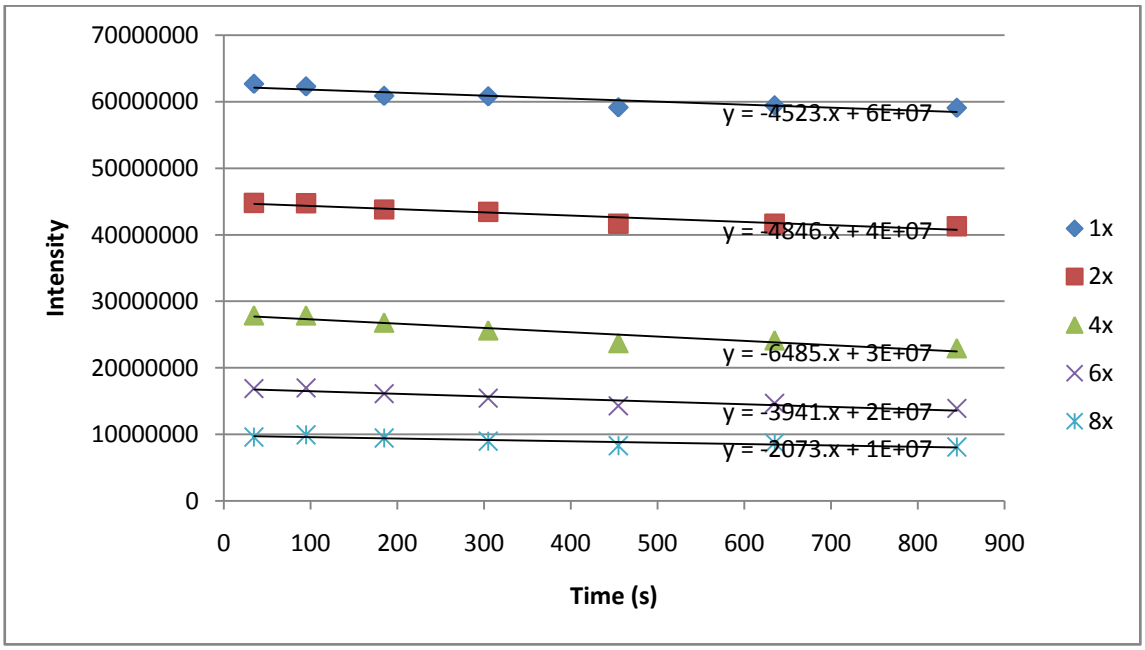

Figure B-3: The effect of UV exposure time on the fuorescence intensity with different photobleaching rate (int/s) for each EGFP concentration (3rd raw data)

Table B-11: The 4th raw data for photobleaching rate

Concentration (µg/ µL) / Time (s)	Intensity				
	1.386	0.694	0.346	0.232	0.174
35	68727091	46698438	26121306	13184390	11197248
95	68955300	45950166	24638700	12414644	10769259
185	67768517	44505527	22178138	11468889	10051557
305	66850223	43233234	20505309	10347448	9399888
455	66728727	42947632	19659525	10381542	9354561
635	65686494	41897525	18493779	9564417	8703576
845	65266804	40726181	17350871	8937060	8094703

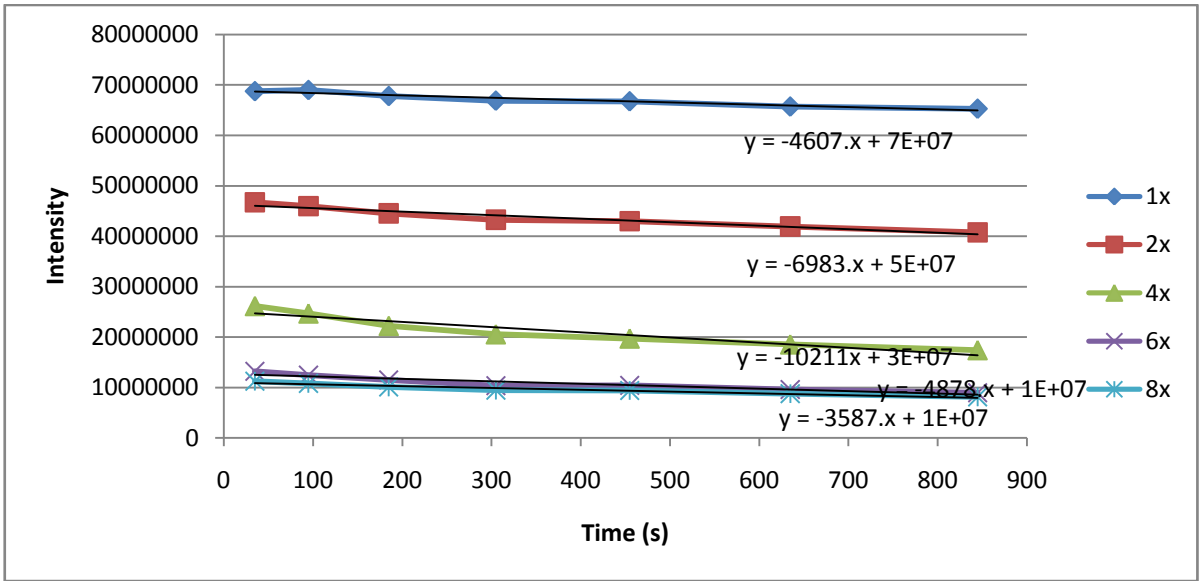

Figure B-4: The effect of UV exposure time on the fuorescence intensity with different photobleaching rate (int/s) for each EGFP concentration (4th raw data)

Table B-12: The average, standard deviation and coefficient of variation of each photobleaching rate (gradient) (4 average data)

Concentration (µg/ µL)	Photobleaching rate (1st)	Photobleaching rate (2nd)	Photobleaching rate (3rd)	Photobleaching rate(4th)	AVG	STD	COV
1.386	3214	2503	4523	4607	3711.75	1027.69	27.68744
0.694	5166	3905	4846	6983	5225.00	1288.42	24.65878
0.346	6813	9344	6485	10211	8213.25	1845.46	22.46928
0.232	5047	6253	3941	4878	5029.75	949.57	18.87905
0.174	2767	4241	2073	3587	3167.00	946.35	29.88146

Table B-13: 1st raw data for the linearity of standard curve (R^2) of different concentration on each UV exposure time

Time (s) \ Concentration (µg/ µL)	Intensity				
	1.386	0.694	0.346	0.232	0.174
5	52742537	44282821	26014815	20155052	12369579
35	54369866	46254637	28132431	21981284	13462831
95	54708030	46731459	28396280	21990259	13345022
185	54193052	46060675	27901889	21339757	13367599
305	54079532	45836388	27469142	20928085	13235516
455	52908366	43862241	24994097	19121458	12040767
635	52948185	43710067	24657503	18847233	12100447
845	51987445	42581373	23142245	18348423	11313992
1085	51392931	41638002	21870034	17596312	10823058
1355	52551361	42320186	22299617	17556828	10855332

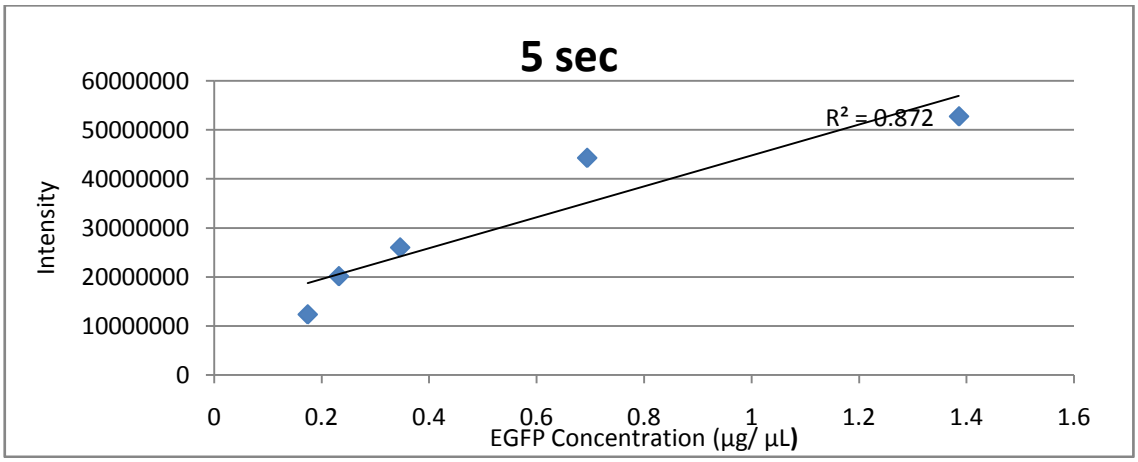

Figure B-5: The effect of EGFP concentration (µg/ µL) on the intensity with linearity of 0.872 at 5 seconds UV exposure time (1st raw data)

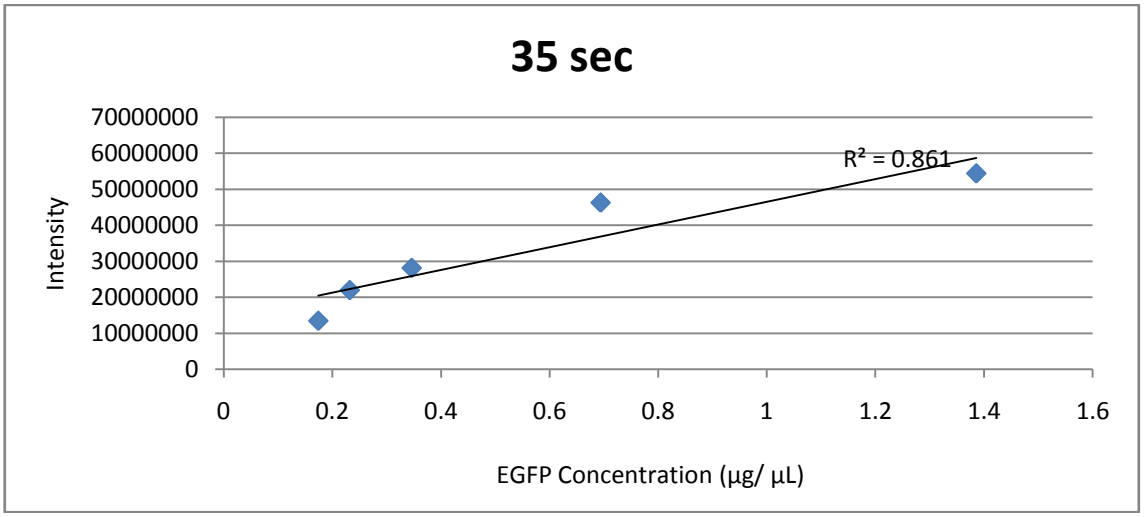

Figure B-6: The effect of EGFP concentration (µg/ µL) on the intensity with linearity of 0.861 at 35 seconds UV exposure time (1st raw data)

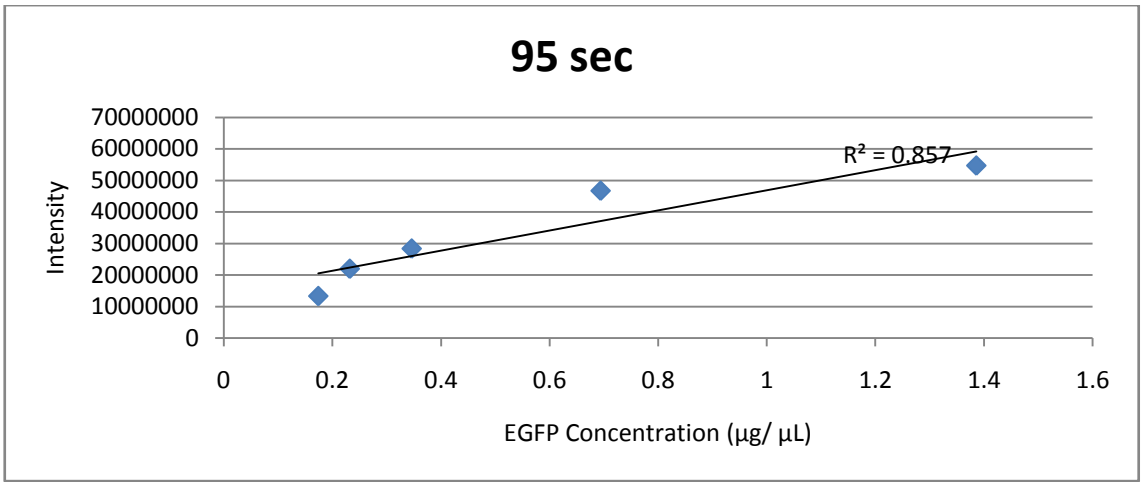

Figure B-7: The effect of EGFP concentration (µg/ µL) on the intensity with linearity of 0.857 at 95 seconds UV exposure time (1st raw data)

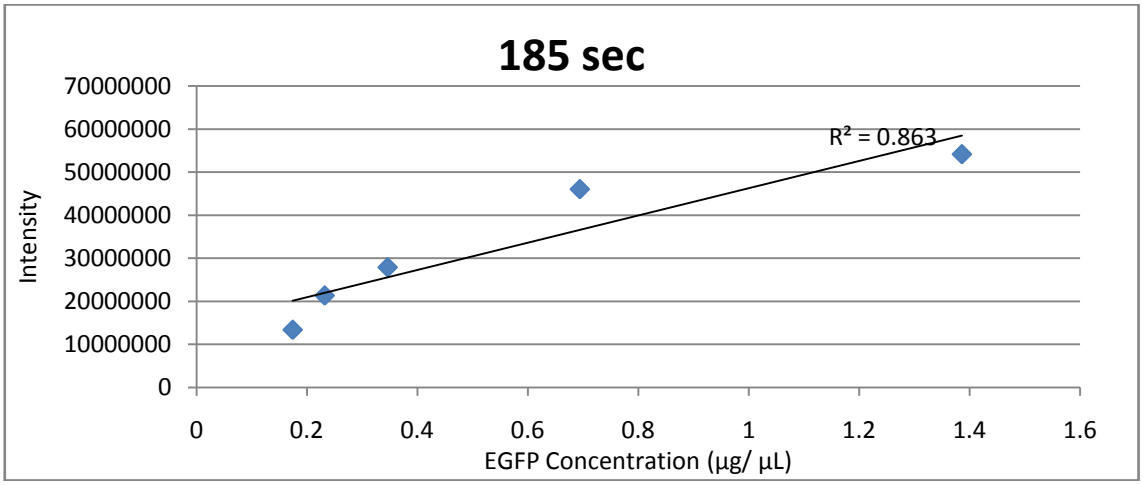

Figure B-8: The effect of EGFP concentration (µg/ µL) on the intensity with linearity of 0.863 at 185 seconds UV exposure time (1st raw data)

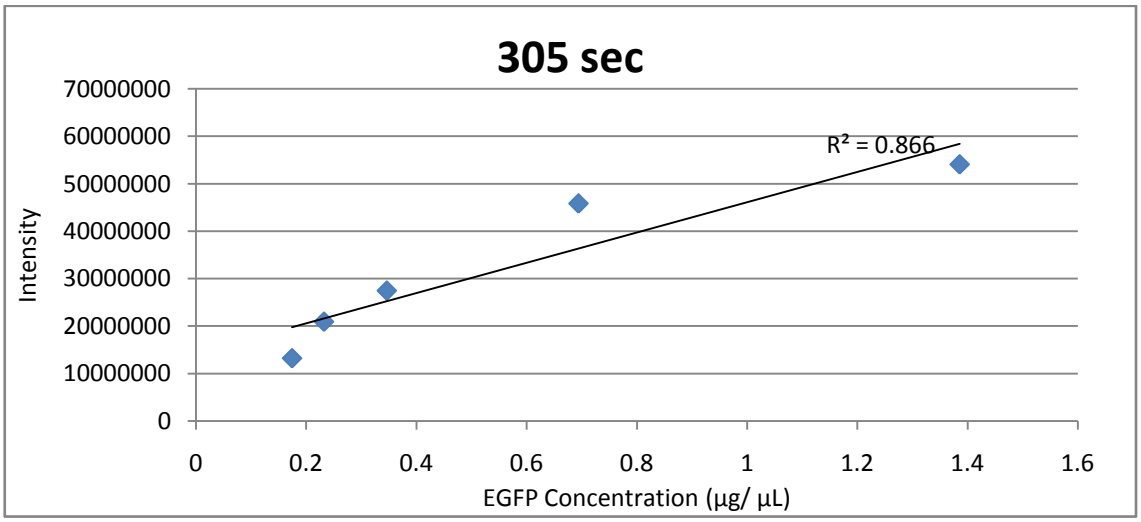

Figure B-9:The effect of EGFP concentration (µg/ µL) on the intensity with linearity of 0.866 at 305 seconds UV exposure time (1st raw data)

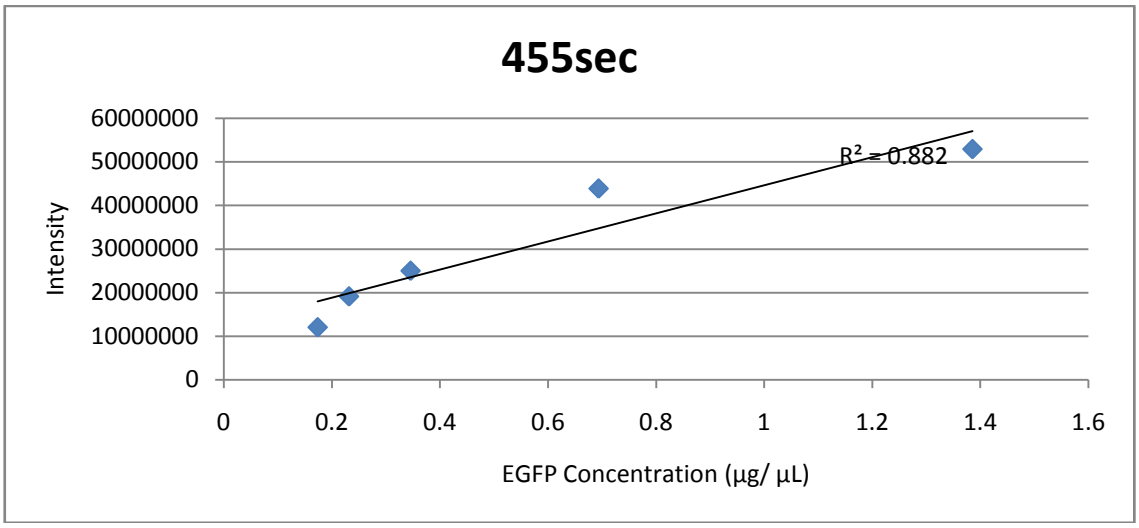

Figure B-10: The effect of EGFP concentration (µg/ µL) on the intensity with linearity of 0.882 at 455 seconds UV exposure time (1st raw data)

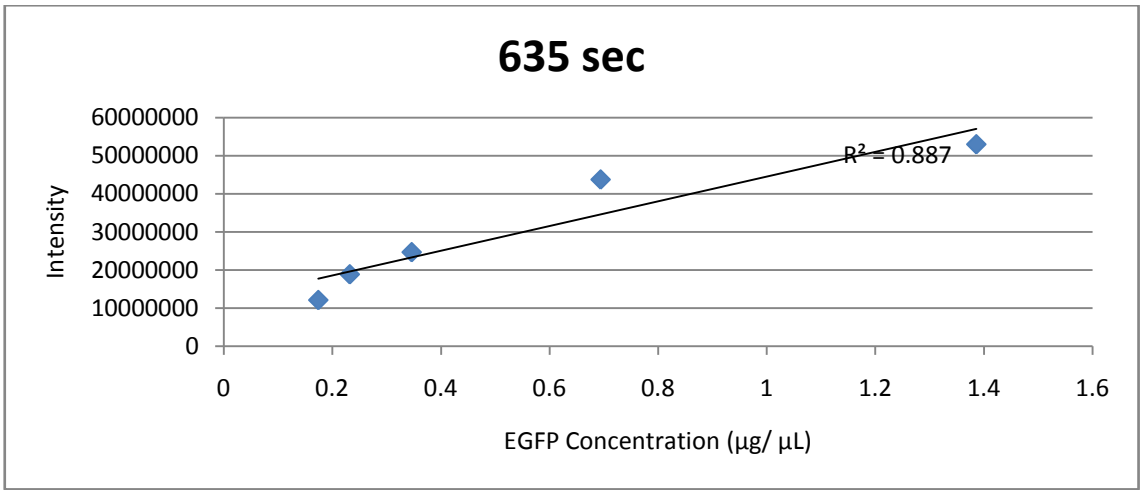

Figure B-11: The effect of EGFP concentration (µg/ µL) on the intensity with linearity of 0.887 at 635 seconds UV exposure time (1st raw data)

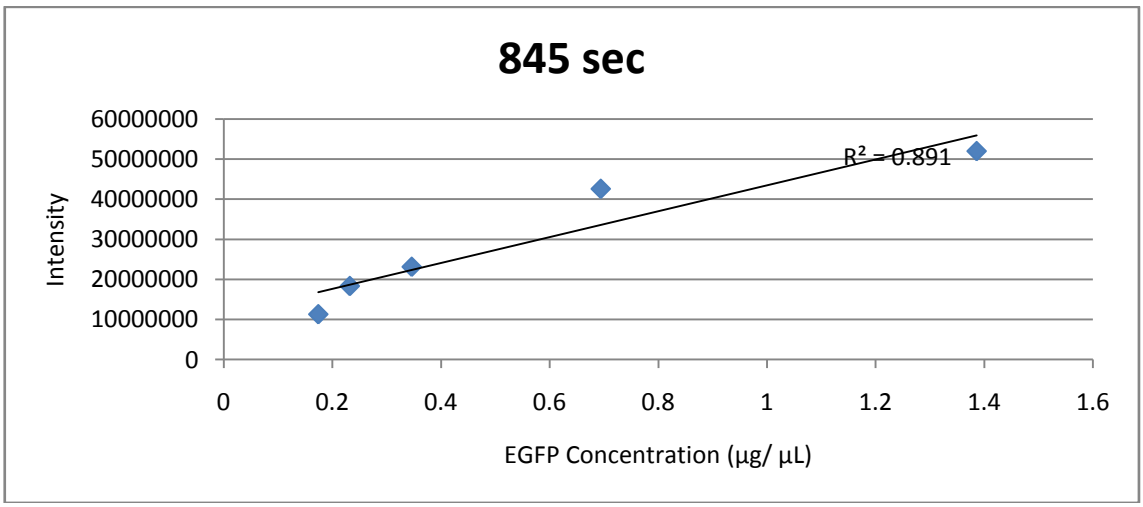

Figure B-12: The effect of EGFP concentration (µg/ µL) on the intensity with linearity of 0.891 at 845 seconds UV exposure time (1st raw data)

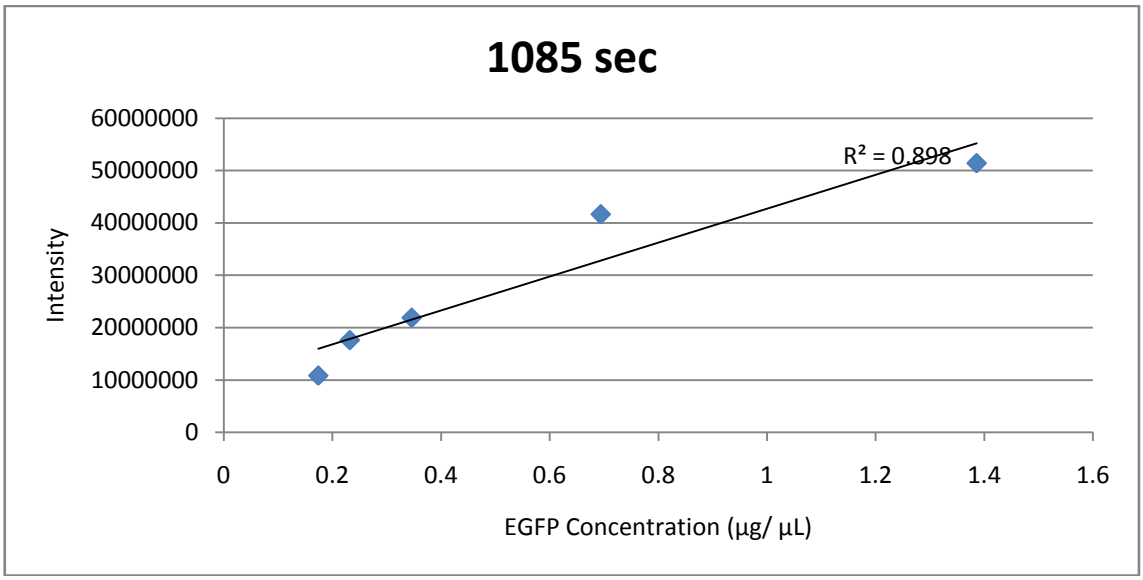

Figure B-13: The effect of EGFP concentration (µg/ µL) on the intensity with linearity of 0.898 at 1085 seconds UV exposure time (1st raw data)

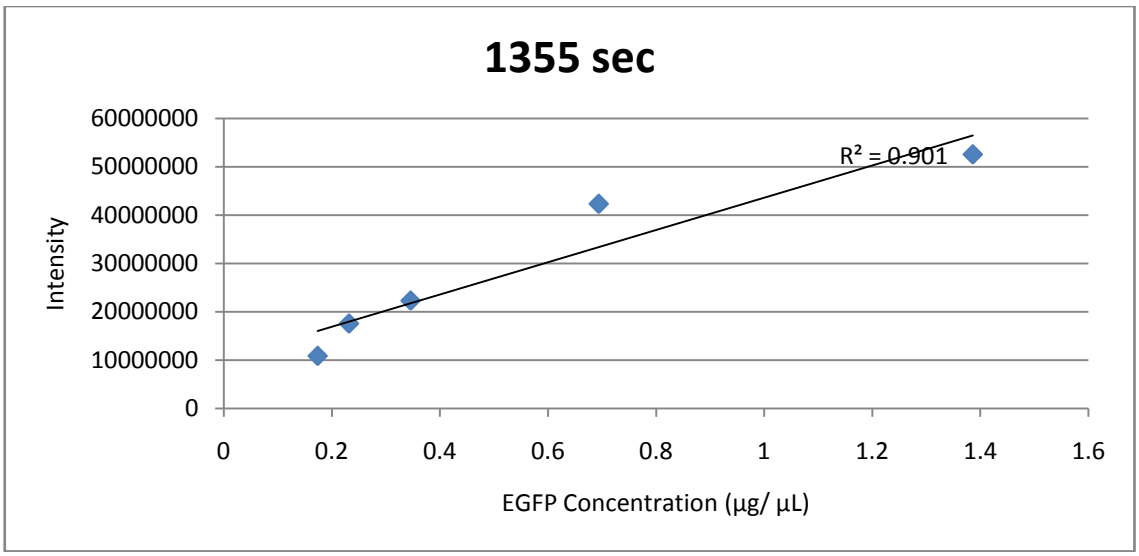

Figure B-14: The effect of EGFP concentration (µg/ µL) on the intensity with linearity of 0.901 at 1355 seconds UV exposure time (1st raw data)

Table B-14: 2nd raw data for the linearity of standard curve (R^2) of different concentration on each UV exposure time

Time (s) \ Concentration (µg/ µL)	Intensity				
	1.386	0.694	0.346	0.232	0.174
5	61219875	42547036	23230903	17105121	13336636
35	62701936	46050264	24001129	17145965	11585032
95	61408604	44862419	22147662	15968699	11589644
185	62401168	44649686	20470590	15163509	11784492
305	61055863	43365067	18594259	13700466	9974071
455	61940325	44196809	18097333	13475728	9913573
635	60670356	43064513	16809672	12623040	8892096
845	60180971	42242326	15808546	11647412	8613366
1085	58177801	40535827	14041322	10592321	7253879
1355	58424119	40027811	13481797	9781019	6784319

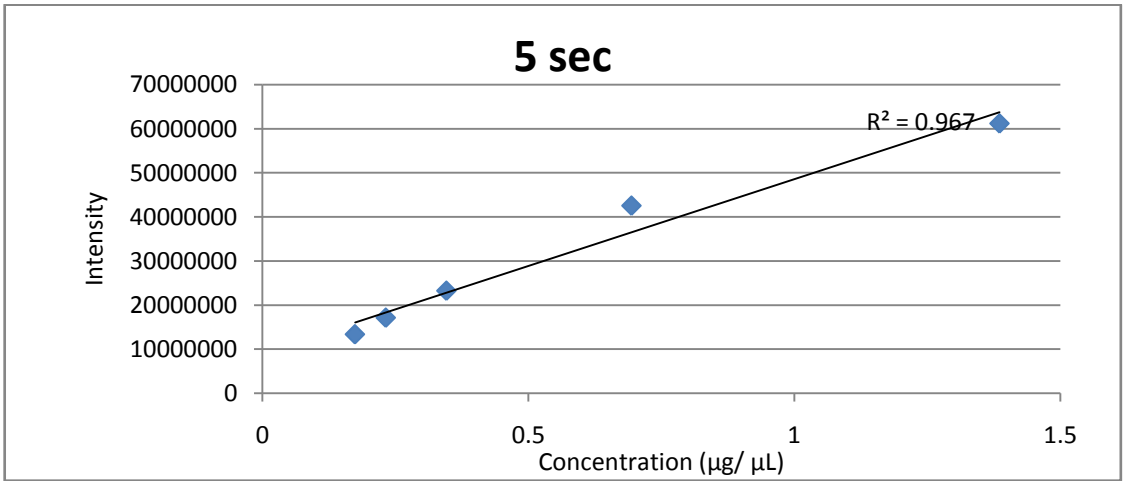

Figure B-15: The effect of EGFP concentration (µg/ µL) on the intensity with linearity of 0.967 at 5 seconds UV exposure time (2nd raw data)

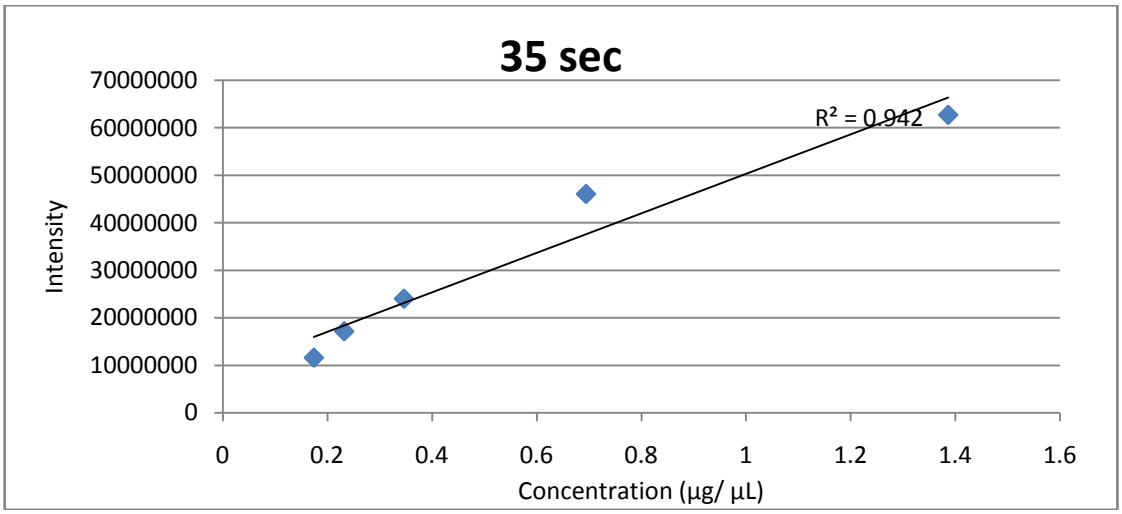

Figure B-16: The effect of EGFP concentration (µg/ µL) on the intensity with linearity of 0.942 at 35 seconds UV exposure time (2nd raw data)

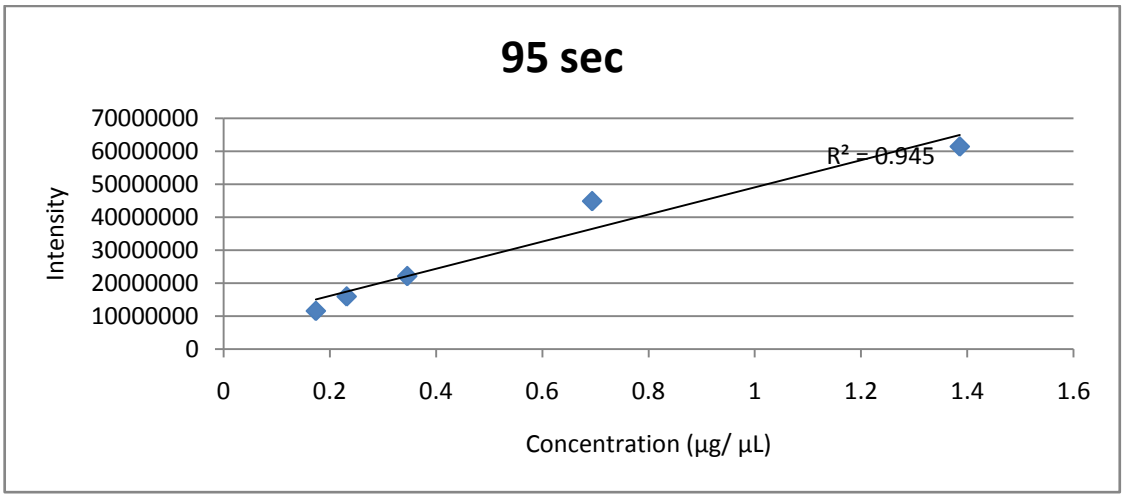

Figure B-17: The effect of EGFP concentration (µg/ µL) on the intensity with linearity of 0.945 at 95 seconds UV exposure time (2nd raw data)

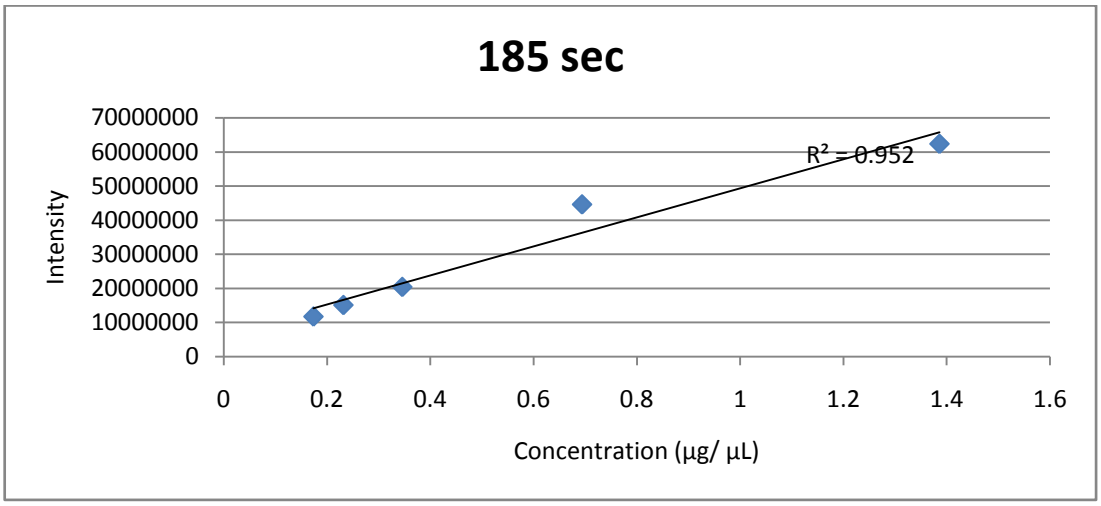

Figure B-18: The effect of EGFP concentration (µg/ µL) on the intensity with linearity of 0.952 at 185 seconds UV exposure time (2nd raw data)

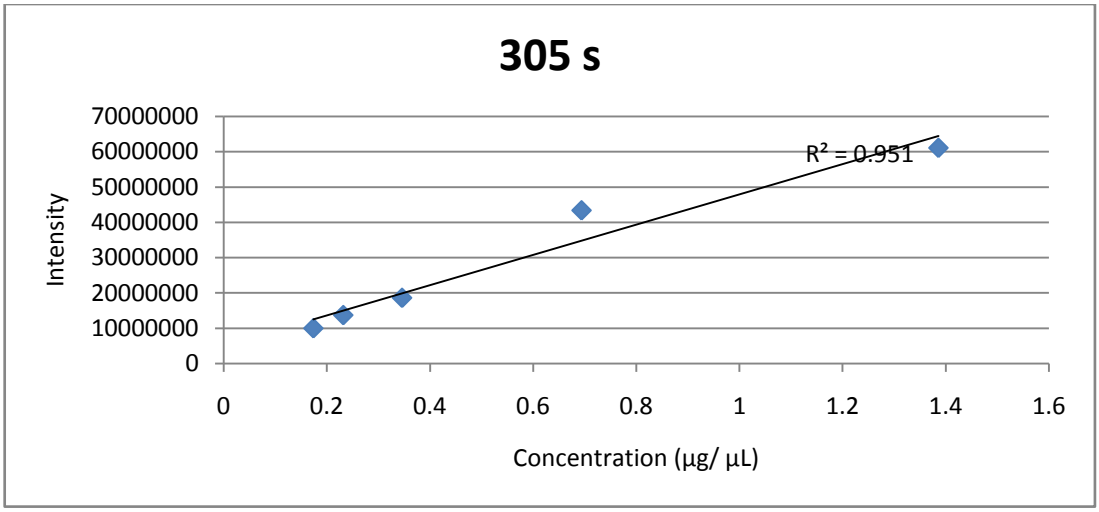

Figure B-19: The effect of EGFP concentration (µg/ µL) on the intensity with linearity of 0.951 at 305 seconds UV exposure time (2nd raw data)

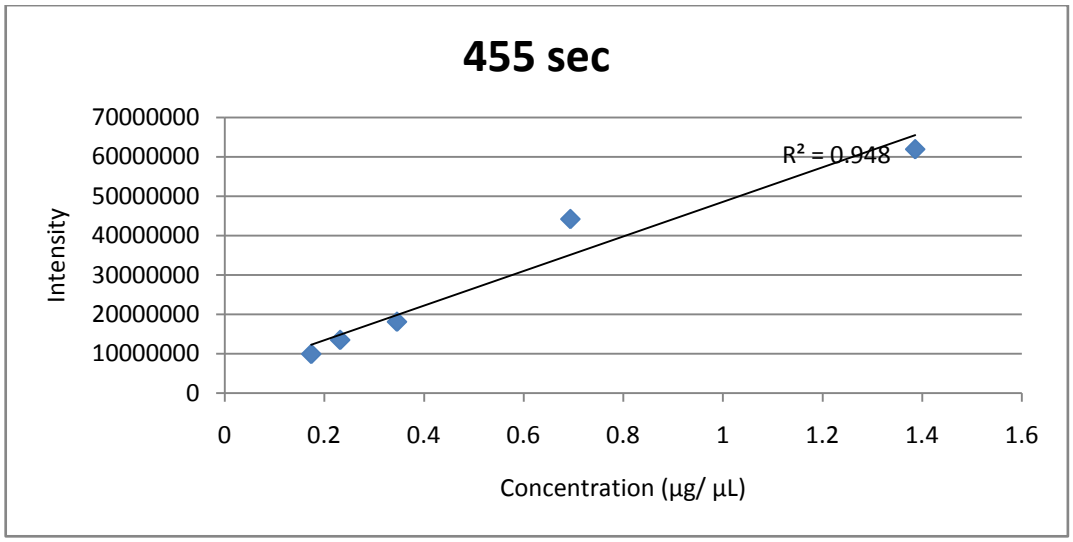

Figure B-20: The effect of EGFP concentration (µg/ µL) on the intensity with linearity of 0.948 at 455 seconds UV exposure time (2nd raw data)

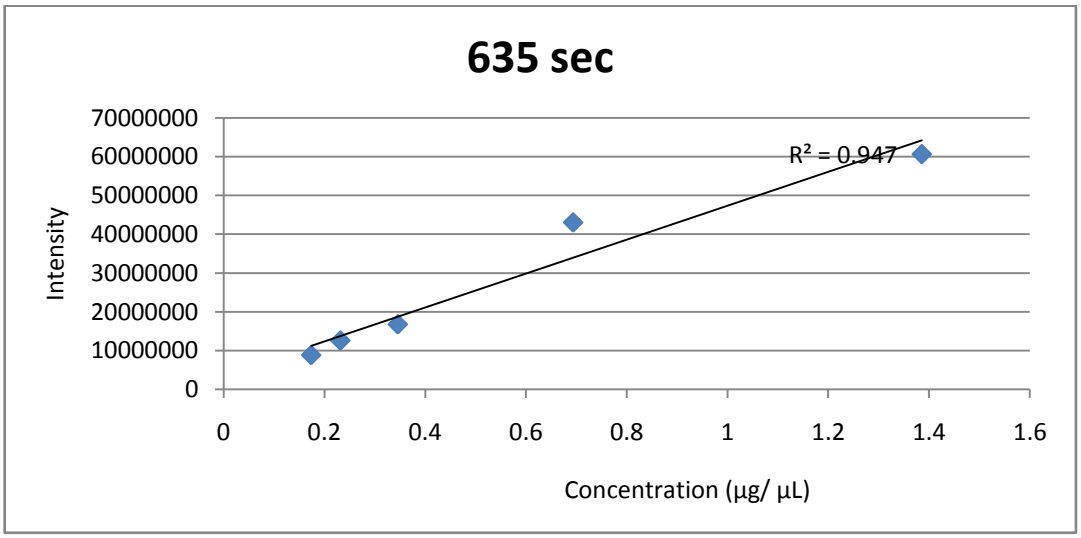

Figure B-21: The effect of EGFP concentration (µg/ µL) on the intensity with linearity of 0.947 at 635 seconds UV exposure time (2nd raw data)

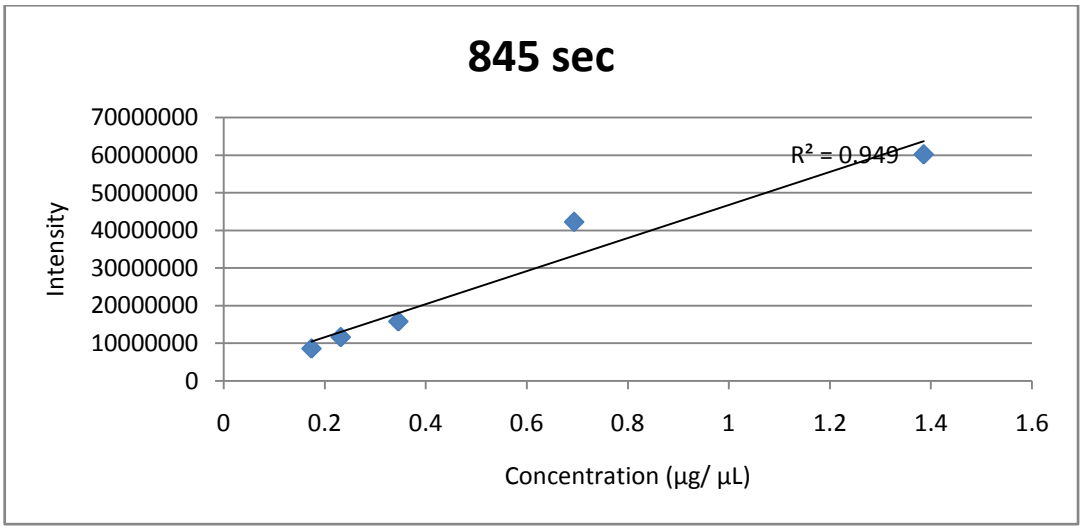

Figure B-22: The effect of EGFP concentration (µg/ µL) on the intensity with linearity of 0.949 at 845 seconds UV exposure time (2nd raw data)

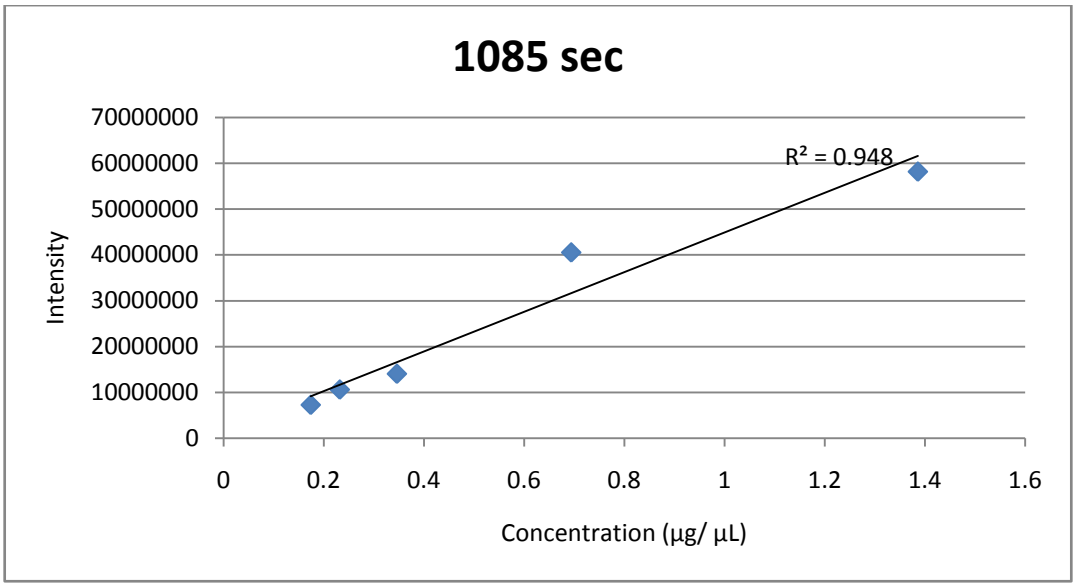

Figure B-23: The effect of EGFP concentration (µg/ µL) on the intensity with linearity of 0.948 at 1085 seconds UV exposure time (2nd raw data)

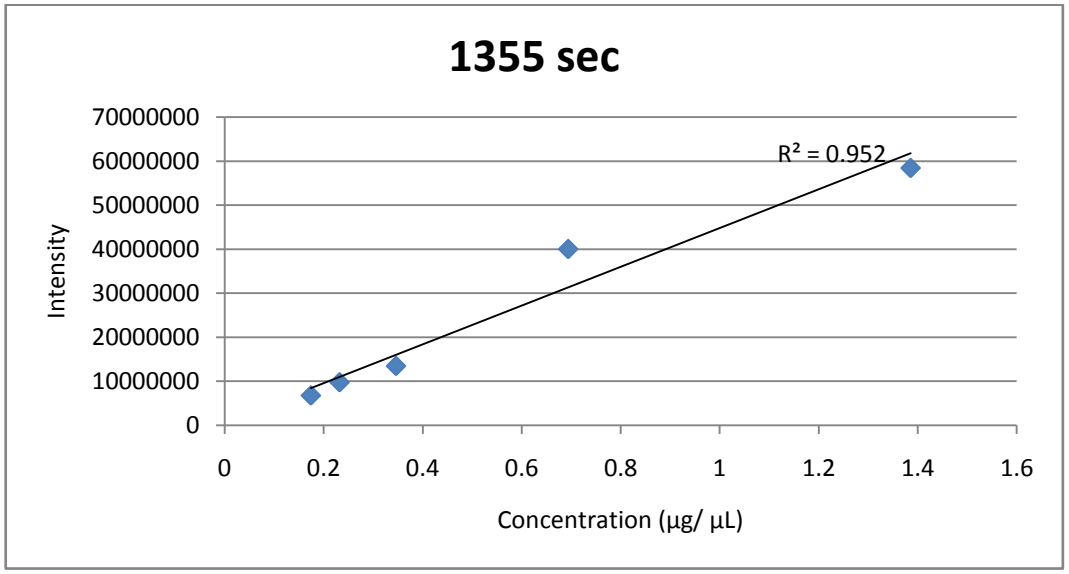

Figure B-24: The effect of EGFP concentration (µg/ µL) on the intensity with linearity of 0.952 at 1355 seconds UV exposure time (2nd raw data)

Table B-15: 3rd raw data for the linearity of standard curve (R^2) of different concentration on each UV exposure time

Time (s) \ Concentration (µg/ µL)	Intensity				
	1.386	0.694	0.346	0.232	0.174
5	60141097	42654446	26353369	15719114	9027672
35	62677345	44796629	27906952	16913659	9607040
95	62284008	44763527	27892932	16995162	9952730
185	60856855	43802578	26813545	16120571	9468982
305	60787572	43453134	25640978	15455686	8982268
455	59121351	41667581	23729624	14273490	8325127
635	59420782	41629843	24142951	14654801	8723683
845	59048134	41261732	22956248	13899610	8123136
1085	57321556	39834255	21652966	13009174	7593878
1355	56594939	38926678	20210536	12095871	7107511

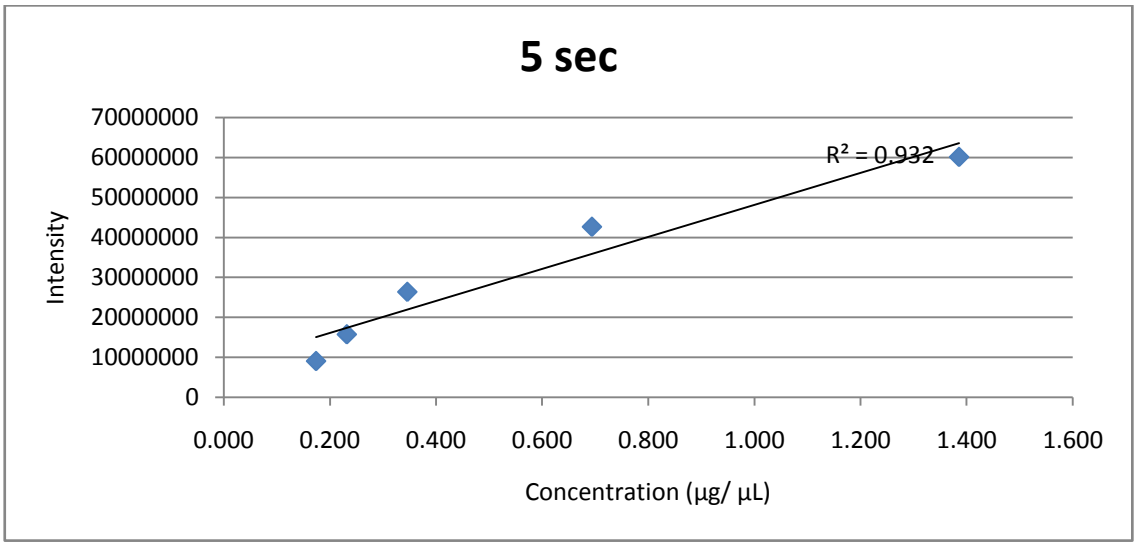

Figure B-25: The effect of EGFP concentration (µg/ µL) on the intensity with linearity of 0.932 at 5 seconds UV exposure time (3rd raw data)

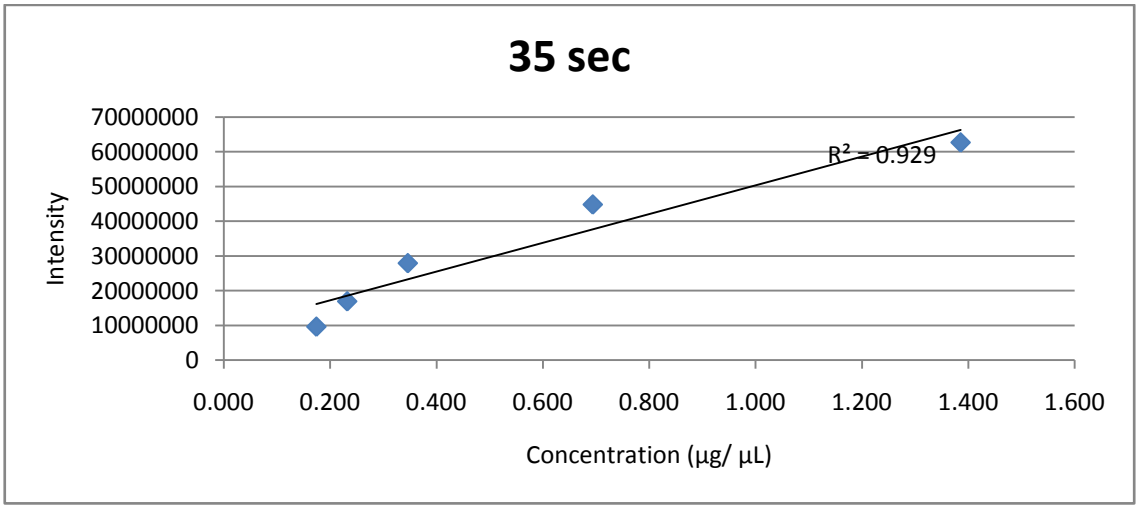

Figure B-26:The effect of EGFP concentration (µg/ µL) on the intensity with linearity of 0.929 at 35 seconds UV exposure time (3rd raw data)

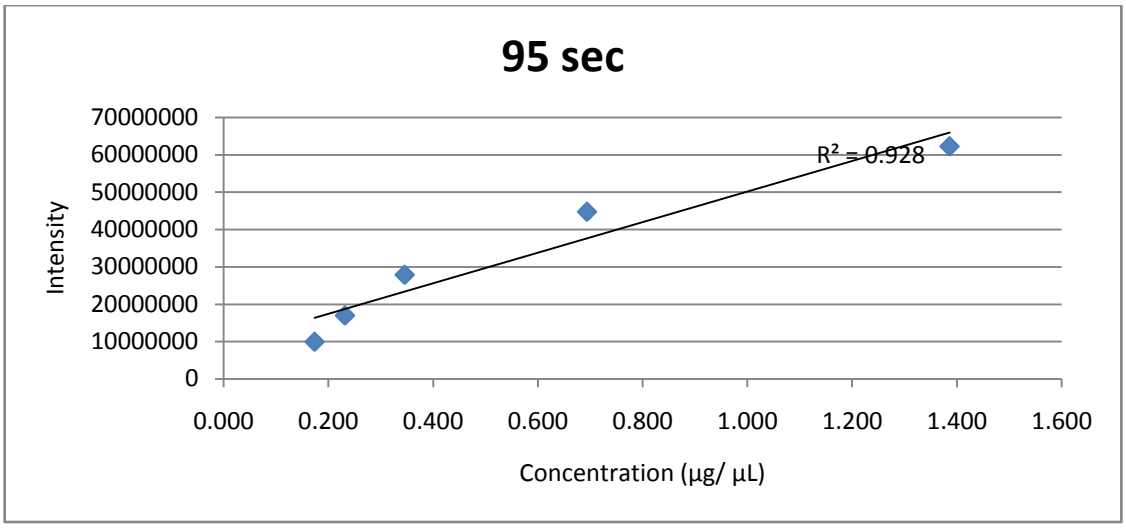

Figure B-27: The effect of EGFP concentration (µg/ µL) on the intensity with linearity of 0.928 at 95 seconds UV exposure time (3rd raw data)

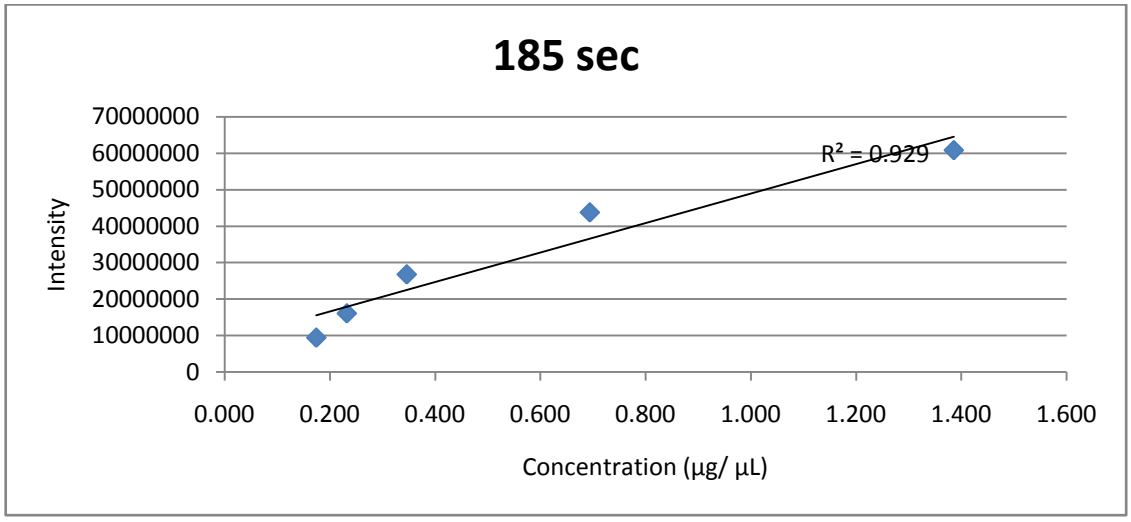

Figure B-28: The effect of EGFP concentration (µg/ µL) on the intensity with linearity of 0.929 at 185 seconds UV exposure time (3rd raw data)

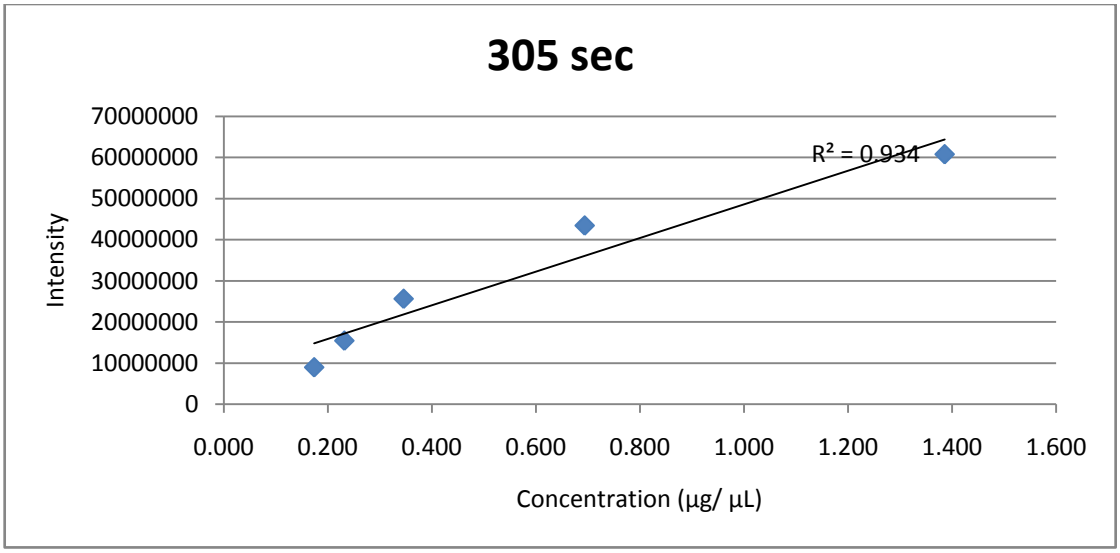

Figure B-29: The effect of EGFP concentration (µg/ µL) on the intensity with linearity of 0.934 at 305 seconds UV exposure time (3rd raw data)

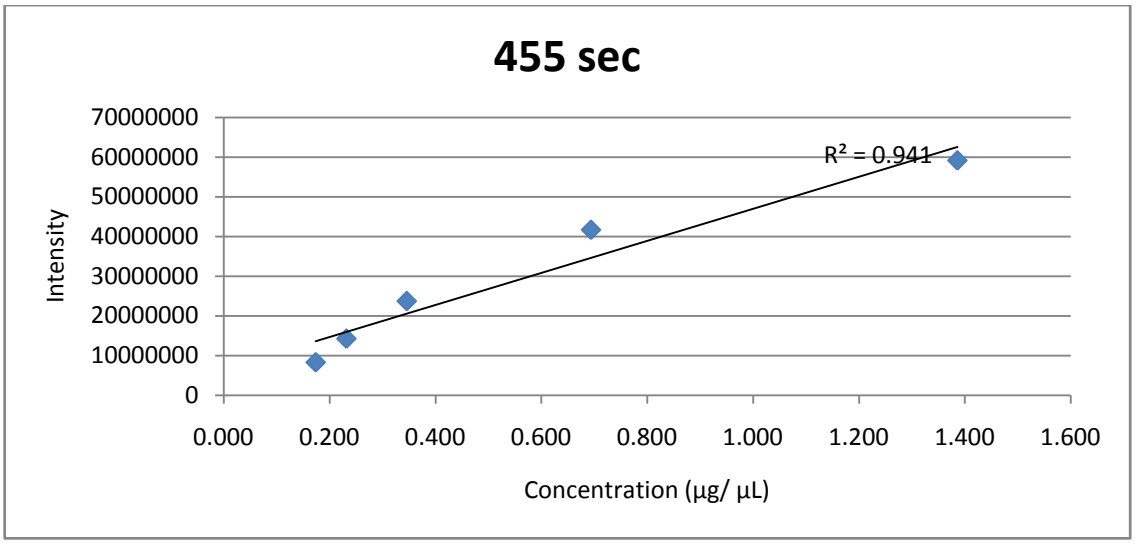

Figure B-30: The effect of EGFP concentration (µg/ µL) on the intensity with linearity of 0.941 at 455 seconds UV exposure time (3rd raw data)

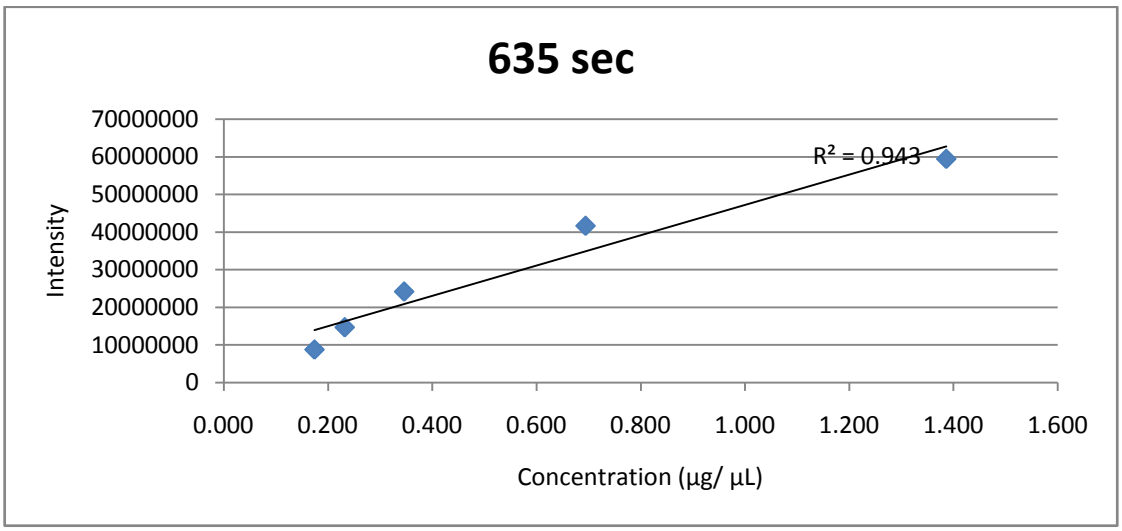

Figure B-31: The effect of EGFP concentration (µg/ µL) on the intensity with linearity of 0.943 at 635 seconds UV exposure time (3rd raw data)

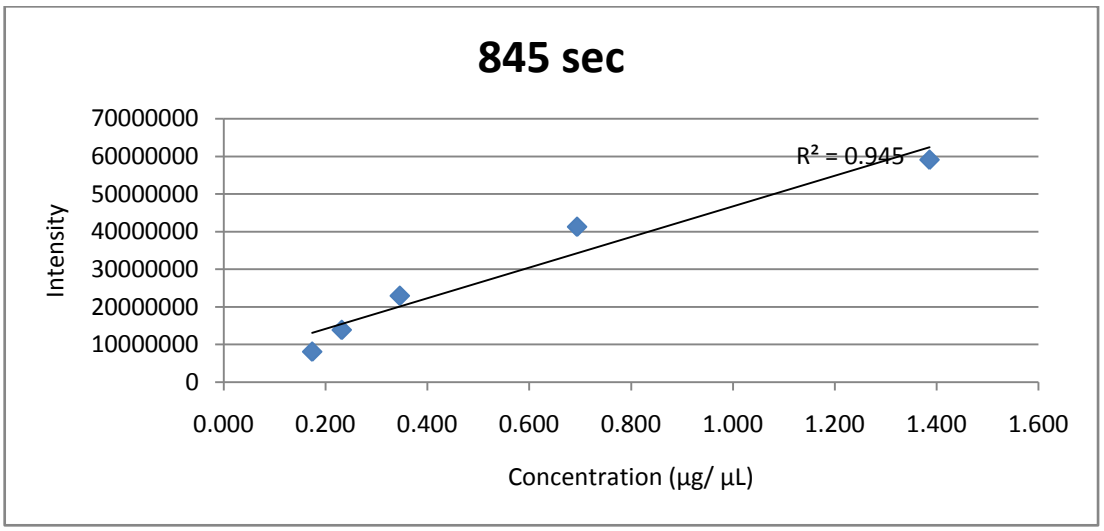

Figure B-32: The effect of EGFP concentration (µg/ µL) on the intensity with linearity of 0.945 at 845 seconds UV exposure time (3rd raw data)

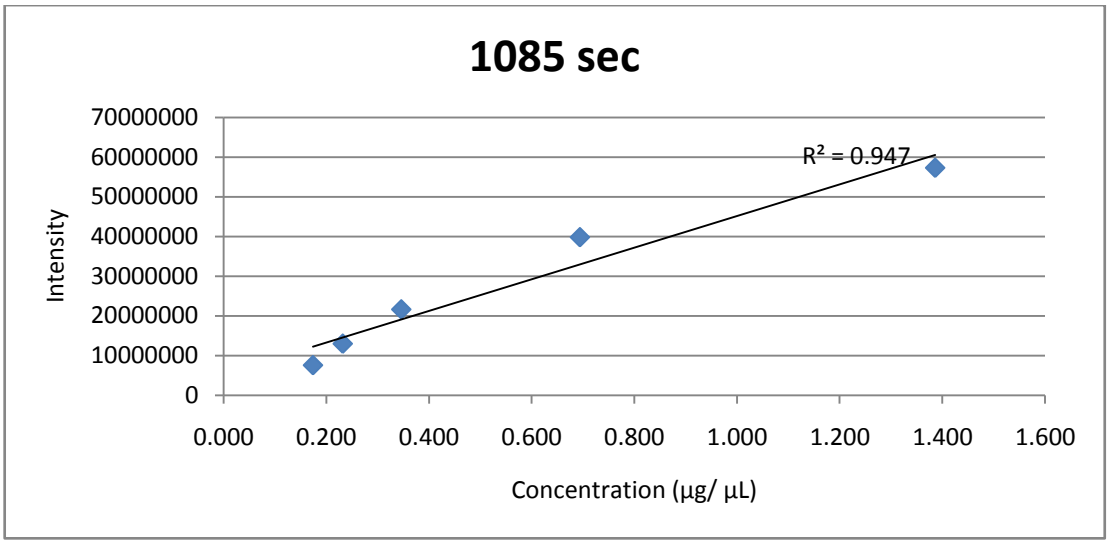

Figure B-33: The effect of EGFP concentration (µg/ µL) on the intensity with linearity of 0.947 at 1085 seconds UV exposure time (3rd raw data)

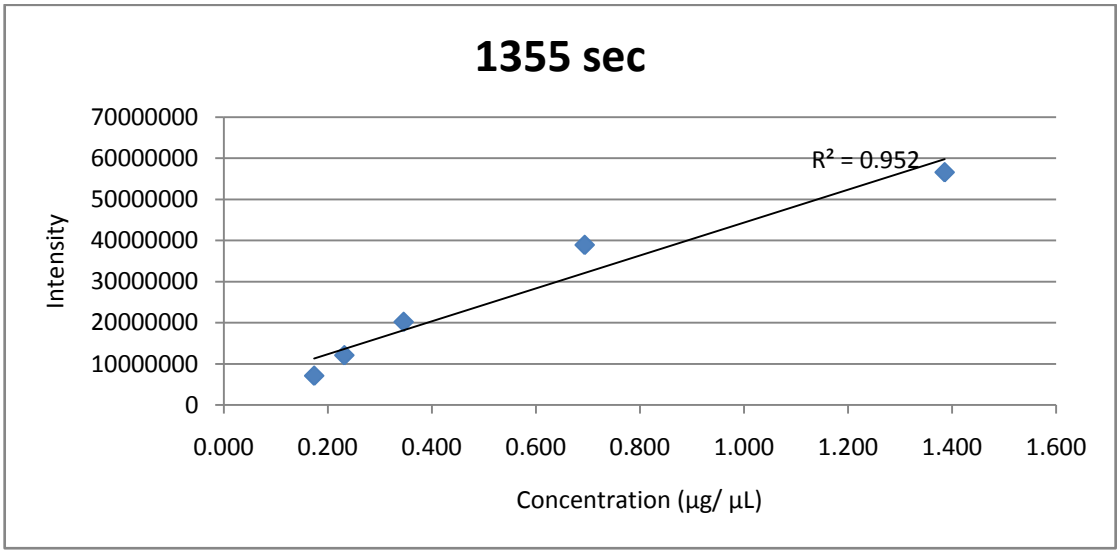

Figure B-34: The effect of EGFP concentration (µg/ µL) on the intensity with linearity of 0.952 at 1355 seconds UV exposure time (3rd raw data)

Table B-16: 4th raw data for the linearity of standard curve (R^2) of different concentration on each UV exposure time

Time (s) \ Concentration (µg/ µL)	Intensity				
	1.386	**0.694**	**0.346**	**0.232**	**0.174**
5	66866522	45045986	25322882	13112099	11390091
35	68727091	46698438	26121306	13184390	11197248
95	68955300	45950166	24638700	12414644	10769259
185	67768517	44505527	22178138	11468889	10051557
305	66850223	43233234	20505309	10347448	9399888
455	66728727	42947632	19659525	10381542	9354561
635	65686494	41897525	18493779	9564417	8703576
845	65266804	40726181	17350871	8937060	8094703
1085	64414332	39833080	16226559	8380953	7465844
1355	63627959	38445816	15292001	7707055	7210934

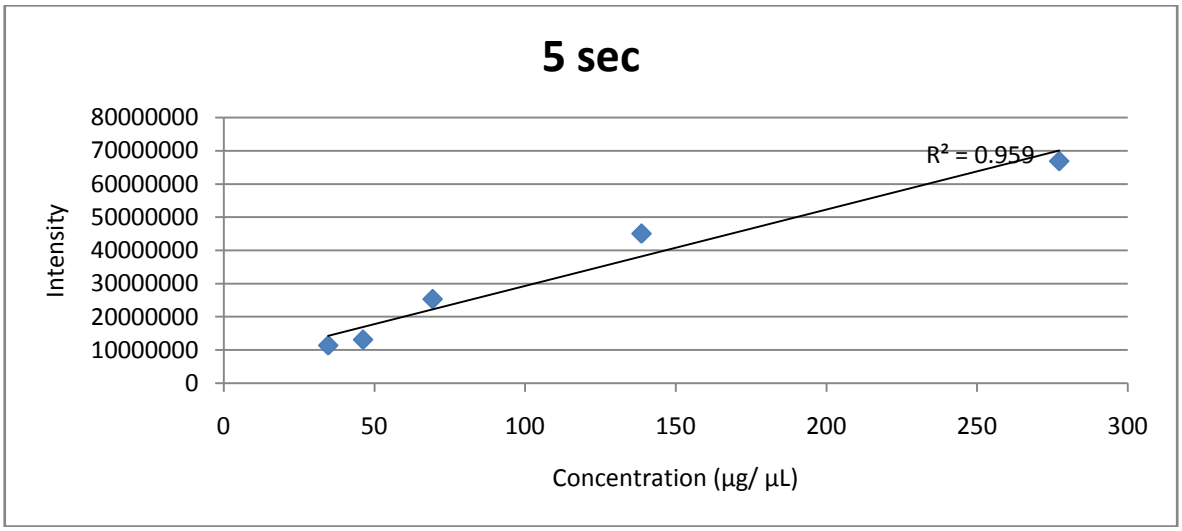

Figure B-35: The effect of EGFP concentration (µg/ µL) on the intensity with linearity of 0.959 at 5 seconds UV exposure time (4th raw data)

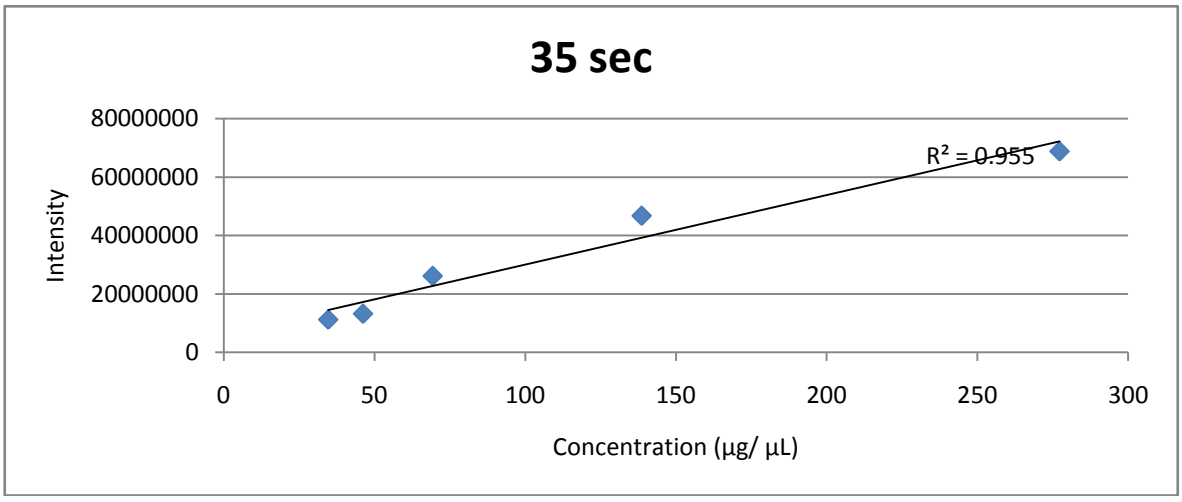

Figure B-36: The effect of EGFP concentration (µg/ µL) on the intensity with linearity of 0.955 at 35 seconds UV exposure time (4th raw data)

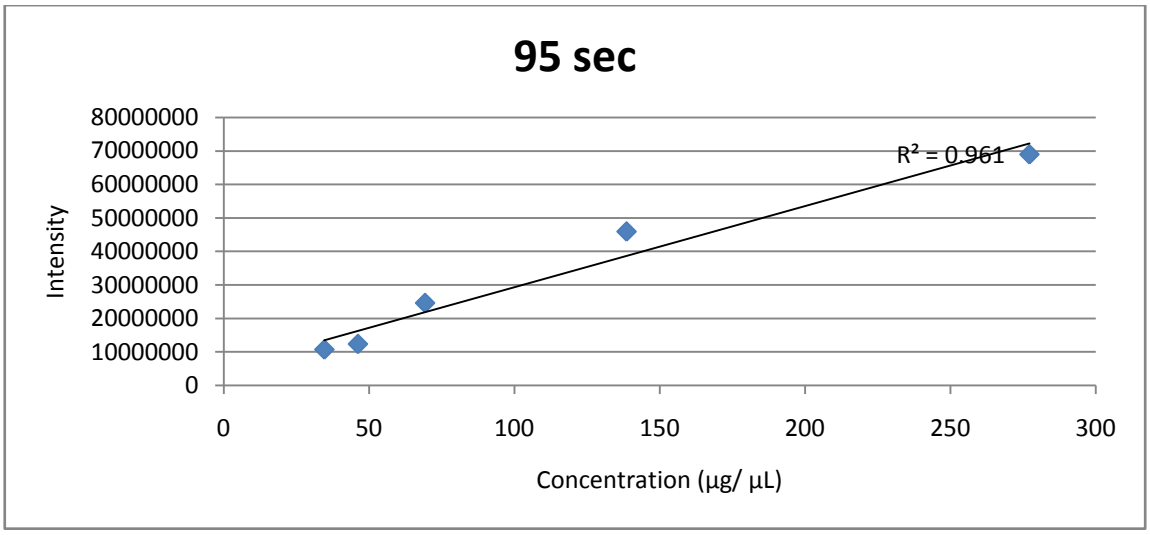

Figure B-37: The effect of EGFP concentration (µg/ µL) on the intensity with linearity of 0.961 at 95 seconds UV exposure time (4th raw data)

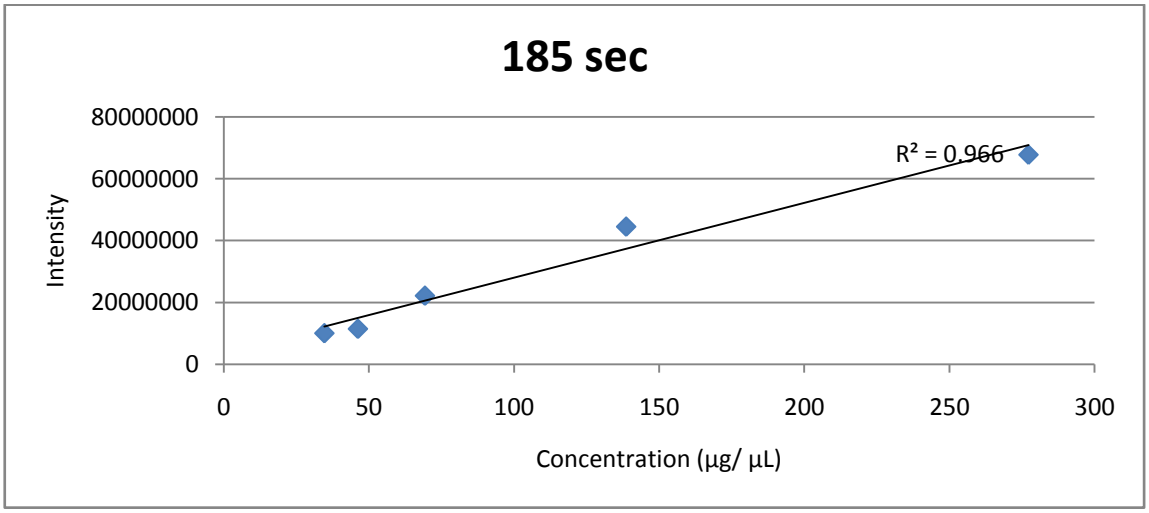

Figure B-38: The effect of EGFP concentration (µg/ µL) on the intensity with linearity of 0.966 at 185 seconds UV exposure time (4th raw data)

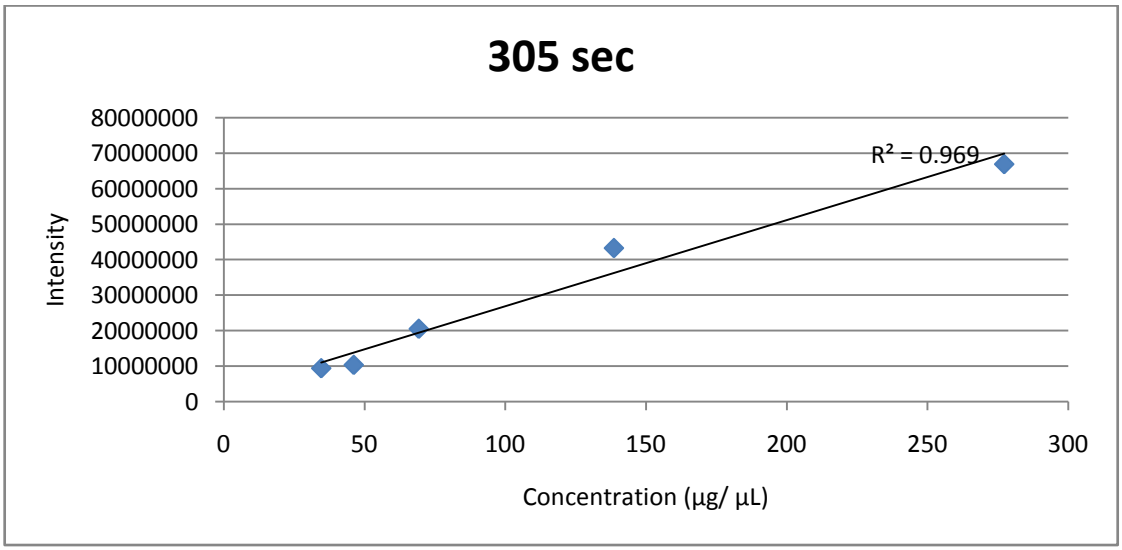

Figure B-39: The effect of EGFP concentration (µg/ µL) on the intensity with linearity of 0.969 at 305 seconds UV exposure time (4th raw data)

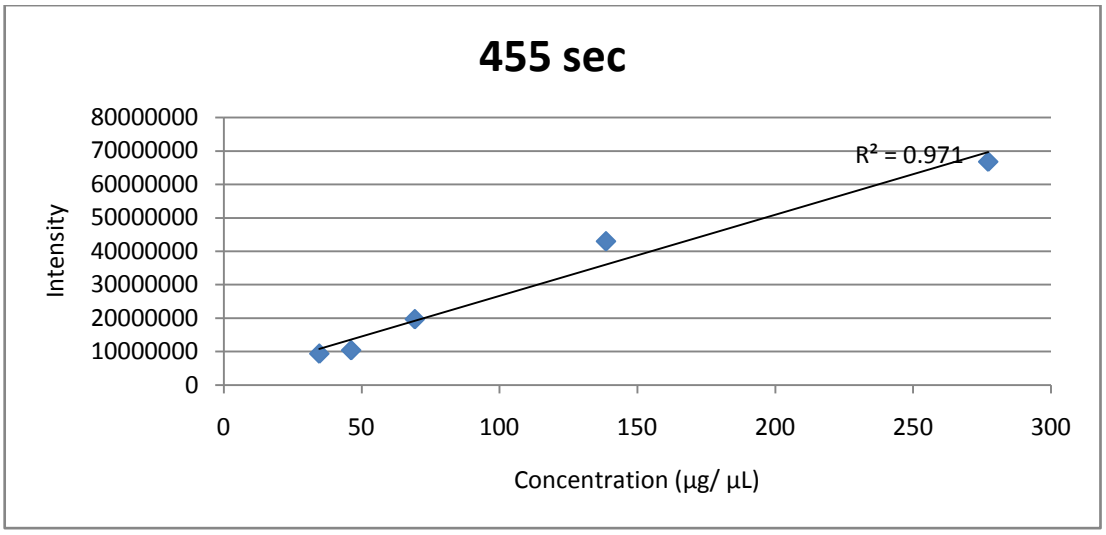

Figure B-40: The effect of EGFP concentration (µg/ µL) on the intensity with linearity of 0.971 at 455 seconds UV exposure time (4th raw data)

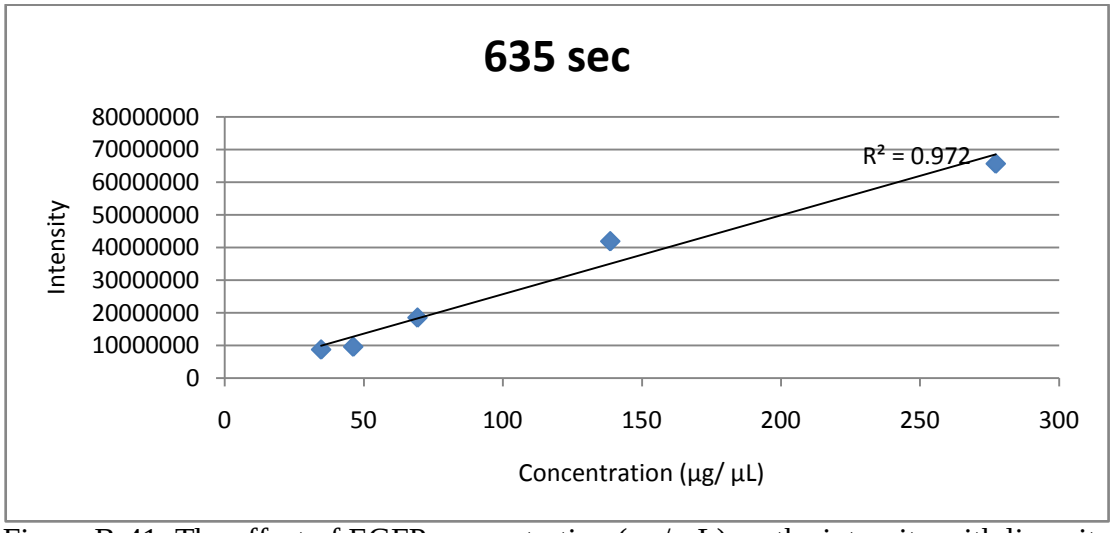

Figure B-41: The effect of EGFP concentration (µg/ µL) on the intensity with linearity of 0.972 at 635 seconds UV exposure time (4th raw data)

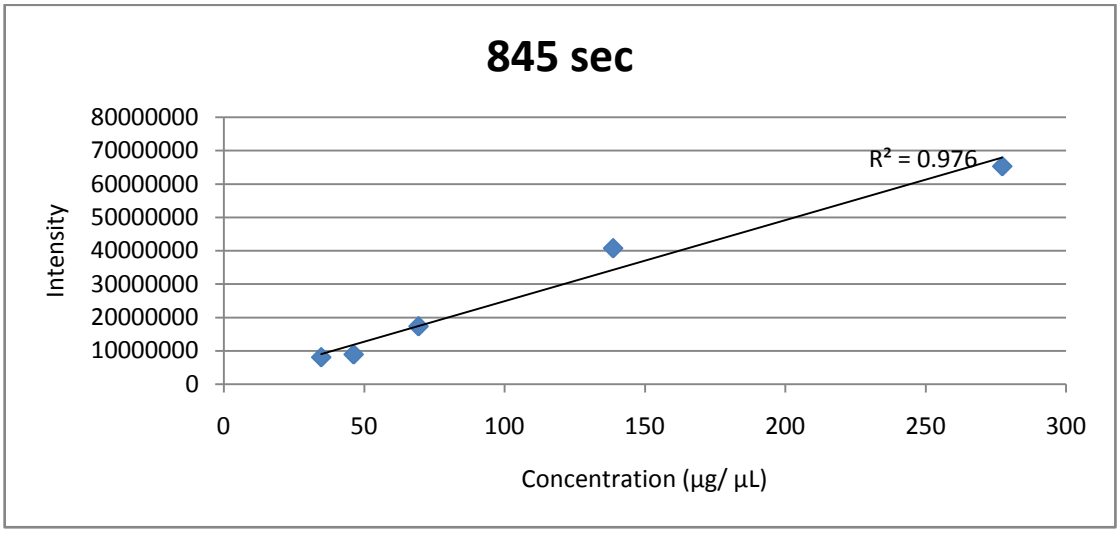

Figure B-42: The effect of EGFP concentration (µg/ µL) on the intensity with linearity of 0.976 at 845 seconds UV exposure time (4th raw data)

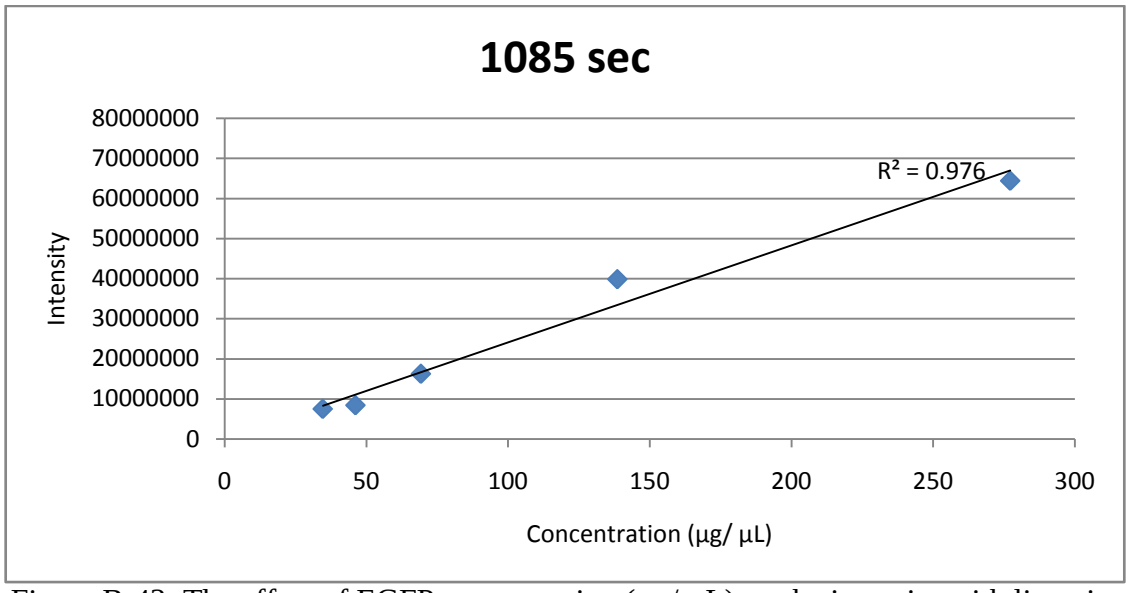

Figure B-43: The effect of EGFP concentration (µg/ µL) on the intensity with linearity of 0.976 at 1085 seconds UV exposure time (4th raw data)

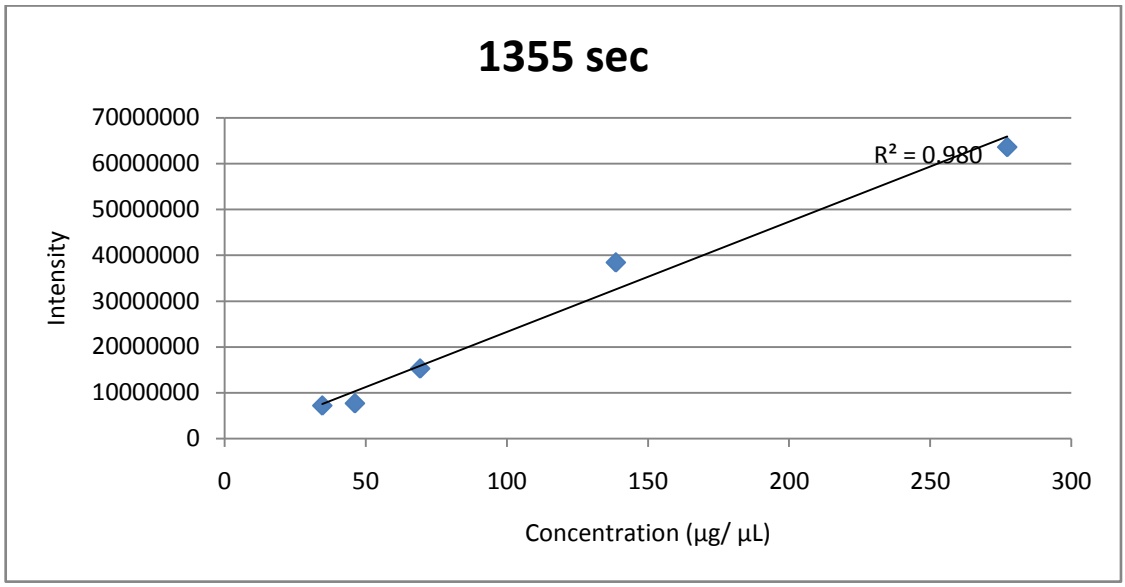

Figure B-44: The effect of EGFP concentration (µg/ µL) on the intensity with linearity of 0.980 at 1355 seconds UV exposure time (4th raw data)

Table B-17: The average data for the linearity of standard curve (R^2) of different concentration on each UV exposure time with standard deviation and coefficient of variance.

Time (s)	Linearity (1st)	Linearity (2nd)	Linearity (3rd)	Linearity (4th)	Average linearity	STD	COV
5	0.872	0.967	0.932	0.959	0.933	0.0430	4.61
35	0.861	0.942	0.929	0.955	0.922	0.0419	4.54
95	0.857	0.945	0.928	0.961	0.923	0.0459	4.97
185	0.863	0.952	0.929	0.966	0.928	0.0456	4.92
305	0.866	0.951	0.934	0.969	0.930	0.0450	4.84
455	0.882	0.948	0.941	0.971	0.936	0.0379	4.05
635	0.887	0.947	0.943	0.972	0.937	0.0359	3.83
845	0.891	0.949	0.945	0.976	0.940	0.0356	3.79
1085	0.898	0.948	0.947	0.976	0.942	0.0324	3.44
1355	0.901	0.952	0.952	0.980	0.946	0.0329	3.48

APPENDIX C: Details and photo of equipment

Figure C-1: The Stuart orbital incubator shaker S1500

Figure C-2: The Eppendorf, centrifuge 5810R centrifuge machine

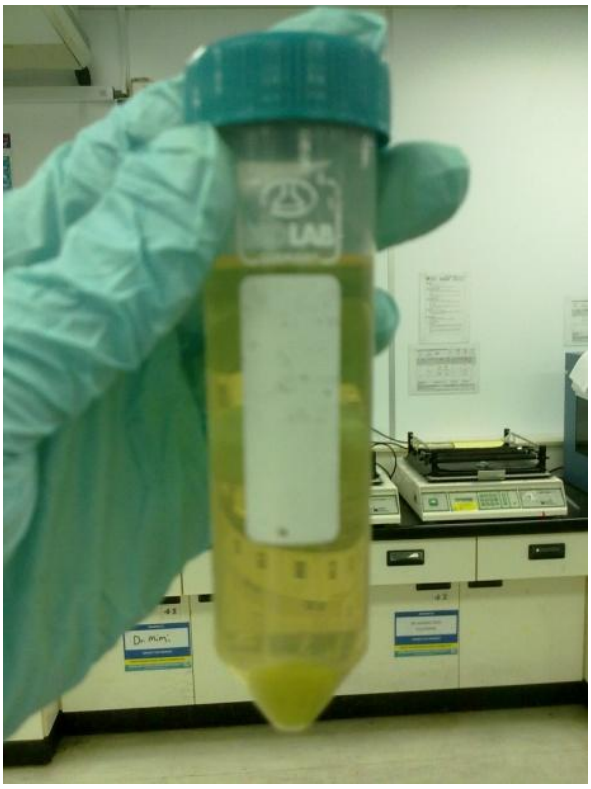

Figure C-3: The light green cell pellet (EGFP) inside the supernatant after centrifugation

Figure C-4: The purification using 1mL histrap column and the purified EGFP

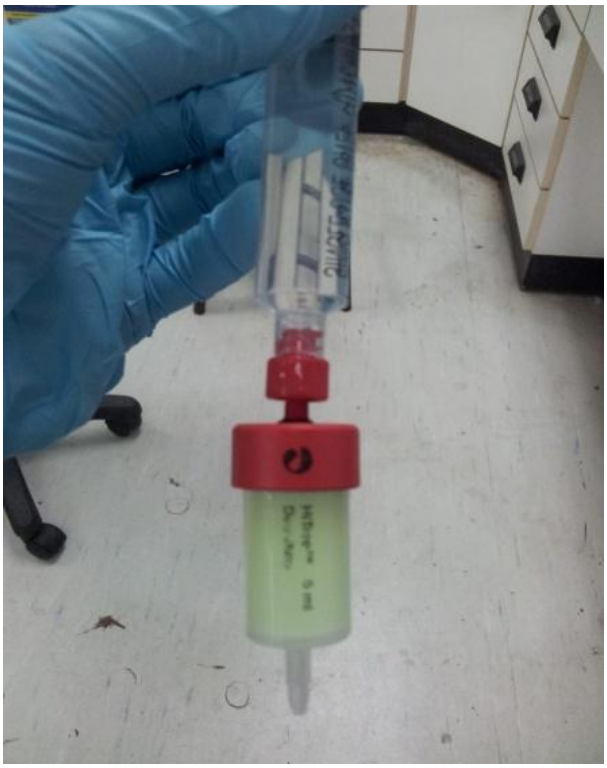

Figure C-5: The 5ml desalting column is used after EGFP purification

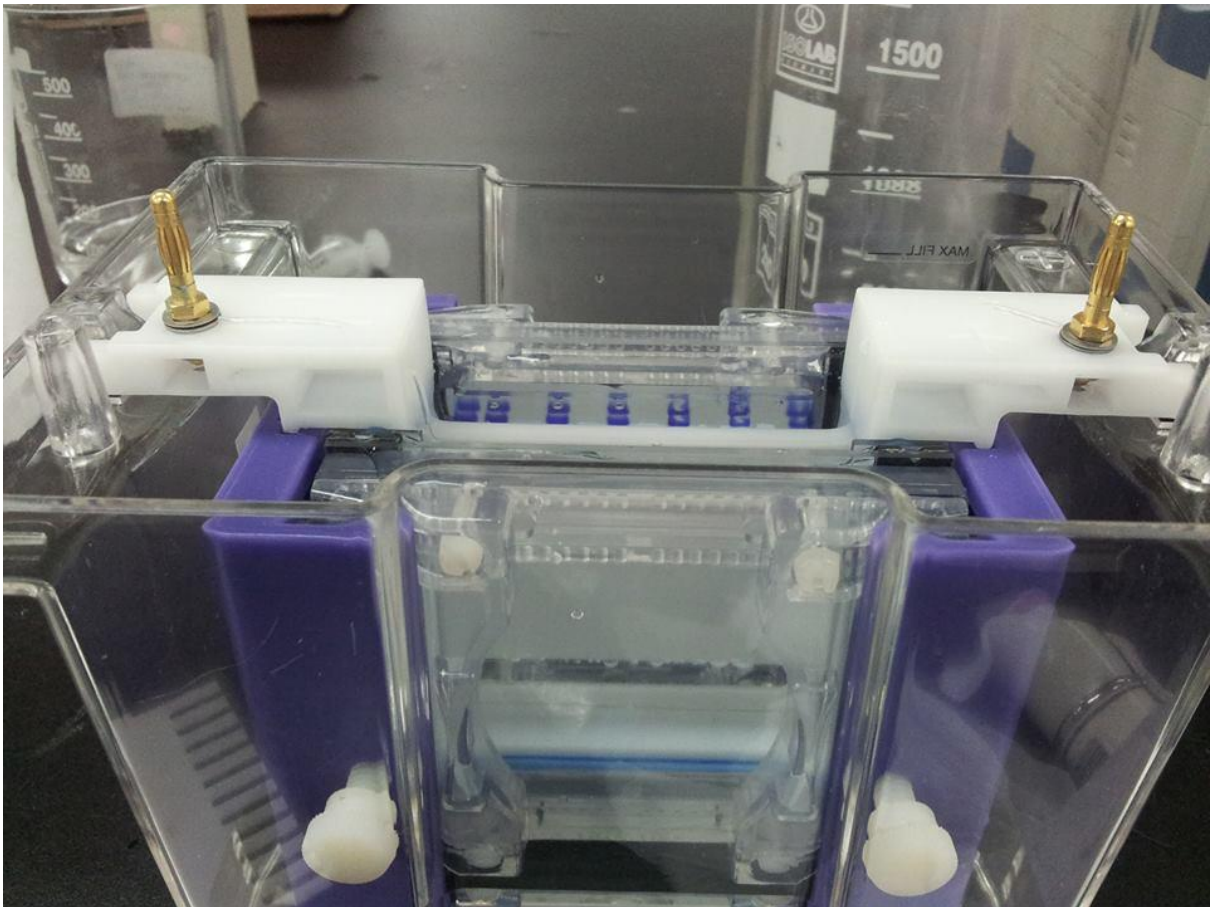

Figure C-6: The mini protean system with the sample dye (dark blue)

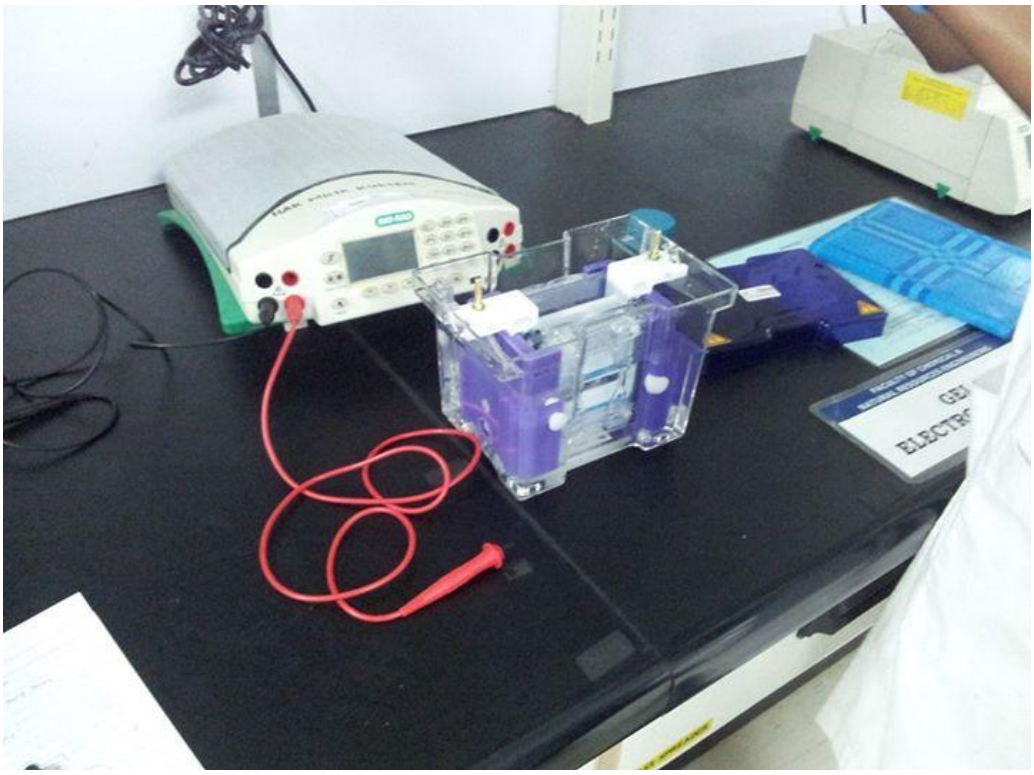

Figure C-7: The electrophoresis apparatus and mini protean system before connection

Figure C-8: The acrylamide gel after electrophoresis

Figure C-9: The outlook of the gel imaging system (Alpha Innotech Fluorochem™)

Figure C-10: The camera setting (Aperture:11; Zoom: 70; Focus: 1.90)

Figure C-11: The setting for the FluorChem™
(Translumination: UV ; Reflective:UV; Fiter type: 4 Fluorescein)

Figure C-12: The wavelength of UV used is 302 nm

Figure C-13: The standard which is used to make sure the gel placement in the same position for every time of analysis

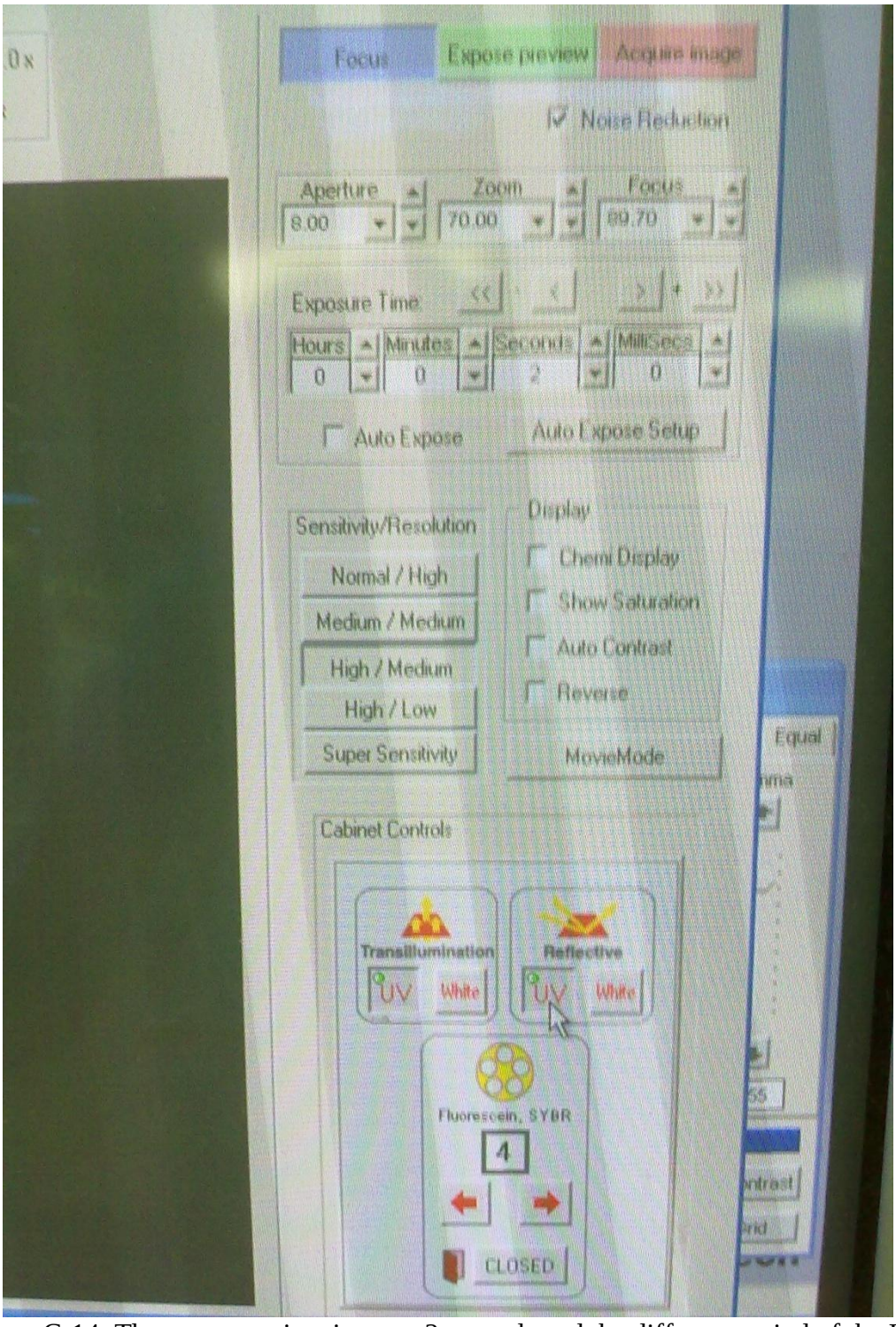

Figure C-14: The exposure time is set at 2 seconds and the different period of the UV irradiation (5, 35, 95, 185, 305, 455, 635, 845, 1085 and 1355 sec) is set after clicking the acquire image button (red color)

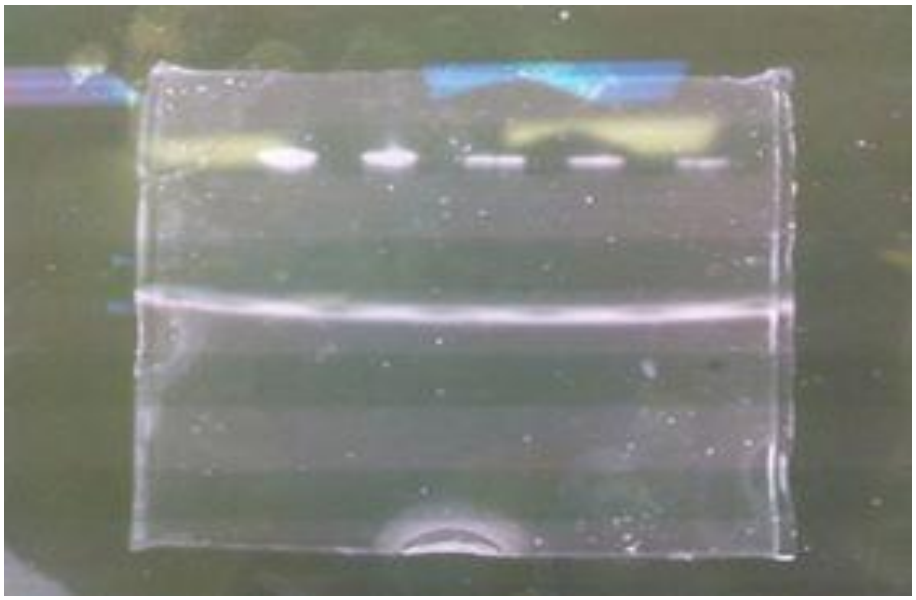

Figure C-15: The intensity of EGFP are shown on the gel inside the gel imaging system (From the left to right: 1x, 2x, 4x, 6x and 8x dilution rate)

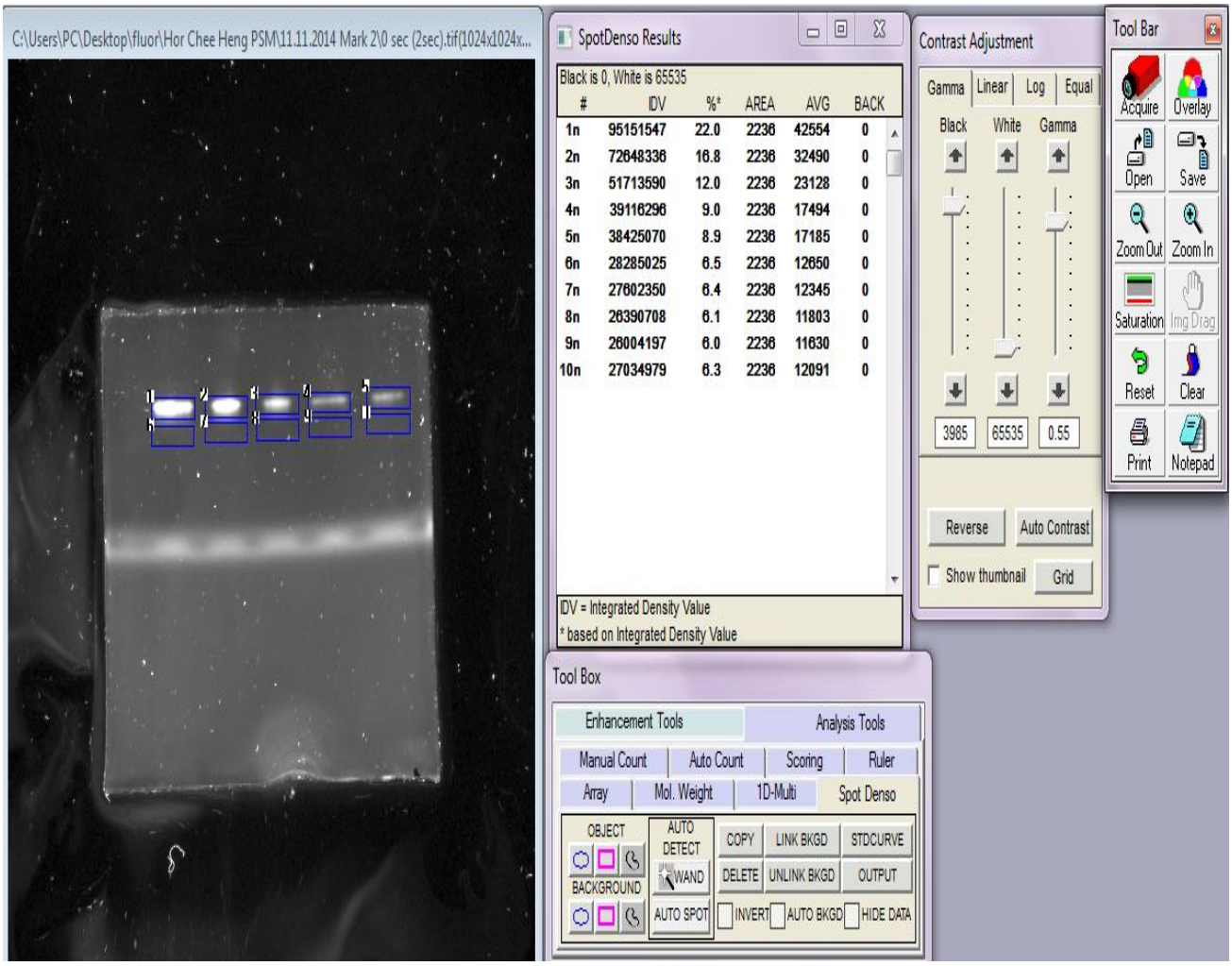

Figure C-16: The analysis of the intensity of the EGFP and its signal to noise ratio inside the gel imaging system.